

Filipe Manuel Coreta Gomes

Quantification of Cholesterol Solubilization by Bile Salt Micelles: Implications in its Intestinal Absorption by Passive Processes

Tese de Doutoramento em Química, especialidade Química Biológica, sob a orientação da Professora Doutora Maria João Pedrosa Ferreira Moreno Silvestre e do Professor Doutor Carlos Frederico de Gusmão Campos Geraldes, apresentada à Faculdade de Ciências e Tecnologia da Universidade de Coimbra

Coimbra, 2013



UNIVERSIDADE DE COIMBRA

• U



C •

FCTUC FACULDADE DE CIÊNCIAS
E TECNOLOGIA
UNIVERSIDADE DE COIMBRA

Departamento de Química

***Quantification of Cholesterol
Solubilization by Bile Salt Micelles:
Implications in its Intestinal Absorption by
Passive Processes***

Tese de Doutoramento em Química, especialidade Química Biológica, sob a orientação da Professora Doutora Maria João Pedrosa Ferreira Moreno Silvestre e do Professor Doutor Carlos Frederico de Gusmão Campos Geraldes, apresentada à Faculdade de Ciências e Tecnologia da Universidade de Coimbra

Filipe Manuel Coreta Gomes

Coimbra

2013

''Now this is not the end. It is not even the beginning of the end. But it is, perhaps, the end of the beginning''

Winston Churchill

Agradecimentos

Um doutoramento é uma viagem maravilhosa pelo mundo do conhecimento, não é contudo uma viagem que se possa dizer que ocorra sem sobressaltos. O importante é não esquecer a pergunta que se fez e acima de tudo não perder a vontade de aprender independentemente das adversidades que possam aparecer. Durante este período maravilhoso ri, chorei, aprendi, experienciei, diverti-me, desiludi-me, duvidei, afirmei, amei, odiei, foram talvez até agora os anos mais intensos da minha vida. Não quis fazer mais um doutoramento, mas sim embrenhar-me da forma mais séria e ambiciosa possível com as capacidades que tinha e que fui adquirido e está aqui o resultado. Certamente não cheguei aqui sozinho e também não parto sozinho. Gostaria de expressar então a minha gratidão a várias pessoas e a várias instituições que me ajudaram neste percurso.

Começaria por agradecer à minha orientadora de doutoramento a Professora Doutora Maria João Moreno, que foi sempre um pilar durante todo o percurso, não só pela sua disponibilidade, mas acima de tudo pela sua exigência, rigor, espírito crítico e dinamismo.

Ao meu co-orientador o Professor Doutor Carlos Geraldês gostaria de agradecer os seus ensinamentos e a disponibilidade demonstrada ao longo deste percurso.

Gostaria ainda de agradecer ao Professor Doutor Winchil Vaz pelas inúmeras conversas e discussões ao longo destes anos, são momentos muito especiais que tenho tido o privilégio de ter.

Ao Professor Doutor Adrián Velázquez Campoy por me acolher no seu laboratório e pela disponibilidade.

Ao Doutor Emeric Wasielewski, por todo o apoio técnico e amizade ao longo destes anos e ainda por todas as discussões e suporte nas longas noites de RMN.

Gostaria ainda de agradecer aos meus colegas de laboratório, mais propriamente à Patrícia, Renato e Hugo, dizer que foi um prazer fazer este percurso convosco, principalmente porque foi um percurso de entreaajuda, de amizade e partilha. Agradecer a todos os outros estudantes com quem partilhamos o gabinete.

Não poderia deixar de agradecer aos meus pais, pois têm sido dos principais responsáveis por ter chegado aqui. Obrigado pelo apoio incondicional e por toda a vossa disponibilidade. Um agradecimento especial à minha avó Maria pela sua presença na minha vida, por todos os seus ensinamentos e principalmente pelo exemplo de vida. Aos

meus tios a quem também estarei eternamente grato por toda ajuda e dedicação que sempre tiveram para comigo.

Obrigado Inês por toda a tua dedicação, paciência, serenidade, foi bom conhecer-te durante este percurso e foi certamente mais uma coisa boa que o doutoramento me trouxe.

A todos os meus amigos que me foram acompanhando ao longo destes anos, um grande abraço e prometo que vou tentar estar mais disponível.

Gostaria de agradecer por fim a várias instituições que permitiram que esta viagem se concretizasse, nomeadamente, a Fundação para Ciência e Tecnologia pela bolsa SFRH/BD/40778/2007, o Departamento de Química da Faculdade de Ciências e Tecnologia da Universidade de Coimbra onde desenvolvi os meus trabalhos e a Organização Europeia de Biologia Molecular (EMBO) pela bolsa de curta duração com a referência ASTF 147-13.

Index

Abstract _____	xvii
Resumo _____	xix
List of abbreviations _____	xxiii
Chapter I A Biophysics View on Cholesterol Solubilization by Bile Salt Micelles: Implications in the Intestinal Passive Absorption Process _____	1
I. 1 - Cholesterol in health and disease: strategies to decrease cholesterol absorption	3
I. 2 - Morphology and physiology of intestinal epithelium _____	9
I. 3 - Properties of gastrointestinal tract (GIT) _____	11
I. 4 - Self-Assembly of amphiphiles: Thermodynamic principles _____	17
I. 5 - Mixed Micelles _____	21
I. 6 - Bile salts structure, diversity and function _____	23
I. 7 - Solubilization processes in the intestinal lumen _____	27
I. 7. 1 - Cholesterol solubility limit in BS micelles: BS-insoluble amphiphiles mixed micelles type _____	27
I. 7. 2 - BS-swelling amphiphiles mixed micelles type _____	30
I. 7. 3 - BS-swelling amphiphiles (lecithin) and cholesterol _____	32
I. 7. 4 - Phytosterols so similar but so different from cholesterol _____	34
I. 8 - Absorption in membranes _____	38
I. 8. 1 - Partition of BS into membranes _____	38
I. 8. 2 - Flip-Flop or translocation _____	41
I. 9 - An overview of passive absorption: Solubilization versus partition phenomena	42
I. 10 - Cholesterol transporters _____	48
I. 10. 1 - Nieman Peak C1 L1 (NPC1L1) (absorption of cholesterol in intestine and liver) _____	48
I. 10. 2 - Regulation by ABC transporters (efflux of cholesterol and phytosterols from apical membrane) _____	49
I. 10. 3 - LDL receptor pathway (transporter of cholesterol from blood to cells) _____	49
Chapter II A Good Choice of Experimental Technique Can Help to Solve a Scientific Problem: NMR and ITC Theoretical Background. _____	51
II. 1 - The NMR spectroscopy _____	53

<i>II. 1. 1 - The NMR experiment</i>	57
<i>II. 2. 1 - Partition Model</i>	63
 <i>Chapter III Direct Non-Invasive Quantification of Cholesterol Solubilized in Bile Salt Micellar Aqueous Solutions</i>	 67
<i>III. 1 - Abstract</i>	69
<i>III. 2 - Introduction</i>	69
<i>III. 3. 1 - Materials</i>	72
<i>III. 3. 2 - Methods</i>	72
<i>III. 4 - Results and discussion</i>	75
<i>III. 4. 1 - Determination of GDCA Critical Micelle Concentration</i>	75
<i>III. 4. 2 - Solubilization of [4-¹³C]cholesterol in GDCA micelles</i>	76
<i>III. 4. 3 - Effects of solubilized cholesterol in GDCA NMR spectra</i>	82
<i>III. 4. 4 - GDCA dynamics</i>	85
<i>III. 5 - Conclusions</i>	86
<i>III. 6 - Supplementary material</i>	87
 <i>Chapter IV Cholesterol Solubility in Bile Salt Micellar Solutions: Dependence on Bile Salt Composition and Competition Effects by Phytosterols, Fatty Acids and Tocopherol</i>	 93
<i>IV. 1 - Abstract</i>	95
<i>IV. 2 - Introduction</i>	95
<i>IV. 3 - Materials and methods</i>	99
<i>IV. 4 - Results and discussion</i>	102
<i>IV. 4. 1 - Determination of CMC of glycine conjugated BS</i>	102
<i>IV. 4. 2 - Determination of Cholesterol Solubilization Index</i>	104
<i>IV. 4. 3 - Effect of phytosterols in cholesterol solubilization in GDCA micelles</i>	109
<i>IV. 4. 4 - Effect of saturated and unsaturated fatty acids in cholesterol solubilization in GDCA micelles</i>	118
<i>IV. 4. 5 - Effect of α-tocopherol in cholesterol solubilization in GDCA micelles</i>	120
<i>IV. 5 - Conclusions</i>	122
<i>IV. 6 Supplementary Material</i>	124

Chapter V Isothermal Calorimetric Study of the Interaction of Bile Salts with Lipid Membranes	131
V. 1 - Abstract	133
V. 2 - Introduction	133
V. 3 - Materials and methods	136
V. 4 - Results and discussion	140
V. 4. 1 - Partition of BS into bilayers in the liquid disordered phase (POPC) using the uptake protocol	140
V. 4. 2 - Partition of BS into bilayers in liquid disordered phase (POPC)-release versus uptake protocol	143
V. 4. 3 - Partition of BS into membranes of POPC/SpM/Chol (1:1:1)-release versus uptake protocol	147
V. 4. 4 - Enthalpy contribution from buffer ionization	149
V. 5 - Conclusions	152
Chapter VI General Conclusions	155
VI. 1 - General conclusions	157
VI. 2 - Pitfalls and future perspectives	161
VII. 1 - Bibliography	163

Index of Figures

<i>Figure I. 1 Small intestine structure and some characteristics from the different anatomic units.....</i>	<i>9</i>
<i>Figure I. 2 Light micrograph (A) and labelled tracing drawing (B) of small intestinal mucosal of monkey.....</i>	<i>9</i>
<i>Figure I. 3 Electron micrographs and labelled trace illustration of glycocalyx.....</i>	<i>14</i>
<i>Figure I. 4 Parameters used for thermodynamic equations of the association of N monomers in an aggregate.....</i>	<i>17</i>
<i>Figure I. 5 The different types of structure and “mesophases” formed by amphiphiles in aqueous solution depending on their packing parameter.....</i>	<i>20</i>
<i>Figure I. 6 Structures of the most common bile salts found in humans.....</i>	<i>23</i>
<i>Figure I. 7 Phase diagram for taurocholate-lecithin system.....</i>	<i>30</i>
<i>Figure I. 8 Schematic models for the structure of the biles salt-lecithin mixed micelle.....</i>	<i>31</i>
<i>Figure I. 9 Triangular phase diagram showing the physical state of all combinations of NaTC, lecithin and cholesterol.....</i>	<i>32</i>
<i>Figure I. 10 Habits of solid and liquid crystals of Chol observed by polarizing light microscopy.....</i>	<i>33</i>
<i>Figure I. 11 Pictorial description of enterocyte in intestinal endothelium.....</i>	<i>43</i>
<i>Figure I. 12 Maximum solubility and passive permeability coefficient for a series of FA and sterols of increasing hydrophobicity. Maximum rates of absorption of different lipids in the presence and absence of the diffusion barrier.....</i>	<i>44</i>
<i>Figure I. 13 Simple model representing passive diffusion of hydrophobic molecules (cholesterol) through apical membrane.....</i>	<i>46</i>
<i>Figure II. 1 Precession orbit defined by the nuclear magnetic moment under an applied field B.....</i>	<i>53</i>
<i>Figure II. 2 Diagram showing the magnetization evolution with several pulses.....</i>	<i>57</i>
<i>Figure II. 3 Spins states and transition probabilities for a coupled two spin system.....</i>	<i>59</i>
<i>Figure II. 4 Scheme sequence of the parameters to define in a NMR experiment to have a ¹³C NMR spectra decoupled with NOE and without NOE.....</i>	<i>60</i>
<i>Figure II. 5 Representative diagram of a typical ITC experiment with power compensation.....</i>	<i>62</i>

<i>Figure III. 1 Molecular structures of GDCA and [4-¹³C]cholesterol and their relaxation times (T_1 in s) obtained for each carbon.....</i>	<i>71</i>
<i>Figure III. 2 Plot A: Fluorescence emission spectra (insert) and integrated intensity of NPN in the presence of different concentrations of GDCA Plot B: Thermogram and heat evolved as a function of the concentration of GDCA in the ITC cell.....</i>	<i>76</i>
<i>Figure III. 3 ¹³C NMR spectra of GDCA obtained on a Varian 600 MHz spectrometer, with ¹H decoupling and NOE.....</i>	<i>77</i>
<i>Figure III. 4 Typical kinetic profile obtained for the solubilization of a [4-¹³C]cholesterol film by GDCA micelles.....</i>	<i>78</i>
<i>Figure III. 5 Concentration of [4-¹³C]cholesterol solubilized by GDCA micelles ($[C_M]_{(\infty)}$) as a function of the total concentrations of cholesterol ($[C]_T$).....</i>	<i>79</i>
<i>Figure III. 6 Resonance shifts observed for GDCA carbons 1, 2, 4, 5, 9, 12, 17, 22 and 23, as a function of the concentration of solubilized [4-¹³C]cholesterol.....</i>	<i>82</i>
<i>Figure III. 7 Solubilization of [4-¹³C]cholesterol (plot A) and cholesterol (plot B) by GDCA micelles ($[C_M]_{(\infty)}$) as a function of the total concentration of cholesterol ($[C]_T$).....</i>	<i>83</i>
<i>Figure IV. 1 Molecular structures of BS (GDCA, GCDCA and GCA); Cholesterol (enriched in C 13 at position 4); phytosterols (stigmastanol and stigmasterol), Vitamine E (α-tocopherol) and Fatty acids (saturated-palmitic acid, unsaturated-oleic acid).....</i>	<i>98</i>
<i>Figure IV. 2 (A) Integrated fluorescence intensity of NPN in different solutions of single, binary and ternary BS mixtures.....</i>	<i>102</i>
<i>Figure IV. 3 Concentration of [4-¹³C]cholesterol solubilized by BS micelles ($[C_M]_{(\infty)}$) as a function of the total concentrations of cholesterol ($[C]_T$).....</i>	<i>104</i>
<i>Figure IV. 4 ¹³C NMR spectra expansion (from 55 to 35 ppm) of GDCA with [4-¹³C]cholesterol: competitor, obtained on a Varian 600 MHz spectrometer, with ¹H decoupling and NOE.....</i>	<i>109</i>
<i>Figure IV. 5 Effect of stigmastanol on cholesterol solubilization.....</i>	<i>110</i>

<i>Figure IV. 6 ^1H NMR spectra of GDCA BS micelles with $[4\text{-}^{13}\text{C}]$cholesterol. The inserts show an expansion from 5.5 to 3.0 ppm showing the peak from cholesterol solubilized at micelles (black line) and the peaks from cholesterol and stigmasterol (gray line).</i>	112
<i>Figure IV. 7 Effect of stigmasterol on cholesterol solubilization.</i>	113
<i>Figure IV. 8 Effect of saturated (palmitic acid-left panel) and unsaturated fatty acids (oleic acid-right panel) on cholesterol solubilization.</i>	118
<i>Figure IV. 9 Effect of tocopherol on cholesterol solubility by the BS micelles.</i>	120
<i>Figure V. 1 (A) Data from an uptake experiment, DCA(cell) and POPC (syringe) (B) Typical titration curve points for DCA and theoretical fit.</i>	140
<i>Figure V. 2 Comparison of titration curves and fit to the experimental results for the partition of conjugated and unconjugated BS to POPC LUV: Panel A. GCDCA, CDCA; Panel B. GCA and CA.</i>	141
<i>Figure V. 3 Titrations curves obtained for uptake and release protocols with POPC membranes. Plot A: CDCA partition profile Plot B: GCDCA partition profile.</i>	143
<i>Figure V. 4 Titrations curves obtained for uptake and release protocols with POPC/SpM/Chol (1:1:1) membranes. Plot A: DCA partition profile Plot B: GCDCA partition profile.</i>	147
<i>Figure V. 5 Enthalpy partition dependence on the buffers enthalpy of ionization..</i>	149

Index of Tables

<i>Table I. 1 BS commonly found in intestinal lumen contents of human beings.....</i>	<i>11</i>
<i>Table I. 2 Concentration of lipids found in duodenum contents according to fractions recovered from the chemical biopsies.....</i>	<i>13</i>
<i>Table I. 3 Lipid composition (%w/w) in biological membranes.....</i>	<i>15</i>
<i>Table I. 4 Physicochemical properties of BS solutions of the unconjugated and conjugated BS.....</i>	<i>25</i>
<i>Table I. 5 Cholesterol saturation limit in BS micelles, CMC, aggregations number.</i>	<i>28</i>
<i>Table I. 6 Molecular structures of sterols and stanols.....</i>	<i>34</i>
<i>Table I. 7 Solubility of cholesterol and phytosterols in simple BS micelles and of cholesterol in binary systems.....</i>	<i>36</i>
<i>Table I. 8 Partition equilibrium constant of BS species to model membranes.</i>	<i>39</i>
<i>Table III. S 1 ¹³C Longitudinal relaxation times (T₁) for GDCA carbons and carbon 4 of [4-¹³C]cholesterol..</i>	<i>87</i>
<i>Table III. S 2 ¹³C-¹H Nuclear Overhauser Effect (NOE) on a solution of GDCA with of [4-¹³C]cholesterol.</i>	<i>88</i>
<i>Table III. S 3 Chemical shifts assignments, peak area, and quantification results from a ¹³C NMR spectra obtained for an aqueous solution of GDCA with [4-¹³C]cholesterol without NOE (correction factor times area with NOE).....</i>	<i>89</i>
<i>Table III. S 4 Chemical shifts of GDCA carbon resonances as a function of solubilized [4-¹³C]cholesterol.</i>	<i>90</i>
<i>Table III. S 5 Concentration of cholesterol solubilized in GDCA micelles calculated from the variation observed in the resonance of GDCA carbons, for the case where unlabeled cholesterol was equilibrated with GDCA.....</i>	<i>92</i>
<i>Table IV. 1 Values of CSI and CMC determined for single, binary and ternary mixtures of BS.</i>	<i>106</i>
<i>Table IV. 2 Poisson distribution of cholesterol per micelle of BS.....</i>	<i>107</i>
<i>Table IV. 3 Comparison between total sterol (cholesterol+ stigmasterol) solubilized in GDCA micelles determined by quantitative ¹³C and ¹H NMR spectroscopy and the total sterol determined from quantitative chemical shift analysis (qCSA)..</i>	<i>116</i>

<i>Table IV. S 1 ^{13}C-$\{^1\text{H}\}$ Nuclear Overhauser Effect (NOE) on a solution of GCA with $[4\text{-}^{13}\text{C}]$cholesterol.....</i>	<i>124</i>
<i>Table IV. S 2 ^{13}C-$\{^1\text{H}\}$ Nuclear Overhauser Effect (NOE) on a solution of GDCA with of $[4\text{-}^{13}\text{C}]$cholesterol.</i>	<i>125</i>
<i>Table IV. S 3 Chemical shift analysis dependence on the total concentration of sterol (stigmasterol+cholesterol) and cholesterol in the micelle.....</i>	<i>126</i>
<i>Table IV. S 4 Chemical shift analysis dependence on the total concentration of sterol (stigmastanol+cholesterol) and determination of stigmastanol solubilized in the micelle.</i>	<i>127</i>
<i>Table IV. S 5 Concentration of palmitic acid solubilized in GDCA micelles calculated from the variation observed in the resonance of GDCA carbons.....</i>	<i>128</i>
<i>Table IV. S 6 Concentration of oleic acid solubilized in GDCA micelles calculated from the variation observed in the resonance of GDCA carbons.....</i>	<i>129</i>
<i>Table IV. S 7 Concentration of tocopherol solubilized in GDCA micelles calculated from the variation observed in some carbon selected resonances of GDCA.....</i>	<i>130</i>
<i>Table V. 1 Partition constant and enthalpy contributions from the interaction of BS (unconjugated and Glycine conjugated) with lipid membranes POPC and POPC/SpM/ Chol (1:1:1).</i>	<i>142</i>
<i>Table V. 2 Variation of pKa observed from partition of BS to membranes of POPC.</i>	<i>150</i>
<i>Table V. 3 Thermodynamic data from partition of several BS to lipid membranes.</i>	<i>151</i>

Abstract

Cholesterol is an important molecule for several functions from structural to hormonal. However, excess of cholesterol is implicated in several diseases, namely atherosclerosis and gallstone disease. Cholesterol absorption takes place at the intestine. The understanding of the mechanism beneath cholesterol absorption is relevant for the effectiveness of strategies to decrease cholesterol intake from the intestinal lumen. Prior to absorption, and due to its low aqueous solubility, cholesterol must be solubilized in bile salts (BS). In this work, focus was given to understand some of the principles related to cholesterol solubilization by BS as well as the interaction of BS with model membranes. First we explored cholesterol solubilization by glycodeoxycholic acid (GDCA), glycochenodeoxycholic acid (GCDCA) and glycocholic acid (GCA) in micelles of single, binary and ternary mixtures as these are the most prevalent BS at the intestinal lumen. Results showed that single micelles of the most hydrophobic BS (GDCA) presented the highest cholesterol solubilization, followed by micelles of GCDCA and of GCA. The 3 compositions of binary micelles, GCA/GCDCA (50:50), GCA/GDCA (50:50) and GCDCA/GDCA (50:50), and the ternary mixture, composed of GCA/GCDCA/GDCA (37.5:37.5:25), presented lower solubilization capacity than the simple micelles of GDCA but higher than GCA micelles. The results from this study suggest that BS mixtures present at duodenum are optimized neither for the highest nor for the lowest solubility of cholesterol; instead the solubilization capacity can be understood as a trade-off between cholesterol supply to membranes and cholesterol excretion. The results showed a linear correlation between cholesterol solubilization by BS micelles and the total concentration of cholesterol, until attaining a plateau that corresponds to the cholesterol saturation index (CSI). Moreover, the sterol occupancy per micelle depends on the BS, being 1 to simple micelles of GDCA and smaller to micelles of either GCDCA or GCA. The interpretation of these results leads to the understanding of solubilization of cholesterol by BS micelles as a partition phenomena rather than a binding event to an available place at the micelle. Solubilization is higher or lower depending on the partition of cholesterol to the considered micelle. However, this does not mean the micelle loses solubilizing capacity for other molecules. The understanding of the solubilization phenomena by the micelles in the presence of several co-solutes can give important information on strategies to decrease cholesterol solubilization and therefore intestinal absorption. Pursuing this objective, the effect of

stigmasterol and stigmastanol (phytosterols), palmitic acid (saturated fatty acid), oleic acid (unsaturated fatty acid) and α -tocopherol (vitamin) on the solubilization of cholesterol by the BS micelles was addressed. The highest effect in the decrease of cholesterol solubility was observed in the presence of phytosterols, followed by α -tocopherol and a very small effect of oleic acid. The upper concentration of co-solutes used was either within the range where each is all solubilized by the BS micelles (α -tocopherol and oleic acid), or above its saturation limit (phytosterols), in the latter case with coexistence of monomeric co-solute and crystals. The presence of palmitic acid in the micelles as co-solute enhanced cholesterol solubility.

In addition to the increase in cholesterol solubility accomplished by the BS micelles, cholesterol absorption in the intestine may also be affected by changes in the properties of the brush border membranes due to partition of BS to the membrane epithelial cells. This was addressed through the determination of the partition coefficient between the aqueous phase and model membranes with lipid compositions representative of biological membranes. From the results it is clear that the most hydrophobic BS partitioned more extensively to POPC and POPC/SpM/Chol (1:1:1) membranes than the most hydrophilic. Also, partition to this latter membrane was lower than to POPC. A more detailed analysis reveals that the general hydrophobicity of the BS is not the only relevant parameter as the partition coefficient of GCDCA is larger than that of GDCA. Additionally, partition to POPC/SpM/Chol (1:1:1) membranes was less favorable than to POPC.

Qualitative data was obtained for translocation in POPC membranes, showing faster values for the most hydrophilic BS, both conjugated and non conjugated BS. The translocation of BS through POPC/SpM/Chol (1:1:1) membranes showed to be faster for both BS measured (DCA and CDCA) as compared with POPC. The enthalpy variation upon BS partition to POPC bilayers (in liquid disordered phase) was negative, being positive for the partition into POPC/SpM/Chol (1:1:1) (with coexistence of liquid disordered and liquid ordered phases [1]). The establishment of the driving forces in the process of solubilization of hydrophobic solutes and BS partition to membranes can give important clues to understand the passive pathways in their absorption process in the intestine.

Resumo

O colesterol é uma molécula com diferentes funções desde estruturais a hormonais. Contudo, excesso de colesterol está relacionado com várias doenças como a aterosclerose e a doença do cálculo biliar. A absorção de colesterol ocorre ao nível do intestino. A compreensão dos mecanismos envolvidos na absorção do colesterol é relevante para a eficácia de estratégias que levem a uma diminuição da absorção de colesterol a partir do lúmen intestinal. Para o colesterol ser absorvido, devido à sua baixa solubilidade em água, precisa de ser previamente solubilizado em ácidos biliares (BS).

Neste trabalho, focamo-nos na compreensão de alguns princípios relacionados com a solubilização do colesterol pelos BS, bem como na interacção de BS com modelos membranares. Primeiramente, explorámos a solubilização do colesterol pelos ácidos glicodeoxicólico (GDCA), glicoquenodeoxicólico (GCDCA) e glicocólico (GCA) em micelas de misturas simples, binárias e ternárias, uma vez que estas são as mais prevalentes no lúmen intestinal. Os resultados mostraram que as micelas simples do BS mais hidrofóbico (GDCA) foram as que demonstraram maior capacidade de solubilização de colesterol, seguindo-se-lhes as de GCDCA e GCA. As 3 composições de micelas binárias, GCA/GCDCA (50:50), GCA/GDCA (50:50) e GCDCA/GDCA (50:50), e a micela ternária GCA/GCDCA/GDCA (37.5:37.5:25) apresentaram uma solubilização inferior à micela simples de GDCA mas superior à micela de GCA. Os resultados deste trabalho sugerem que as misturas de BS presentes no duodeno não estão optimizadas nem para a maior nem para a menor solubilização de colesterol; de facto, a capacidade de solubilização pode ser compreendida como um compromisso entre a entrega de colesterol às membranas e a sua excreção. Os resultados mostram uma correlação linear entre o colesterol solubilizado pelas micelas de BS e a concentração total de colesterol, até se atingir um patamar que corresponde ao índice de saturação de colesterol (CSI). Para além disto, a ocupação de esterol por micela depende do BS, sendo 1 para micelas de GDCA e inferior para as micelas de GCDCA e GCA. A interpretação destes resultados conduziu à compreensão da solubilização de colesterol como um fenómeno partição em vez de um mecanismo de ligação a um local disponível na micela. A solubilização será maior ou menor dependendo da partição do colesterol para a micela considerada. Uma vez atingido o limite de solubilidade não é possível solubilizar mais colesterol, mas tal não significa que a micela não possua capacidade de

solubilizar outras moléculas. A compreensão do fenómeno de solubilização pelas micelas na presença de vários co-solutos pode revelar informação pertinente no desenho de estratégias que levem a um decréscimo de solubilização e, portanto, a uma diminuição da absorção intestinal de colesterol. Com este objectivo em mente, foi averiguado o efeito do estigmaesterol e estigmaestanol (fitoesteróis), ácido palmítico (ácido gordo saturado), ácido oleico (ácido gordo insaturado) e α -tocoferol (vitamina) na solubilização do colesterol por micelas de BS. O maior efeito na diminuição da solubilidade do colesterol foi observado na presença de fitoesteróis, seguido pelo α -tocoferol e por um efeito muito reduzido na presença de ácido oleico. A concentração máxima de co-solutos usados pode englobar-se em dois regimes distintos, por um lado os co-solutos completamente solubilizados pelas micelas de BS (α -tocoferol e ácido oleico) e por outro lado co-solutos acima do seu limite de saturação (fitosteróis), apresentando coexistência de co-soluto monomérico e cristais. A presença de ácido palmítico nas micelas de ácido biliar resultou no aumento da solubilidade do colesterol.

Para além do aumento da solubilidade de colesterol mostrado pelas micelas de BS, a absorção de colesterol no intestino pode ser afectada por alterações nas propriedades da membrana intestinal. Isto foi determinado através da quantificação de coeficientes de partição entre a fase aquosa e modelos membranares com composições lipídicas representativas de membranas biológicas.

Os resultados mostram que BS mais hidrofóbicos particionam mais extensamente para as membranas de POPC e POPC/SpM/Chol (1:1:1) do que os mais hidrofílicos. Uma análise mais detalhada revela que a hidrofobicidade geral dos BS não é o único parâmetro relevante pois o coeficiente de partição do GCDCA é maior que o do GDCA. Ainda é de salientar que a partição para a membrana composta por POPC/SpM/Chol (1:1:1) foi menor do que a partição para a membrana de POPC. Resultados qualitativos para a translocação de BS quer conjugados quer não conjugados em membranas de POPC mostram que são os BS mais hidrofílicos que translocam mais rapidamente. A translocação de BS para membranas de POPC/SpM/Chol (1:1:1) apresentou-se mais rápida para ambos os BS medidos (DCA e CDCA) do que para membranas de POPC.

A variação de entalpia observada para a partição de BS para bicamadas lipídicas constituídas por POPC (fase líquido desordenado) foi negativa, sendo positiva para membranas de POPC/SpM/Chol (1:1:1) (coexistência de fase líquido ordenado/líquido desordenado [1]). O estabelecimento de forças motrizes no processo de solubilização de

solutos hidrofóbicos e partição de BS para membranas pode dar pistas importantes para perceber a difusão passiva no processo de absorção intestinal.

Nota: não se encontra escrito de acordo com as regras do novo acordo ortográfico.

List of abbreviations

Aggregation Number

AZ - Azulene

Azo - Azobenzene

BBB - Blood Brain Barrier

BBM - Brush Border Membrane

BS - Bile Salt

CE - Cholesterol Ester

Chol - Cholesterol

CL - Cardiolipin

CMC- Critical Micellar Concentration

CSA - Chemical Shift Analysis

CSI - Cholesterol Saturation Index

DAG - Diacylglycerol

DMM - Dietary Mixed Micelle

EPC - Egg Phosphatidylcholine

ESM - Egg Sphingomyelin

FA - Fatty Acid

GCA - Glycocholic acid

GCDCA - Glycochenodeoxycholic acid

GDCA - Glycodeoxycholic acid

GICA - Glycolithocholic acid

GICAS - Glycolithocholic sulphate

ITC - Isothermal Titration Calorimetry

L.S - Light Scattering

LPC - Lyso- Phosphatidylcholine

MAG - Monoacylglycerol

MDCK - Madin Darby Canine Kidney Cultured Epithelial Cells

NMR - Nuclear Magnetic Resonance

NMRSS - Resonance Spectral Shift

NOE - Nuclear Overhauser Effect

NPC1L1 - Nieman Peak C1 Like 1

OA - Oleic Acid

PA - Palmitic Acid

PC - Phosphatidylcholine

PE - Phosphatidylethanolamine

PI - Phosphatidylinositol

PL - Phospholipids

POPC - 1-Palmitoyl-2-Oleoyl-Sn-Glycero-3-Phosphocholine

PS - Phosphatidylserine

Pyr - Pyrene

RhSS- Rhodamine 6-G Spectral Shift

R-Radius

S.F.- Surface Tension

SpM - Sphingomyelin

T - Orange OT (1- O-Tolyl Azo-2-Naphthanol)

TAG - Triacylglycerol

TCA - Taurocholic acid

TCDC - Taurochenodeoxycholic acid

TDCA - Taurodeoxycholic acid

TG - Triglycerides

TLCA - Taurolithocholic acid

TICAS - Taurolithocholic sulphate

U.C. - Ultracentrifugation

UWL - Unstirred Water Layer

**Chapter I A Biophysics View on
Cholesterol Solubilization by Bile Salt Micelles:
Implications in the Intestinal Passive Absorption
Process**

I. 1 - Cholesterol in health and disease: strategies to decrease cholesterol absorption

Cholesterol is both vital and lethal for human beings. On one hand, cholesterol is a structural building block of membranes that maintains its integrity and rigidity. It is also the precursor of hormones and bile salts (BS) which are required for the solubilization of several hydrophobic molecules in intestinal lumen, including fatty acids (FA), cholesterol and vitamins, playing an important role to guarantee lipid homeostasis [2]. Cholesterol is also implicated in phase separation in biological membranes known as rafts which are described to be scaffolds for the function of several membrane proteins [3]. On the other hand, high cholesterol levels in blood are the main factor responsible for atherosclerosis, one of the major causes of cardiovascular diseases, and are also involved in the gallstone disease.

Several efforts have been made to decrease cholesterol absorption. On average in human adult, cholesterol absorption through the intestine is 1800 mg per day of which 1200 mg are linked with endogenous production and 600 mg are supplied from the diet. One of the strategies to decrease endogenous cholesterol production has been the use of statins. Statins is a drug blocking the endogenous production of cholesterol by inhibiting of the enzyme 3-Hydroxy-3-methylglutaryl-CoA synthetase involved in the conversion of 3-hydroxy-3-methylglutaryl-CoA into mevalonate, one of the steps of cholesterol biosynthesis.

Currently the process of cholesterol absorption is not completely elucidated. There are two main mechanisms explaining cholesterol absorption through intestinal epithelium, namely the passive diffusion and the mediated transport. There is strong evidence that both processes occur, but efforts should be done to clarify what is the effective contribution of each pathways to the overall process. This is not known as yet and a better understanding of cholesterol absorption process can lead to more effective strategies to decrease cholesterol absorption.

In the passive diffusion mechanism the highly hydrophobic cholesterol is solubilized in the intestinal lumen with the help of BS to bypass its low solubility. Once solubilized in the BS micelle, it can diffuse to the neighbourhood of the membrane and be delivered from the micelle to the membrane as an aqueous monomer. The monomer is then inserted in the membrane, translocating from the outer monolayer to the inner monolayer and delivered to the cytosol. This process is ruled by the cholesterol

Chapter I

diffusion from the lumen to the membranes through the unstirred water layer. The solubilization of cholesterol in BS micelles has been addressed by several research groups [4; 5; 6; 7; 8; 9], but some open questions still remain. The solubility of cholesterol in several simple mixtures of BS and also its dependence with lecithin content is known. From the literature, it is clear that more hydrophobic BS present higher solubilization of cholesterol and that solubilization of cholesterol increases with the presence of lecithin. The typical aggregates formed by these lipids depend on the ratio BS/lipid and are usually self aggregated as mixed micelles and mixed vesicles. They can also form crystals, one of the ways used to excrete cholesterol through the intestine. Cholesterol solubilization by BS micelles seems to be crucial for its absorption, contrary to FA which, as monomers, are more soluble in aqueous solution. Information gathered since more than sixties years shows that nowadays there are still puzzling questions regarding solubilization of cholesterol by BS micelles. BS present in intestinal lumen are mainly glycine conjugated BS with the following proportions: glycocholic acid (GCA) 37.5%, glycochenodeoxycholic acid (GCDCA) 37.5% and glycodeoxycholic acid (GDCA) 25%. It is not clear why this is the physiological proportion of BS and if any modification of it would involve an increase or a decrease of cholesterol solubility. Another question concerns the effect of the increase of cholesterol solubility and its meaning in terms of cholesterol absorption through the membrane. The effects of the presence of each BS in the micelles, and particularly the additive effects of each BS in their mixtures were never systematically investigated. It was assumed the mixture of BS behaves similarly to the average behaviour of single micelles. In some examples in literature focus was given to mixtures that could mimic the *in vivo* scenario but the understanding of the effect of mixing different BS was not addressed. This study can give a significant contribution to predict ways to avoid or enhance cholesterol solubilization in micelles. In fact, the mimesis of the physiological scenario *per se* gives only a quantitative answer of cholesterol solubilization in that particular environment, which will be a mixture of several effects making the system very hard to interpret. The idea is to understand which kind of synergies occurs between the most representative BS in the human lumen and what this result can tell us. If we have two BS with different affinities for cholesterol (i.e. different solubilizations) what would be the outcome in terms of cholesterol solubilization when we increase the proportion of one relatively to the other? Can we use this information to selectively avoid cholesterol solubilization? Does the mix of both BS gives ideal cholesterol

solubilization capacity? These questions are currently not answered in the literature and to look at the solubilization phenomena can bring new insights in the development of inhibitory cholesterol absorption strategies. The dependence of cholesterol solubilization and absorption on the BS composition can also be useful to interpret individual variations in their efficiency in cholesterol absorption. After the characterization of cholesterol solubilization in BS micelles with a robust experimental method, the next step will be to follow its partition into the membrane.

As previously mentioned cholesterol absorption can occur by passive diffusion or by mediated transport. The latter is dependent on proteins involved in cholesterol transport. One of these proteins is Nieman Peak C1 Like1 (NPC1L1) that has been described to be involved in transport of cholesterol from the lumen to the interior of intestinal epithelium. In the other hand ABC transporters are responsible for the efflux of cholesterol and also phytosterols. The inhibition of cholesterol transporters is another strategy to decrease cholesterol absorption. One very popular drug, usually used in combination with statins is Ezetemibe which has been considered an inhibitor of NPC1L1. However it is not known whether this drug affects the elastic properties of the membrane and by this way the efficiency of passive process. Therefore the inhibitory properties of this drug can be either due to inhibition of cholesterol carriers and/or change of membrane permeability.

Another strategy commonly used in a daily basis to reduce cholesterol absorption is the addition of phytosterols and esterified phytosterols to several food products consumed by humans. However the mechanism by which phytosterols induced a reduction of cholesterol absorption is not completely solved. One hypothesis is the physicochemical processes happening when cholesterol and phytosterols are together in intestinal lumen. The duodenum content is a complex mixture of BS, FA, phospholipids (PL) and monoacylglycerol (MAG) forming a structure called dietary mixed micelles (DMM) which solubilize cholesterol. If phytosterols are available in solution they can compete with cholesterol for solubilization in the dietary micelles, inhibiting in this way cholesterol absorption. Another proposed mechanism suggests the presence of phytosterols enhances cholesterol precipitation, leading to a decrease of cholesterol absorption due to its excretion in feces in a so called co-precipitation mechanism [10]. The ABC transporters are also involved in these mechanisms. This is mainly related with the fact that ABC transporters regurgitate both cholesterol and phytosterols [11; 12]. Once cholesterol and phytosterols are internalized through the apical membrane,

Chapter I

cholesterol is immediately esterified and carried upstream to be further processed to chylomicrons and enter in the blood stream. On the other hand phytosterols and some non-esterified cholesterol are effluxed by the ABC transporters. Sitosterolemia is a disease leading to the accumulation of phytosterols in enterocytes due to the malfunctioning of ABC transporters.

Like most hydrophobic molecules cholesterol needs the help of surfactants to increase its solubility in aqueous environment. The effect of different BS on this process has been extensively studied in the sixties but was mainly focused on the healing strategies for gallstone disease. The main interest was to maximize the dissolution of cholesterol gallstones which were mainly precipitated cholesterol with salts in the gallbladder. Because enterohepatic recirculation occurs, BS are reabsorbed in the intestine and delivered again to liver, being then deposited in the gallbladder. Consequently the strategy was to administrate BS with high solubilizing power and partition properties to decrease gallstones in gallbladder.

The paradigm can be thought the other way around, putting the focus on preventive absorption of cholesterol to avoid one of the most lethal human diseases in developed countries: atherosclerosis. In this case the operative solution is the minimization of cholesterol absorption, maximizing its precipitation in duodenum content and minimizing the solubilized cholesterol, being the cholesterol crystals excreted in feces. One approach to understand these complex phenomena can be to reduce the system complexity and to increase it back stepwise.

The study of cholesterol solubility in single component micelles of the most prevalent BS in duodenum content seems to be a reasonable starting point. Observation of the cholesterol solubilization while changing BS hydrophobicity in the mixed micelles can give hints on what is happening in the physiological scenario. Literature shows us that several attempts were made to reveal the significant physicochemistry underneath these processes. In this chapter we will investigate the work done on this topic as some drawbacks and unsolved questions. Studying the effect of mixing BS with different hydrophobicities and their effect on cholesterol solubilization can give us insights for strategies to decrease cholesterol absorption. Based on available data in literature a quantitative analysis is addressed to understand the effects of each components, namely BS, FA and PL in the different proportions studied. The action of phytosterols, unsaturated FA and other hydrophobic nutrients such as vitamins on cholesterol solubilization by the BS micelles is also subject to study. A clarification on

the mechanism of action, either co-precipitation or co-solubilization, can suggest us clearer strategies to decrease cholesterol solubilization and by this way decrease cholesterol intake. Once the main determinants for phytosterols action on the decrease of cholesterol solubilization are known, sterols with more effective inhibitory skills can be targeted. Again this could be done using a quantitative approach where the system variables are under control. In order to efficiently understand the effect of one component in the solubilization we need to characterize it in such way we observe only its effect and not the overall effect from several variables.

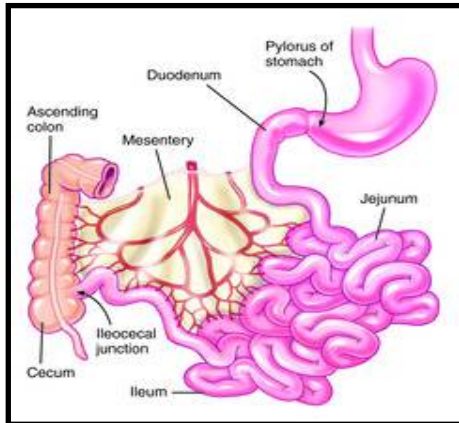
So far we mainly focused on solubilization of cholesterol and we also highlighted the mechanisms by which absorption of cholesterol can occur. As previously mentioned absorption of cholesterol occurs in intestinal epithelium. This epithelium is subjected to continuous contact with several molecules including PL, vitamins, FA and also the already mentioned BS. BS are known by their surfactant properties, meaning they have perturbing and destabilizing effects on membranes, even leading to their solubilization depending on Lipid/BS ratio. Although this continuous exposure can have harmful effects on the membrane, they have protective mechanisms against these agents, namely a structured area called water unstirred layer (UWL) composed by the glycocalyx behaving as a biological protective barrier. In cases of large changes in pH, which can occur in some diseases, the partition of BS into membranes can be a harmful health issue. Nevertheless the partition of BS into the membrane will lead to a change in its fluidity with potential effects on cholesterol passive diffusion. In this sense it is crucial to understand the effects of surfactants and other drugs used or present in the intestine as they can affect membrane permeability. This is even more problematic if the effect is not only directed for cholesterol but also for others essential nutrients and drugs. The partition coefficient of BS can help us to know the effective concentration of BS in the membrane and allows the understanding of their partitioning upon different BS hydrophobicities. This can be useful to elucidate which BS is more efficient to enhance cholesterol absorption. This understanding can have major implications in drug delivery design because BS can be thought as vehicles to carry molecules but also as enhancers for drug absorption. On the one hand BS can promote the absorption that should be prevented in case of cholesterol intake issues; on the other hand they can usefully promote drug delivery. Which BS are more effective and what should be their effective concentrations are the parameters that must be addressed.

Chapter I

Having introduced some general considerations about how to avoid cholesterol absorption and presented some strategies mainly focused on the understanding of solubilization prior to absorption, we will now review some basic knowledge starting with the morphology and physiology of the intestinal epithelium.

I. 2 - Morphology and physiology of intestinal epithelium

Absorption in intestine is the pathway taken by nutrients from intestinal lumen to blood and lymphatic system. The intestine is constituted by three anatomic units, namely duodenum, jejunum and ileum. The Figure I. 1 shows the anatomic structure of the small intestine and also some characteristic properties: diameter (d), length (l), exposed surface area (s) and the variation in pH (ΔpH) along each unit.



Anatomic unit	l (cm)	d (cm)	s (m ²)	ΔpH
Duodenum	25	5	~ 0.09	5-7
Jejunum	300	5	~ 60	6-7
Ileum	300	5	~ 60	7

Figure I. 1 Small intestine structure and some characteristics from the different anatomic units [13].

Morphologically the small intestine was built to maximize the absorption of nutrients making use of villi and microvilli (Figure I. 2). These structures increasing the surface area for absorption can be hundred times larger than the human body surface area.

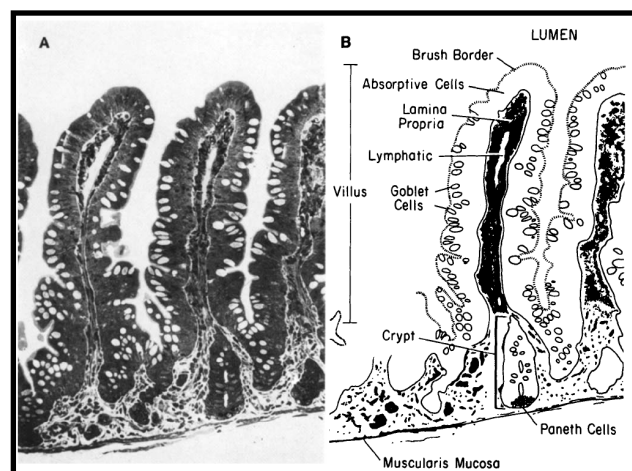


Figure I. 2 Light micrograph (A) and labelled tracing drawing (B) of small intestinal mucosal of monkey (source [14]).

Chapter I

Nutrients absorbed by intestine do not enter directly into the general circulation. First they go to the liver through the capillaries network present in the digestive tract being drained into the hepatic portal vein. The liver is the largest internal organ mainly constituted by hepatocytes cells, arranged into hepatic plates of two cells thick [15]. The bile is produced in the hepatocytes and then secreted into thin channels called bile canaliculi, localized in each plate, and is drained at the periphery of each lobule into the bile ducts. These bile ducts end up in hepatic ducts that carry the bile away in a separate route and in opposite directions of the blood stream. In addition to the regular components of bile that we will mention later, a wide variety of xenobiotics are secreted by the liver into the bile ducts. This is a major route of elimination of some drugs from blood stream, excreting them into the intestine and expelled by the feces. However some of these compounds released with the bile into the intestine are not excreted in the feces, but instead can be re-absorbed by the intestine and enter the portal vein. So they are re-cycled into the liver where they can be either re-secreted from the hepatocytes or undergo other treatments. This recirculation between liver and intestine is a process called enterohepatic circulation. Bile is continuously produced by the liver and is drained into the bile ducts and then into duodenum. When the small intestine is in fasted state, a sphincter at the end of the duct closes and forces the bile to enter cystic duct which converges into a saclike organ that stores bile, called gallbladder. This organ has a capacity of 30 to 100 mL. In the fed state the gallbladder contracts and expels the bile into cystic duct entering in the small intestine.

I. 3 - Properties of gastrointestinal tract (GIT)

The most gastrointestinal absorption, 99 %, is localized in jejunum and ileum. The pH in these intestine sections varies depending whether the organism is in fed or fasted state. In the fasted state the pH in stomach is around 1.7. Leaving stomach, the acidic mixture proceeds to duodenum, where it is neutralized by bicarbonate ions secreted by the pancreatic duct, resulting in pH increase to 4.6. Between the proximal jejunum and distal ileum the pH increases gradually from 6 to 8 what represents a considerable pH gradient along small intestine. While food can be retained in stomach from half an hour as long as 13 hours, the transit time on jejunum and ileum is only from 3 to 5 hours and from 7 to 20 hours in the colon. Thus, the absorption process in the intestine occurs during a period of 3-5 hours with a pH ranging from 4.5 to 8. The presence of food in the intestine boosts the segregation of bile acids from bile which will emulsify fat, mainly Chol, PL and FA in the so-called mixed bile salt micelles (MBS) or also dietary mixed micelles (DMM).

The first description of the luminal contents was done by Borgstrom [16; 17] describing the existence of three phases: an upper phase less dense, a middle phase presumed to be micellar and a precipitated phase (pellet). These phases are mainly composed by BS, Chol, PC, triacylglycerides (TAG), diacylglycerides (DAG), monoacylglycerides (MAG), cholesterol esters (CE) and FA. The most common BS present in human intestinal lumen are shown in Table I. 1 with their relative compositions (in mole percentage: mol%).

Table I. 1 BS commonly found in intestinal lumen contents of human beings [16].

BS species	mol%
GCA	24
GCDCA	24
GDCA	16
GLCA	0.7
GLCAS	3
TCA	12
TCDCA	12
TDCA	8
TLCA	0.3
TLCAS	1

Chapter I

These BS presented at Table I. 1 are mainly conjugated with taurine and glycine under the following names: GDCA, GCDCA, GCA, taurodeoxycholic acid (TDCA), taurocholic acid (TCA), taurochenodeoxycholic acid (TCDCA), glycolithocholic acid (GICA), glycolithocholic sulphate acid (GICAS), tauroolithocholic acid (TLCA) and tauroolithocholic sulphate (TICAS).

Composition and concentration of lipids present in duodenum were determined from duodenum aspiration and revealed several interesting results (Table I. 2). The most abundant lipids in duodenum are FA, TG, MG, DG and PL and are more soluble in the oil fraction than in the aqueous sub phase and oil/water interphase. Although some of these lipids present considerable concentration at the interface, their concentrations clearly decreases at the aqueous phase.

Data shows BS are the lipids having similar concentrations along the different phases, meaning they are equally soluble and suggesting their primary role in the absorption of hydrophobic molecules. Indeed, in their hydrophobic core, BS accommodate very low water soluble molecules what eases the transport of these molecules from the oil phase to the apical membrane of epithelium, therefore, increasing, their availability in the apical membrane of epithelium.

Values reported in Table I. 2 are commonly used as standard lipids concentrations to mimic DMM.

Table I. 2 Concentration of lipids found in duodenum contents according to fractions recovered from the chemical biopsies [18].

Fractions	[] mM								
	Chol	FA	MG	DG	TG	PL	BS	CE	CT
Unfractioned lipid compositions	2.4±2.0	20.4±14	5.4±4.5	7.3±6.3	34.6±44.5	4.8±1.8	14.5±8.8	0.2±0.4	89.4±62.2
Lipid composition of oils	29±22	801±468	145±54	18±24	371±169	80±72	9.9±6.5	6.5±5.4	1458±718
Lipid composition of interfaces	7.6±7.1	166±176	24.4±9	3.0±4.3	134±131	19.6±11.3	9.6±5.8	10.1±3.5	374±321
Lipid composition of subphases	0.77±1.6	9.3±7.4	2.8±2.9	0.1±0.2	0.06±0.2	3.2±2.5	13.1±10.8	0.01±0.03	29.4±19.7
Lipid composition of precipitates	4.4±2.2	86.5±37.4	12.9±6.0	5.3±2.9	2.3±1.6	8.3±7.3	5.0±2.1	n.d.	124.9±24.3
total	44.2	1083.2	190.5	33.7	542.0	115.9	52.1	16.8	2078.3

% of each component at intestinal duodenum	2.1	52.1	9.2	1.6	26.1	5.6	2.5	0.8
--	-----	------	-----	-----	------	-----	-----	-----

Chapter I

Prior to epithelial absorption, molecules have to cross the unstirred water layer (UWL), a mucus layer composed of proteoglycans coated with a structure named glycocalyx. Glycocalyx is composed of glycoproteins, digestive enzymes and oligosaccharides chains enriched in sialic acid, conferring it a negative charge character. The size of this layer ranges between 30 to 100 μm , what is 2 to 5 times the size of the brush border membrane (approximately 18 μm) [19]. Unlike intestinal lumen (pH 6.5), the UWL exhibits an acidic microclimate, pH 5.2, due to both the negative charge hindrance of sialic acid by protons and the low proton diffusion resulting from the more structured and viscous character of UWL [19]. Together size, composition and physicalchemical characteristics confer UWL a pivotal role in the process of absorption of hydrophobic molecules as will be explored (section I. 14). To the best of my knowledge, so far, the importance of UWL has been overlooked.

After crossing UWL, molecules reach the apical membrane of the epithelium. The intestinal epithelium is composed of enterocytes which are epithelial polarized cells, having the apical membrane in contact with the intestinal lumen, and by basolateral cells which are U shaped and in contact with lymphatic and blood vessels. It is worth to underline that molecules had faced pH change along the gastrointestinal tract (6 to 8), from lumen (6.5) to UWL (5.2) and again from UWL to the capillary network where pH is 7.4.

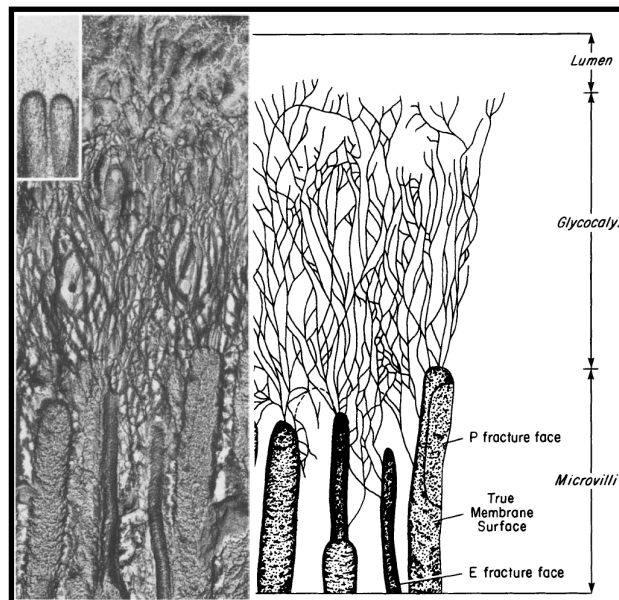


Figure I. 3 Electron micrographs (left and inset) and labelled trace illustration (right) of glycocalyx [14].

After crossing the apical membrane the molecule has to cross another unstirred layer localized in the cytosol which should be accounted when considering absorption across intestinal epithelium.

The lipid composition of several biological membranes is shown in Table I. 3. In the intestinal epithelium, the apical membrane is rich in cholesterol (Chol) and SpM whereas the basolateral is composed of POPC, Chol and SpM. Other lipids like PE, PS, and PI are also present in both membranes but more abundant in the basolateral.

Table I. 3 Lipid composition (%w/w) in biological membranes [19].

Lipid composition	BBM^a	MDCK^b	BBB^c
PC	20	22	18
PE	18	29	23
PS	6	15	14
PI	7	10	6
SpM	7	10	8
FA	-	1	3
CL	-	-	2
Chol+CE	37	10	26
TG	-	1	1
Negative/Zwitterionic lipid ratio	1:3.5	1:2.3	1:1.8

a) Reconstituted brush border membrane of rat b) Madin-Darby canine kidney cultured epithelial cells c) Blood brain barrier lipid model, RBE4 rat endothelial immortalized cell line

The plasma membrane of the brush border membrane shows high polarity and sizes from 10 to 11 nm larger than the average size of eukaryotic plasma membranes (7-9 nm) [19]. This is mainly assigned to the high Chol:PL and protein:lipid ratios [13].

Intestinal epithelium composition, in what respects to lipid composition of epithelial cells and pH changes along intestinal segments, UWL and blood stream, was just described. It's now time to detail knowledge about the solubilization of hydrophobic molecules in the intestine and their partition to membranes. At this point it is convenient to consider the different sources supplying cholesterol to intestine endothelial cells. Diet furnishes around 600 mg of cholesterol *per* day while the synthesized cholesterol is around 1200 mg [2]. Cholesterol delivered by the gallbladder can also have various sources. The main one is the endogenous synthesis of cholesterol in the liver. Another source is the cholesterol delivered from lipoproteins to the liver from peripheral tissues.

Chapter I

Cholesterol delivery and consumption is an excellent interplay between several mechanisms that enable proper supply and consumption. These mechanisms use BS as strategy for cholesterol excretion. This is achieved by converting cholesterol, a hydrophobic molecule, into BS which properties enable them to solubilize cholesterol itself. This shows to be a sophisticated system able to regulate, on the one hand, cholesterol excretion and on the other hand guarantee its intake.

From what has just been said it is clear that several phenomena are important to handle cholesterol homeostasis. In the next two sections we will highlight some concepts regarding self-assembly phenomena.

I. 4 - Self-Assembly of amphiphiles: Thermodynamic principles

Self aggregation of amphiphiles is a process occurring when the chemical potential of the aggregate is lower than the chemical potential of the monomer [20; 21]. Equilibrium between micelle and monomer is illustrated in Figure I. 4.

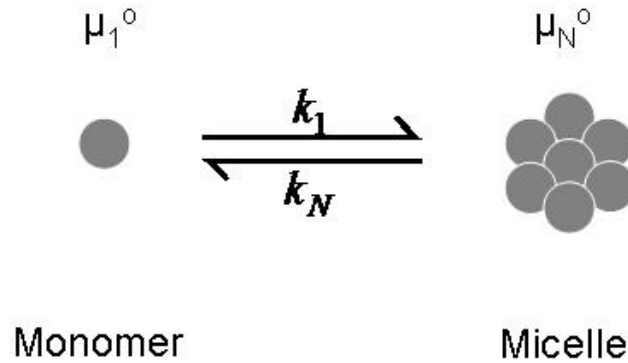


Figure I. 4 Parameters used for thermodynamic equations of the association of N monomers in an aggregate.

The chemical potential, μ_1 , associated to the monomer can be defined by the following equation,

$$\mu_1 = \mu_1^0 + RT \ln X_1 \quad \text{Equation I. 1}$$

where, μ_1^0 is the standard chemical potential for the monomer, X_1 the molar fraction of the monomer, R the gas constant and T the absolute temperature. By analogy the chemical potential, μ_N , associated to micelles with N monomers is defined as

$$\mu_N = \mu_N^0 + \frac{RT}{N} \ln \frac{X_N}{N} \quad \text{Equation I. 2}$$

where X_N is the molar fraction of amphiphiles incorporated in micelles. At equilibrium the chemical potential of the micelle must be equal to the chemical potential of the monomer, therefore

$$\mu_N^0 + \frac{RT}{N} \ln \frac{X_N}{N} = \mu_1^0 + RT \ln X_1 \quad \text{Equation I. 3}$$

From the mass law we can get the association and dissociation rate constants.

$$\text{rate of association} = k_1 X_1^N \quad \text{Equation I. 4}$$

$$\text{rate of dissociation} = k_N \frac{X_N}{N} \quad \text{Equation I. 5}$$

The ratio between association and dissociation defines the equilibrium constant (K)

$$K = \frac{k_1}{k_N} = \exp \left[-\frac{N (\mu_N^o - \mu_1^o)}{RT} \right] \quad \text{Equation I. 6}$$

Developing this equality provides the expression correlating the molar fraction of amphiphiles in an aggregate of N monomers with the molar fraction of a monomer:

$$X_N = N \left\{ X_1 \exp \left(\frac{\mu_N^o - \mu_1^o}{RT} \right) \right\}^N \quad \text{Equation I. 7}$$

Aggregation occurs only when there is a difference in the cohesive energies between molecules in the aggregated and monomer states. If molecules in aggregates and in monomers experience the same kind of interactions with their surroundings the value of chemical potential will be the same ($\mu_M^o = \mu_1^o$). In these conditions the Equation I. 7 can be simplified to,

$$X_N = NX_1^N \quad \text{Equation I. 8}$$

Therefore, if $X_1 < 1$ this indicates that molecules will be in the monomer state ($X_N \ll X_1$). The monomer state will also be favoured when μ_N^o increases with N. We can have a coexistence of several structurally different populations of aggregates within a single phase in thermodynamic equilibrium with each other. However, the necessary condition for the formation of stable aggregates remains that the chemical potential of the aggregate is lower than the chemical potential of the monomer ($\mu_N^o < \mu_1^o$).

There are three main contributions for the chemical potential of a molecule with an average superficial area (S) in an aggregate of N molecules which the origin is mainly related with interface attractive and repulsive events and bulk interaction. These contributions can be described by the following Equation I. 9.

$$\mu_N^o = \gamma S + \frac{C}{S} + H_N \quad \text{Equation I. 9}$$

The term γ refers to the attractive interfacial tension responsible for the stabilization of the interaction between interfaces of two liquids. The second term refers to the repulsive interactions including those geometric and electrostatic (S). Meanwhile there are some forces leading molecules to associate and other forcing them to be further apart. They are expressed in the Equation I. 9 by the constant C, C determining the optimal density of packing in the aggregate. The optimum value of S is given by the minimization of free energy relatively to the molecular surface area ($\frac{\mu_N^0}{dS}$), the molecular surface area being given by $S_0 = \sqrt{\frac{C}{\gamma}}$. The third term on equation is related to free energy of acyl chains, being responsible for the dependence of CMC with the increasing of acyl chain.

From what was just been said the formation of aggregates depend of different factors which can condition the formation of aggregates but also their shape. Aggregates can assume different shapes namely, spherical, distorted spheres (ellipsoids or globular), cylinders or bilayers. The most favourable geometry for the aggregate is dependent on the surface area (S_0), the length of acyl chain (l) and the volume occupied by the acyl chain (V). The packing parameter is therefore defined by $\frac{V}{lS_0}$ which can predict the type of aggregate more favoured for a defined set of molecules. If we consider a total area for a micelle of M molecules equal to MS_0 of radius r, and its volume equal to MV, the radius obtained is equal to $r = \frac{3V}{S_0}$, being the radius for the micelle inferior to the length of acyl chain. The packing parameter for the micelles is defined by the Equation I. 10.

$$\frac{V}{lS_0} \leq \frac{1}{3} \quad \text{Equation I. 10}$$

Figure I. 5 illustrates different type of structures that can be formed by amphiphiles in aqueous solution and their dependence with the critical packing parameter.

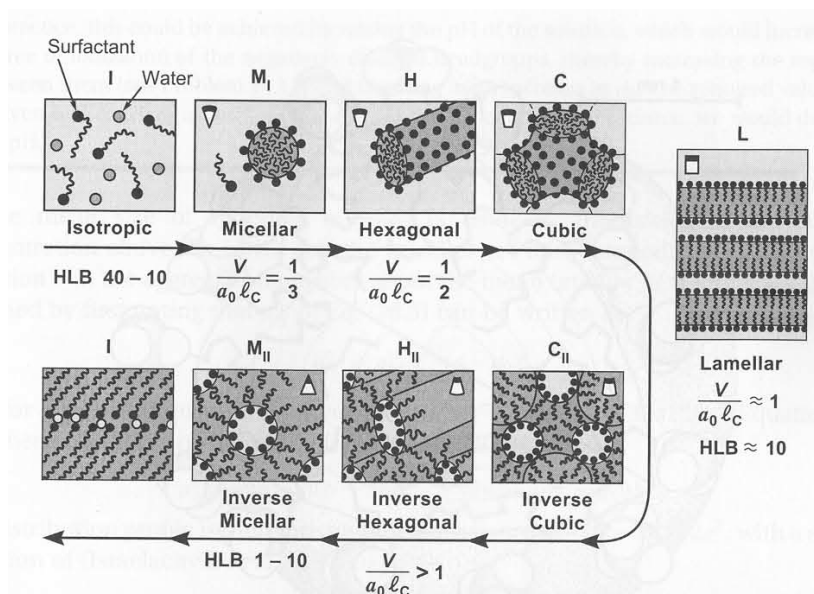


Figure I. 5 The different types of structure and “mesophases” formed by amphiphiles in aqueous solution depending on their packing parameter. Isotropic solutions of monomers are illustrated and additionally, M for micellar, H hexagonal (cylindrical), C for cubic (usually isotropically interconnected) and L for lamellar. The subscripts I and II stand for normal and inverted (aqueous core) structures. HLB is the Hydrophile-Lipophile balance [21].

I. 5 - Mixed Micelles

Mixed micelles are micellar solutions composed of more than one component. The mixture of two surfactants in a solution is a typical example of a mixed micelle. The mixture of two surfactants is said ideal when there is no net interaction between the two species. To well predict the CMC of a mixed micelle composed of two surfactants we need to use the definition of chemical potential described in the above section. Assuming a generic aggregate type, with a concentration, C_i , the chemical potential can be defined as

$$\mu_i = \mu_i^0 + RT \ln C_i \quad \text{Equation I. 11}$$

considering that at critical micellar concentration, $C_i = x_i CMC$. Therefore the chemical potential of the surfactant is given by

$$\mu_i = \mu_i^0 + RT \ln x_i CMC \quad \text{Equation I. 12}$$

and in similar manner the chemical potential of component i in the mixed micelle (mm) is given by,

$$\mu_{i,mm} = \mu_{i,mm}^0 + RT \ln C_i = \mu_{i,mm}^0 + RT \ln CMC x_i^{mm} \quad \text{Equation I. 13}$$

where x_i^{mm} is the mole fraction of the i^{th} component in the mixed micelle and $\mu_{i,mm}^0$ is the chemical potential of component i in the reference state. If only a single specie exists in solution then $x_i^{mm} = 1$, $\mu_i = \mu_{i,mm}$ and $\mu_i^0 = \mu_{i,mm}^0$. Chemical potential of component i in the solution is the same than in the micelle at equilibrium and CMC value from mixed micelle can be predicted by

$$\frac{1}{CMC} = \sum \frac{x_i}{CMC_i} \quad \text{Equation I. 14}$$

when insoluble lipids are incorporated into simple micelles they also form mixed micelles and the process of incorporation is called solubilization.

The mixed micelles with BS can be divided in four main categories, A - mixed micelles with nonpolar hydrocarbons; B - insoluble nonswelling amphiphilic lipids; C - insoluble swelling amphiphilic lipids; and D - soluble amphiphilic lipids. The first class of mixed micelles is not physiological relevant. On contrary the other classes of

Chapter I

micelles are very relevant for the understanding of solubilization and absorption phenomena of hydrophobic molecules ranging from vital nutrients to xenobiotics. Example of mixed micelles with nonswelling lipids is the cholesterol BS micelles, and also their interaction with nonswelling amphiphiles like palmitic acid, oleic acid, phytosterols and tocopherol. Regarding the insoluble swelling amphiphilic class of mixed micelles, BS-lecithin micelles are the canonical example.

After the introduction of the self-assembly of amphiphiles, some of these relevant features will be described considering the BS and their primordial role in the cholesterol solubilization process. Thus the coming section will focus on the state of knowledge about the BS structure, diversity, function and physicochemical parameters.

I. 6 - Bile salts structure, diversity and function

Bile salts are biological ‘detergents’ while they can be classified as surfactants. Surfactants come from the agglutination of the words surface active agents, which highlights the main action of surfactants at an interface: they reduce the surface tension at the surface between two phases. Detergents are characterized by an amphiphilic nature which enables them to have a part liking non aqueous environments (hydrophobic) and another part liking aqueous hydrophilic molecules. Their main function in an *in vivo* scenario is to increase the solubility of hydrophobic molecules in aqueous environments. They are atypical surfactants in the sense they are not constituted by a hydrophobic alkyl chain and a polar head group, but instead two faces (hydrophilic-convex and hydrophobic- concave) equatorial segmented. The most common structures of the BS found in humans are presented in Figure I. 6.

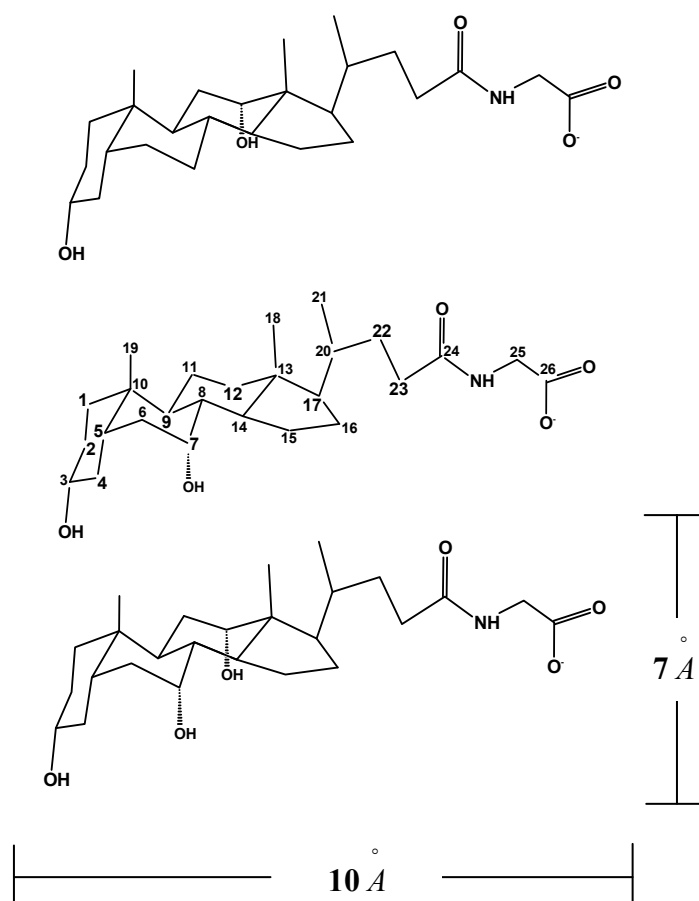


Figure I. 6 Structures of the most common bile salts found in humans: GDCA (top), GCDCA (middle) and GCA (bottom).

GDCA and GCDCA have both two hydroxyl groups, respectively placed on carbons 3 and 12, and on carbons 7 and 12. GCA has an additional hydroxyl group, being a trihydroxy bile salt. Solubility as a monomer in aqueous solution is considerably higher when compared to cholesterol or lecithin solubilities. The presence of hydroxyl groups gives them a more hydrophilic character, which allows them to be soluble in the monomer state in the millimolar range. The cholesterol and lecithin are soluble as monomers from the nanomolar to micromolar range. The CMC, which is the concentration where aggregation starts, is higher for the trihydroxy BS. Unconjugated BS are not usually found in human bile, because they have a pKa of approximately 6, at the pH range values found in duodenum such pKa can lead to some precipitation in the acidic form (at some extremes it forms a gel). Conjugation of BS with glycine or taurine lowers their pKa and enables them to be in the ionized form at the broad range of pH occurring in the intestine (pH ranging from 6 to 8). The conjugation with glycine or taurine is the most prevalent and leads to an elongation and increase of the polarity of side chain [22]. The characterization of several BS properties like pKa, CMC and their dependence to pH, ionic force and temperature have been extensively described in literature. The next section intends to present a review on the fundamental knowledge obtained by others. Whenever relevant, systematization is done in tables. Several physicochemical characteristics of unconjugated and conjugated BS are presented in Table I. 4. The CMC is strongly influenced by the number of hydroxyl groups. The trihydroxy BS display a greater aqueous solubility as a monomer than the dihydroxy BS. Considering the dihydroxy BS, GDCA shows a higher solubility than GCDCA. It should be emphasized that depending on the pH and ionic force used, values of CMC will be quite different. The pKa can also vary depending whether if the BS is in solution, in membrane or other hydrophobic environment. Data shows a pKa increase with the increase of BS concentration. Before reaching the CMC the pKa show a lower value than compared with a concentration above the CMC [23]. One common approach to measure the pKa was potentiometry, another was to follow carboxyl ¹³C NMR chemical shift dependence on pH being very sensitive to the environment of the bile salt and on its ionization state. The pKa of cholic acid can vary from 4.6 as a monomer in solution to 6.8 if inserted in egg-PC vesicles [24]. The ionization behaviour of BS in different environments is certainly important because bile salts secreted by the duodenum can find environments where large changes in pH (5 to 8) occur, and can vary upon partition to membranes.

Table I. 4 Physicochemical properties of non-conjugated and conjugated BS.

BS	CMC (mM)								R at CMC Å	̄A		pH	T °C	
	dye titration				S.T.	L.S	ITC	Spectral shift		U.C.	L.S.			
	OT	AZ	Pyr	Azo				RhSS						RMNSS
DCA	8.0 ^[25]	10.0 ^[25]			6.0 ^[25; 26]							8	n.d.	
			2.4 ^[27]									n.d.	35	
										13 ^[9]		8-9	36	
										15 ^[9]		8-9	20	
CDCA	4.0 ^[9; 25]	5.0 ^[25]			4.0 ^[25; 26]							8	n.d.	
										11 ^[9]		8-9	36	
										11 ^[9]		8-9	20	
					2.0 ^[25]	3.2 ^[28]		1.5 ^[25]		12 ^[28]	5 ^[28]	10	37	
CA			3.0 ^[27]									n.d.	35	
	16.0 ^[25]	14.0 ^[25]			11.0 ^[25]							8	n.d.	
							9.4 ^[29]					7.4	37	
										5 ^[9]		8-9	36	
GDCA										5 ^[9]		8-9	20	
			6.2 ^[27]									n.d.	35	
	2.2 ^[25]	3.0 ^[25]			2.0 ^[25]							8	n.d.	
			1.2 ^[30]									7.5	35	
GCDCA				1.9 ^[25]								6.3	37	
						1.1 ^[25; 26]						6.0	37	
							2.0 ^[29]					7.4	37	
											16 ^[9]	8-9	36	
GCA												19 ^[9]	8-9	20
	2.0 ^[25]				1.8 ^[25; 26]							8	n.d.	
				2.4 ^[25]								6.3	37	
							2.2 ^[29]					7.4	37	
GCDCA								1.1 ^[25; 26]		17 ^[9]	13 ^[9]	10	37	
											18 ^[9]	8-9	36	
											20 ^[9]	8-9	20	
GCA	9 ^[25]	10.0 ^[25]			1.0 ^[25; 26]							8	n.d.	
			4.0 ^[30]									7.5	35	
							8.5 ^[29]					7.4	37	
										6 ^[9]		8-9	36	
TDCA										6 ^[9]		8-9	20	
	3.0 ^[25]	6.0 ^[25]			2.4 ^[25; 26]							8	n.d.	
			1.1 ^[30]									7.5	35	
				1.9 ^[25; 26]								6.3	37	
TDCA							1.8 ^[29]					7.4	37	
								1.2 ^[25; 26]				22 ^[9]	7.0	37
										18 ^[9]		8-9	36	
TCDCA	4.0 ^[25]	7.0 ^[25]			2.8 ^[25; 26]							8	n.d.	
				2.5 ^[25; 26]								6.3	37	
							2.0 ^[29]					7.4	37	
								2.8 ^[31]				n.d.	n.d.	
TCA									17.5 ^[28]			7.0	37	
										16 ^[9]		8-9	36	
	9.0 ^[25]	4.0 ^[25]			6.0 ^[25; 26]							8	n.d.	
			2.0 ^[30]									7.5	35	
TCA							7.6 ^[29]					7.4	37	
								4.0 ^[25; 26]				n.d.	20	
										5 ^[9]		8-9	36	

Chapter I

T- orange OT(1- O-tolyl azo-2-naphthanol), AZ- azulene, Azo- azobenzene, Pyr- pyrene. L.S.- light scattering, U.C.- ultracentrifugation, ITC- isothermal titration calorimetry, RhSS- rohdamine 6-G spectral shift, NMRSS- resonance spectral shift, S.T.- surface tension R- radius \bar{A} - aggregation number, n.d.- not defined

The numbers of monomers per micelle depend on the BS hydrophobicities. The general rule is that more hydrophilic BS have a lower aggregation number. The aggregation can also be dependent on the ionic strength and temperature used. The aggregation number (size) of BS micelles increases at lower temperature and higher ionic strengths. It is also observed that non conjugated BS have lower values of aggregation number.

Had explored the physicochemistry parameters of micelles of BS is time to describe what happen when BS are in the presence of other lipids with relevance for the solubilization process at intestinal lumen.

I. 7 - Solubilization processes in the intestinal lumen

I. 7. 1 - Cholesterol solubility limit in BS micelles: BS-insoluble amphiphiles mixed micelles type

Mechanism for the solubilization of cholesterol in micelles is not yet understood. If the incorporation of cholesterol molecules in the micelle is faster than the diffusion of micelle itself to the cholesterol we are facing a diffusion controlled process (solubilization). Otherwise if the incorporation of cholesterol in the micelle is slower than the diffusion of micelle in the vicinity of cholesterol we are facing a non-diffusion controlled process, in the so called chemically controlled reactions. The dissolution of cholesterol monohydrate is a non-diffusion controlled process [32].

A review of the literature shows some studies on solubilization of cholesterol through simple BS micelles. Some available information on solubilization of cholesterol by BS is shown in the Table I. 5. Depending on the method used, ionic force and pH, values can be quite different. In fact most of these results are obtained with filtrations or chromatographies techniques which are invasive. These methods can perturb the equilibrium between crystal precipitate phase and aqueous BS micelles phase explaining some differences between some experimental results. Methods differentiating micellized cholesterol from crystals of cholesterol in solution of BS micelles would be very straightforward, and NMR spectroscopy is good candidate for such study (see Chapter III). The results of solubilization between different experimental settings are sometimes difficult to compare due to the use of different concentrations of BS. To better compare them one strategy is to use the amount of sterol per micelle that is shown in the Table I. 5. This is given by the highest concentration of cholesterol solubilized (Cholesterol Saturation Limit-CSI) divided by the concentration of micelles. The concentration of micelles is given by the difference of BS concentration and the CMC divided by the aggregation number.

Table I. 5 Cholesterol saturation limit in BS micelles, CMC, aggregation numbers.

BS	[Chol] (mM)	[BS] (mM)	\bar{A}	CMC (mM)	[BS] micellar (mM)	chol per micelle	T (°C)	pH	[NaCl] (mM)	Ref.
DCA	6.1	100	15	1.0	6.6	0.9	37	10.0	150	[32]
	3.0	60	11	3.4	5.1	0.6	35	7.5	150	[30]
CDCA	12.1	240.0	5	2.0	47.6	0.3	37	10.0	150	[28]
CA	0.6	60.0	13	6.3	4.1	0.1	35	7.8	100	[33]
UDCA	0.8	240.0	5	5.5	46.9	0.02	37	10.0	150	[28]
	0.3	100.0	5	5.5	18.9	0.02	37	10.0	150	[32]
GDCA	3.3	60.0	16	1.2	3.7	0.9	35	7.5	150	[30]
	10.0	200.0	16	1.2	12.7	0.8	37	7.0	n.d.	[34]
GCDCA	5.4	240.0	13	1.1	18.4	0.3	37	10.0	150	[28]
	2.2	100.0	13	1.1	7.6	0.3	37	10.0	150	[32]
	6.0	200.0	13	1.1	15.3	0.4	37	7.0	n.d.	[34]
GCA	1.0	60.0	6	4.0	9.3	0.1	35	7.5	150	[30]
	6.0	200.0	6	4.0	32.7	0.2	37	7.0	n.d.	[34]
GUDCA	0.65	240	13	1.7	18.3	0.04	37	10.0	150	[28]
	0.2	100.0	13	1.7	7.6	0.03	37	10.0	150	[32]
TDCA	9.0	200.0	16	1.1	12.5	0.7	37	7.0	n.d.	[34]
TCDCA	3.32	240	15	2.2	15.9	0.2	37	7.0	150	[28]
	2.2	60	16	1.1	3.7	0.6	37	7.0	150	[28]
	1.5	100	15	2	6.5	0.2	37	10.0	150	[32]
TCA	0.6	60	6	2	9.7	0.06	35	7.5	150	[30]
TUDCA	0.37	240	17	1.3	14.0	0.03	37	7.0	150	[28]
	0.13	100	17	1.3	5.8	0.02	37	10.0	150	[32]

The data shown in Table I. 5 clearly shows that the most hydrophobic BS have a higher solubilizing capacity. This is true for non-conjugated as for conjugated BS. It is also needful to keep in mind that pH has a considerable influence in solubilization capacity of micelles to cholesterol. If the pH is lower than the pKa of the BS there will be presence in solution of the acidic form of the BS. Because this protonated specie is less soluble in aqueous environment than the ionized one, once in solution it will compete for a place in the micelle. This will have influence not only in the CMC of BS but also affects the solubilization of cholesterol decreasing drastically the solubilized sterol. The ionic strength can also affect the solubilization of cholesterol in a canonical away. The increase of ions in solution will decrease repulsion between BS, enhancing the solubilizing power of the micelles [35]. Higher temperature also increases the solubilizing power of BS micelles for cholesterol. Although consequent work done on

solubilization of cholesterol by BS micelles, no one tried to understand the effect of binary mixtures in this process while this could give clues on the solubilization process by mixed BS systems. Although these *in vivo* systems are quite complex they can be reduced to the three most common species conjugated with glycine in the following proportions (GCA 37.5 %, GCDCA 37.5% and GDCA 25%). The first one is the one that has three hydroxyl groups and is solubilizing the less cholesterol. This can be probably explained by the highest solubility in water characterized by the higher CMC [30], being this micelles less hydrophobic than the micelles composed only by two hydroxyl groups. This could be an explanation for the phenomena but comparing both of the dihydroxy BS, they show a very different solubility capacities while similar CMC. This seems to be related with the hydroxyl position at carbon position 12 of sterol backbone of BS (Figure I. 5). Aggregation numbers for GCA seem to be much lower than the ones of GCDCA and GDCA.

The type of relations that these BS have with each other *in vivo* is not completely clear. The reason behind the variability of BS and the type of synergies occurring between them seem to be interesting starting points on the way to the understanding of cholesterol solubilization in the intestinal lumen

Some published works characterized these systems but it usually approached using the BS more representative. The main conclusion is that the solubility power of BS mixture is ruled by the BS solubilizing less cholesterol [34], being the behaviour similar to the GCA and GCDCA solubilizing capacities. The system is not optimized to solubilize the highest quantity of cholesterol, which is consistent with the main role of BS to be a pathway for cholesterol excretion. Even so, physiology selected BS with different solubilities for cholesterol. The question is why? An investigation on the properties of binary and ternary mixtures of different BS could give some clues regarding this question (Chapter IV). Moreover the study of these systems can lead to a better knowledge on strategies to decrease cholesterol absorption by reducing the available cholesterol in the micelles. We have just reviewed in this section the effects of an insoluble amphiphile (cholesterol) in BS micelles. It should be by now realized that other amphiphiles are in action at intestinal lumen. Among them is lecithin, a phospholipid that once in aqueous environment become swollen and form vesicles (liquid crystal phase). The coming section will now review all the known aspects of the solubilization of lecithins with BS.

I. 7. 2 - BS-swelling amphiphiles mixed micelles type

Some of the most abundant lipids in lumen contents are phospholipids (PL). PL are known by their swelling properties and by their tendency to form liquid crystal phases. Depending on the lipid/BS ratio three scenarios can happen: 1- mixed micelles coexisting with simple micelles; 2- only mixed micelles; 3- only bilayers. The Figure I. 7 shows a phase diagram obtained for the taurocholate-lecithin system at 20 °C.

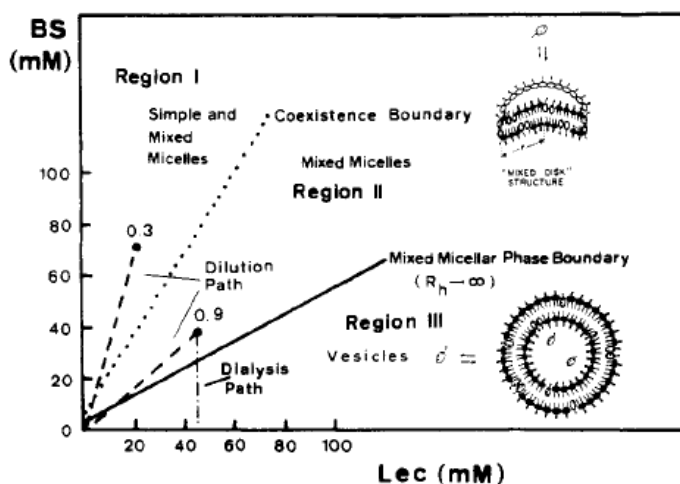


Figure I. 7 Phase diagram for taurocholate-lecithin system at 20 °C [36].

The determination of these structures is normally achieved using dynamic light scattering and transmission electron microscopy to obtain the different aggregates sizes. Diluting a mixture in the region I or II of the phase diagram depicted in Figure I. 7, shows that both coexistence boundaries can be crossed, with eventual divergence on aggregates composition and shape, at the phase limit. Upon further dilution the system is gradually transformed into unilamellar vesicles. The hydrodynamic radius increases upon dilution, contrary to what is observed in simple BS systems, where the size of micelles tend to decrease upon dilution [37]. The concept of intermixed bile salt concentration is very important when diluting these samples without changing the size of the micelles. At low lecithin/BS ratio mostly simple micelles exist with very sparse mixed micelles. The mixed micelles become dominant when an increase in the Lecithin/BS ratio occurs and the simple micelles population decreases due to the increase of BS in the lipid-BS micelles. This will happen until a coexistence boundary above which the solubilization of more lipid requests a reorganization of the micellar

size and structure. The mixed micelles of lecithin-BS are described by two models, the Small and the Mixed Disc Model (Figure I. 8).

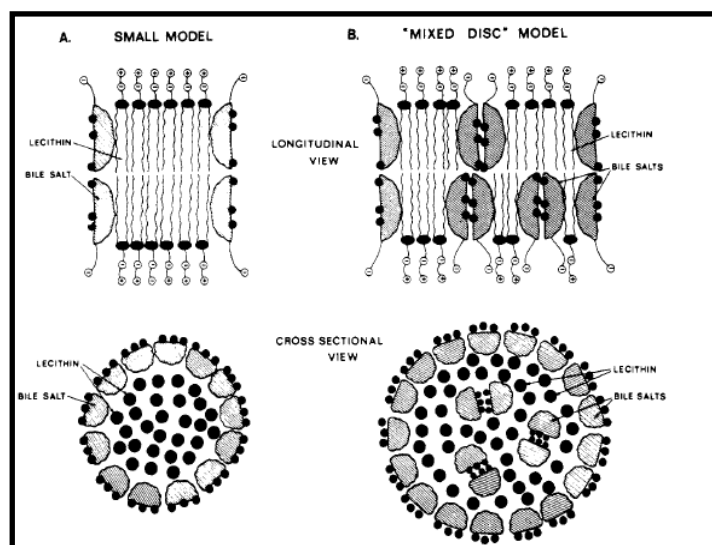


Figure I. 8 Schematic models for the structure of the bile salt-lecithin mixed micelle, shown in longitudinal and cross sectional view [37].

There are some differences between both models. In one hand the Small model consists of a lecithin bilayer disc surrounded by the BS, with their hydrophilic face exposed to water and the hydrophobic face in contact with alkyl chains of phospholipids. On other hand the Mixed Disc Model introduces some higher order of complexity, namely assuming BS are not only in the perimeter but also incrustrated has hydrogen bonded dimers in the lecithin discs. This second model is better accepted because it can fit well the behaviour of the hydrodynamic radius dependence on lipid/BS ratio. As lipid/BS ratio is increased there are huge changes in the self aggregate forms obtained. The mean hydrodynamic radius grows extremely at increasing lipid/BS ratio because initially there are micelles mixed with lecithin, but at some point a rich domain of lecithin is formed (liquid crystal phase). This different self-aggregated species have very important solubilization functions in intestinal lumen. This is the strategy used to solubilize several hydrophobic nutrients that otherwise would not be accessible for absorption at the membrane. The intestinal lumen composition is a very complex mixture where PL, BS and cholesterol join together. The coming section will revisit some of the properties of this mixture.

I. 7. 3 - BS-swelling amphiphiles (lecithin) and cholesterol

Precipitation of cholesterol is a phenomena associated since a long time with gallstone disease [38]. The development of this disease is related with the phase equilibrium between the different intervenients in the gallbladder, namely cholesterol, BS and PL. These systems were extensively studied in the past and some interesting knowledge was obtained. The Figure I. 9 shows the ternary phase diagram obtained for taurocholic acid, lecithin and cholesterol.

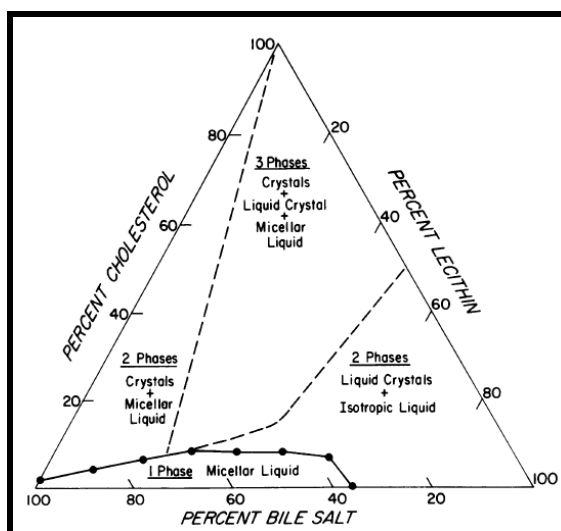


Figure I. 9 Triangular phase diagram showing the physical state of all combinations of NaTC, lecithin, cholesterol as 20-g/dL solutions in 0.15 M NaCl at 24 °C [35].

The ternary phase diagram BS – phospholipid - cholesterol shows a one phase zone constituted only by micelles, a left two-phase zone with micelles and cholesterol crystals, a central three-phase zone where micelles, vesicles and cholesterol crystals cohabit and a right two-phase zone with micelles and vesicles. From the studies of the phase diagram (Lecithin, Cholesterol, BS) considering higher proportions of BS and $\frac{\text{lecithin}}{(\text{lecithin} + \text{BS})} < 0.2$, it was observed that crystals precipitate at higher rates and various forms of anhydrous cholesterol were present (needles arcs, spirals or tubules), as can be seen in Figure I. 10. Increasing contribution of lecithin showed a decrease in precipitation rates of cholesterol with the predominant formation of cholesterol monohydrate crystals. These crystals have shown to be solubilized by BS micelles

slower than the anhydrous cholesterol form [35]. When reaching some limit of lecithin, cholesterol precipitation as crystals vanishes and cholesterol starts to be completely soluble in vesicles. The dependence of these processes on the hydrophilicity of the BS showed that the most hydrophilic BS have lower capacity to solubilize cholesterol precipitates, reducing the zone of one micellar phase.

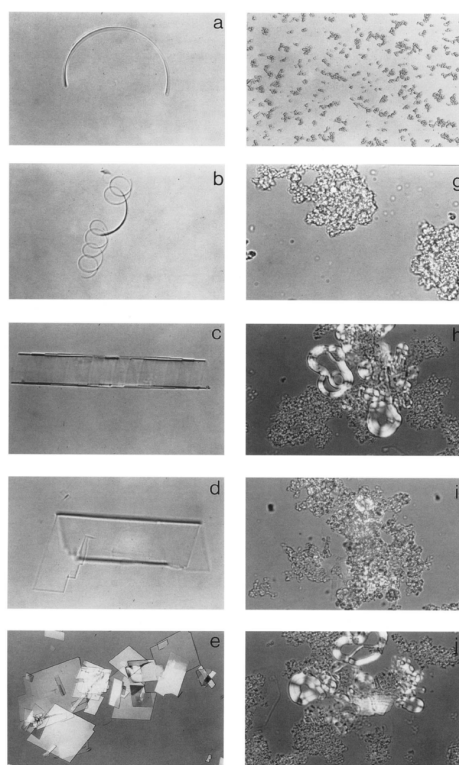


Figure I. 10 Habits of solid and liquid crystals of Chol observed by polarizing light microscopy: a) arc-like crystal; b) irregular right-handed helical crystal; c) tubular crystal with helical stripes; d) tube-like crystal fracturing at ends to produce plate-like Chol monohydrate crystals; e) typical Chol Monohydrate crystals, with 79.2° and 100.8° , and often a notched corner; f) small non birefringent liquid crystal (labeled small); g) aggregated non birefringent liquid crystal (labeled aggregated); h) typical fused liquid crystals (labeled fused) with Maltese-cross birefringence and focal conic textures; i) Chol monohydrate crystals emerging from an aggregated liquid crystal; j) same, from fused liquid crystals. Magnifications x 800 [35].

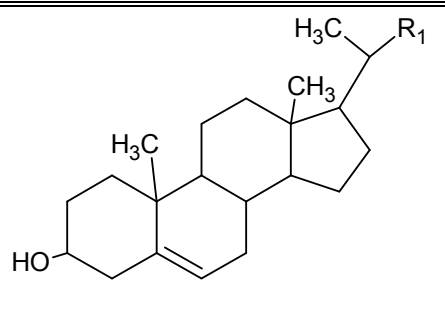
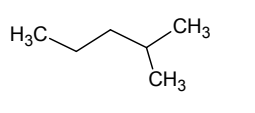
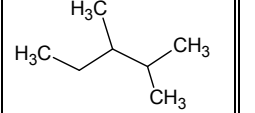
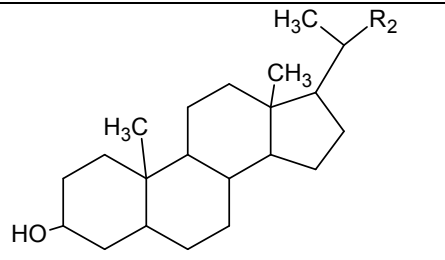
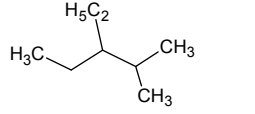
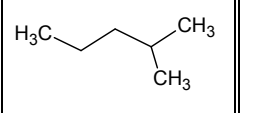
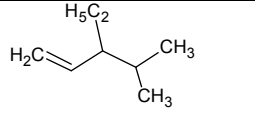
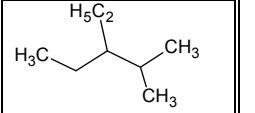
Intestinal lumen has a mixture of aggregates responsible for the solubilization of several hydrophobic molecules. Lecithin was shown to clearly increase the cholesterol solubility. However, there are other compounds that can affect solubilization of cholesterol. One of the most known and effective compounds are the phytosterols.

I. 7. 4 - *Phytosterols so similar but so different from cholesterol*

Sterols and stanols from vegetal origin, usually referred as phytosterols (the term will be used from now on to describe both classes) are known by their inhibiting capacities of cholesterol absorption in the intestine.

Some intriguing questions arise when considering the structures of the most common phytosterols. Some of them are quite similar to cholesterol and only small changes are noticed in the side chain, staying the backbone similar to cholesterol. Some of the most common phytosterol are illustrated in Table I. 6. The daily intake of phytosterols ranges from 150 - 400 mg/day with 65% intake of β -sitosterol, 30% of campesterol and 5 % of stigmasterol [39].

Table I. 6 Molecular structures of sterols and stanols.

Sterol		R ₁ Cholesterol	R ₁ Campesterol
			
Stanol		R ₁ Sitosterol	R ₂ Cholastanol
			
		R ₁ Stigmasterol	R ₂ Sitostanol
			

The aqueous solubility of these phytosterols is also very low as monomer, being in the nanomolar range [40], similar to cholesterol. Above this concentration they precipitate as well as cholesterol. Currently two mechanisms explain how sterols of vegetal origin can inhibit cholesterol absorption. In one hand, phytosterols compete for solubilization in the micelle formed by the BS molecules, FA and PL. Therefore a co-solubilization mechanism can occur between the sterol and the cholesterol. If cholesterol and sterol have the same affinity or similar affinities for the micelle, there will be less cholesterol solubilized due to the presence of phytosterols. In the presence

of similar amounts of cholesterol and phytosterols a fraction of each of them will be solubilized in the micelles. Consequently less cholesterol is solubilized in a phenomenon that can be understood as dilution of cholesterol by other sterol. On the other hand a co-precipitation mechanism can also explain the decrease of cholesterol absorption. In this mechanism phytosterols enhance precipitation of cholesterol by decreasing its solubility in water, preferring to be mostly in a crystal aggregate than in the micelle content. This will lead to a decrease in the available cholesterol to be absorbed because is no longer soluble, instead is aggregated in sterol precipitate crystals. Another possible scenario is that both processes can happen. Several published works account the effects of phytosterols on the cholesterol solubilization. Most of them use a mixture of different components, PL, FA, BS, cholesterol and phytosterols. Usually the idea is to use a system that can better mimic the *in vivo* scenario [16]. In such a complex mixture it is possible to lose information about particular properties of the involved compounds during solubilization. Keeping this in mind we will present a review starting with simple systems and increasing the complexity of the mixtures. The simplest system studied is a simple mixture using one BS and one sterol. The information collected for the solubilization of sterols in simple BS micelles is presented in Table I. 7. From these results, cholesterol solubilization in simple BS micelles is always higher than the most common phytosterols. This happens not only for taurine conjugated BS but also for glycine conjugated BS [8]. The solubility of cholesterol and phytosterols alone in TCA BS decreases when compared with its homologous glycine conjugated BS. Comparing the taurine conjugated BS, there is a decrease of solubility of phytosterols with the increase of hydrophilicity of BS. The same happens with cholesterol. The solubilization of stigmasterol appears in some systems with higher solubility than sitosterol in GDCA [41].

Results presented in Table I. 7 show that the values obtained for cholesterol solubilization can be quite different between different reports. The introduction of phytosterols in the systems with cholesterol and a BS leads to a decrease of cholesterol solubility. From those results, the most effective phytosterols for reduction of cholesterol solubility are sitostanol (44 %) and sitosterol (44%), while stigmasterol (22%) is the less effective the. These results from less complex micelles could help the understanding of more complex systems.

Table I. 7 Solubility of cholesterol and phytosterols in simple BS micelles and of cholesterol in binary systems (BS micelles plus cholesterol/phytosterols in proportion 1:1).

	BS species	Sterol composition	T(°C)	pH	[BS] mM	[Sterol] solubilized	ref	
						mM		
Single BS	GCA	chol	37	7	50	1.57	[23]	
	GCDCA	chol	37	10	100	2.20	[19]	
		chol	37	7	50	1.89	[23]	
	GDCA	chol	37	7	50	3.08	[23]	
		chol	24	10	50	2.20	[32]	
		sitosterol	24	10	50	0.31	[32]	
	GDCA	stigmasterol	24	10	50	0.94	[32]	
		GUDCA	chol	37	10	100	0.13	[19]
			TCA	chol	35	7.5	15	0.025
	sitosterol	35		7.5	15	0.015	[30]	
	chol	24		7	50	0.45	[32]	
	sitosterol	24		7	50	0.19	[32]	
	stigmasterol	24		7	50	0.20	[32]	
	chol	37		7	50	1.49	[23]	
	TCDCA	chol	37	7	100	1.50	[19]	
		chol	37	7	50	1.53	[23]	
	TDCA	chol	35	7.5	15	0.50	[30]	
		sitosterol	35	7.5	15	0.30	[30]	
		stigmasterol	35	7.5	15	0.20	[30]	
		sitostanol	35	7.5	15	0.25	[30]	
		chol	35	7.5	15	0.39	[31]	
		sitosterol	35	7.5	15	0.22	[31]	
		chol	37	7	50	2.65	[23]	
TUDCA	chol	37	7	100	0.19	[19]		
Binary Mixed Micelles	TCA	chol:sitosterol	35	7.5	15	0.02	[31]	
		chol: sitosterol	35	7.5	25	0.04	[31]	
	TDCA	chol: sitosterol	35	7.5	15	0.30	[30]	
		chol: stigmasterol	35	7.5	15	0.48	[30]	
		chol:sitostanol	35	7.5	15	0.25	[30]	
		chol:sitosterol	35	7.5	25	0.50	[30]	
		chol: stigmasterol	35	7.5	25	0.70	[30]	
		chol:sitostanol	35	7.5	25	0.50	[30]	
		chol:sitosterol	35	7.5	15	0.38	[31]	
		chol:sitosterol	35	7.5	25	0.56	[31]	

In some published works where more complex models were used like DMM, used to mimic the intestinal lumen content, phytosterols effect on cholesterol solubilization diverges from the results obtained in simple mixtures. In this study stigmasterol has shown to be the most efficient phytosterol in cholesterol solubility decrease, followed by stigmastanol and sitosterol [42]. Using also a complex system, other study showed that sitosterol has a higher effect on decreasing cholesterol solubilization in single systems but also in the presence of monoolein, oleic acid and phospholipids [40]. The reason for these different effects of phytosterols on cholesterol solubilization is not yet understood and should be addressed.

Solubilization of hydrophobic molecules in the intestinal lumen is only one of the features of BS. Another important aspect to have in consideration is their partition into membranes. The partition of BS into biological membranes can alter their fluidity properties and affect the partition of other molecules through the membrane. It is also important for the understanding of the enterohepatic circulation of BS. What is the extent of partition and what is the local concentration of BS in the membranes should also be addressed. The coming section will review the state of knowledge about partition of BS to model membranes with biological relevance.

I. 8 - Absorption in membranes

I. 8. 1 - Partition of BS into membranes

Membranes are made of several lipids, the most representatives being PL, sphingomyelin and cholesterol [3]. The interaction of BS with membranes is of huge importance due to the resistance they need to have against the surfactant properties of BS which are present in the milimolar range in the intestine [43]. This high concentration of a surfactant combined to the solubilizing action of BS for hydrophobic molecules (such as sterols and phospholipids) raises some questions concerning partition of BS into membranes. The determination of partition equilibrium constant to membranes can give information on the local concentration of BS in the membrane. This is a fundamental parameter to predict the effects of BS on the structure of gastrointestinal membranes. The order parameter profile of acyl chains of model membranes in the presence of increasing BS concentrations can explain the effect on membrane structure fluidity by the action of BS, the effect of cholic acid being a good example [44]. Contrary to the cholesterol condensing effect in membranes [45; 46], BS shows an increase of the disorder inside the membranes by a decrease on the order parameter. This raises the following question: can the presence of BS in membrane enhance permeation of hydrophobic molecules such as cholesterol? To answer this question a quantitative study on partition of several BS must be addressed. Some previous investigations quantitatively addressed the partition of BS to membrane, by using radiolabelled probes and doing ultrafiltration [47; 48] or using ITC [49; 50]. The available experimental data on BS partition into membranes is summarized in Table I. 8. From the reported values most of the works are done with a lipid to bound BS ratio to high. Partition equilibrium constants show that at the middle of some titration experiments there are ligand to bound BS ratios of 1. High ligand concentration at the membranes leads to aggregation of BS on the surface of the membrane therefore providing erroneous partition data [49; 50]. Ideally the ratio of lipid to bound ligand at 50 % titration should be higher than 20 to recover the intrinsic partition coefficient.

Table I. 8 Partition equilibrium constants of conjugated and non-conjugated BS to model membranes (LUV 100 nm).

BS	Lipid	NaCl (mM)	T (°C)	pH	K_p	Lipid/ bound BS 50% of titration	Ref.	
GCA	lecithin	150	20	8	1.0×10^2	2	[36]	
		150	40	8	1.0×10^2	2	[36]	
		500	20	8	3.0×10^2	2	[36]	
		GCDCA	150	20	8	6.6×10^2	2	[36]
		UDCA	150	25	7.4	1.3×10^4	50	[48]
CDCA	150	25	7.4	1.6×10^4	7	[48]		
CA	lecithin/ PS 7:3	150	25	7.4	2.8×10^3	10	[48]	
	lecithin/ PE 7:3	150	25	7.4	2.6×10^3	17	[48]	
	lecithin/ Chol 7:3	150	25	7.4	3.7×10^3	36	[48]	
	lecithin/ SpM 7:3	150	25	7.4	4.9×10^3	13	[48]	
	lecithin	150	25	7.4	6.3×10^3	17	[48]	
	EPC	140	25	7.4	1.6×10^2	19	[49]	
	POPC	100	20	7.4	8.8×10^2	2	[50]	
		100	30	7.4	8.8×10^2	2	[50]	
		100	40	7.4	3.3×10^2	2	[50]	
		100	50	7.4	8.9×10^2	2	[50]	
100		60	7.4	1.2×10^3	3	[50]		
DCA	EPC	140	25	7.4	5.4×10^2	7	[49]	
	ESM	140	25	7.4	2.9×10^3	14	[49]	
	POPC	100	20	7.4	1.7×10^4	1	[50]	
		100	30	7.4	2.3×10^3	1	[50]	
		100	40	7.4	2.5×10^3	2	[50]	
		100	50	7.4	2.8×10^3	1	[50]	
		100	60	7.4	2.0×10^3	1	[50]	

Considering the experimental results that were obtained in ideal conditions (bold highlighted in Table I. 8), with ligand to bound BS ratio at 50% of the titration around 20 or higher, some generalizations can be made. UDCA a dihydroxy BS partitions more into lecithin membranes than the trihydroxy CA BS. This is expected due to the higher hydrophobicity the most hydrophobic BS (UDCA). Results obtained for the partition of CA to lecithin and a lecithin/cholesterol (7:3) membrane shows a decrease for the membrane in presence of cholesterol. This is consistent with the order increase of these membranes relatively to the membranes in absence of cholesterol. The increase of phosphoethanolamine proportion in lecithin membranes show a decreasing effect on the observed partition obtained. Phosphoethanolamine presences in membranes can

Chapter I

establish hydrogen bonding between them which may explain the observed decrease in the partition. The decrease observed between the partition of CA to lecithin and EPC could be due to the different PC lipid composition and also to the low ionic strength used which would lead to a lower partition, due to the lowest charge compensation.

A clear determination of the partition of glycine conjugated BS to POPC, POPC/Chol/SpM (1:1:1) and SpM/Chol (1:1) membranes is crucial to understand the solubilizing capacities of BS in an *in vivo* scenario and also the permeability effects of BS in membranes. These lipid compositions can help to mimic the apical and basolateral membranes of enterocytes in the intestinal epithelium and also the composition of the external monolayer of canicular membrane from where BS are expelled from liver into the gallbladder. Although the constitution of this membrane is SPM and POPC, gallbladder content shows a higher presence of phospholipids. The mechanism by which this happens is not known but revealing what are the partitions of BS between these different membranes can give valuable information.

The partition of BS to membranes is also an important process for the understanding of their re-absorption through the intestine. Each BS recycles several times between intestine and liver. Before being delivered to the blood stream, after partition into the membrane, BS needs to translocate between the apical and basolateral membranes.

We will now review the current state of knowledge about translocation of BS. We should highlight that BS can also be transported by mediated transport (this topic will not be covered but further information can be found elsewhere [51]).

I. 8. 2 - Flip-Flop or translocation

Depending on their environment BS can change their ionization state. This alters significantly the translocation rate from one monolayer to the other in the membrane. As an example, when solubilized in water below its CMC, cholic acid can change its pKa from 4.98 to 5.5 in micelles or to 6.8 when inserted in a lecithin membrane. If the pKa is increasing from micellar to membrane environment, this means that at the same pH we will have less charged BS molecules in the membrane than in the micelles [52], increasing this way the fraction of protonated form. The determination of translocation of unconjugated BS was studied by ^{13}C NMR spectroscopy, both at low and high pH [24]. Results show that for low pH (3.5) at 35 °C the characteristic time for translocation was 7.2 s for cholic acid and lower for the more hydrophobic BS (CDCA and DCA, in this order). Increasing the pH (around 10) decreases the flip-flop rate to characteristic times higher than 24 h. The BS flip-flop for Taurine conjugated BS, TDCA, was addressed using centrifugation ultrafiltration and the results showed that the average time for translocation in egg yolk phosphatidylcholine (EYPC) membranes was 2.5 h [53]. Upon raising the hydrophilicity of BS (TCA) an increase in average time for translocation in the lipid membrane was obtained (3 h). In the same study GDCA showed to have a translocation of 15 min. The translocation of DHE (cholesterol analogue) in POPC membranes is around 40 s, which should be faster than that of cholic acid at physiological pH [54]. One question still unsolved is if the translocation of other hydrophobic molecules can be enhanced by the presence of BS in the membranes and in such case which are the more effective in this process. This can be very important for drug delivery field.

Translocation of BS is key point to understand the enterohepatic re-circulation of BS from lumen to liver. There is no information regarding the translocation of BS conjugated with glycine through lipid membranes containing POPC, SpM/Chol and also POPC/Chol/SpM, namely with the most prevalent BS in lumen, GCA, GCDCA and GDCA.

I. 9 - An overview of passive absorption: Solubilization versus partition phenomena

The hydrophobic molecules present in the lumen need to be solubilized prior the absorption through epithelium surface. Once the solubility as monomer is overcome, different type of hydrophobic molecules show different aggregation behaviour, cholesterol has a very low solubility in water (1×10^{-9} M) [55] and forms crystal phases at higher concentrations. PL has higher solubility than cholesterol as monomer in water, but once the aqueous solubility is reached it forms liquid crystal phases (bilayers). FA and BS form micelles.

In the duodenum content we find PL, cholesterol, BS and FA solubilized in mixed micelles and vesicles. This means the duodenum is characterized by a complex mixture with a wide variability of molecules with different solubilities arranged in different types of aggregates. In fact luminal contents are described through three phases, a upper less dense phase, a middle phase presumed to be micellar and a precipitated phase (pellet) [16]. In a more detailed picture we can find liquid crystal phases (mixed vesicles), mixed micelles, simple micelles and cholesterol crystals and other precipitates.

The solubility in water of a given molecule as a monomer is inversely proportional to its hydrophobicity. On one hand the increase of the hydrophobicity of a molecule is normally reflected in a decrease of its solubility in aqueous environment. On the other hand the permeability of hydrophobic molecules, which is the ability of a molecule to cross a membrane, increases with the increase of hydrophobicity.

The permeability of hydrophobic molecules through the membrane can be analyzed considering the solubility-diffusion model. This assumes the rate limiting step of the molecule crossing the membrane is the diffusion through the membrane, the steps of entering the membrane and exiting from the membrane being negligible in the overall process. In these conditions permeability can be defined as proportional to the diffusion and partition coefficient and being inversely proportional to the length of the membrane to be crossed. The equation for permeability (P) is therefore given by,

$$P = \frac{K_p D_m}{l} \qquad \text{Equation I. 15}$$

where K_p is the partition coefficient defining the equilibrium of the hydrophobic molecule between the aqueous and membrane phases; D_m is the diffusion within the membrane and l is the length of the membrane. Observations from Meyer-Overton noticed that partitions of a solute from an aqueous solvent to a membrane were related with the partition coefficient from an aqueous phase to a non-polar solvent [56]. However some deviations to the Meyer-Overton rule were noticed and could be explained by the variation in the value of diffusion constant of solute through the membrane. Diffusion of molecules in a polymer is quite dependent on their size and shape like in a membrane. It is given by the Stokes-Einstein equation, assuming a sphere, which states that translational diffusion through a polymer or membrane is inversely proportional to the radius of the diffusing molecule. The diffusion in this hydrodynamic analysis is thought to occur in several steps depending on free volume being formed along the fluctuations in membrane. The diffusion will depend on how many holes of right size will be formed that can accommodate the molecule and how fast they will be formed.

Figure I. 11 shows a profile of enterocyte cells from intestinal epithelium emphasizing the sizes of different structures, namely the UWL, the size of the enterocyte and also the pH range from lumen to blood stream.

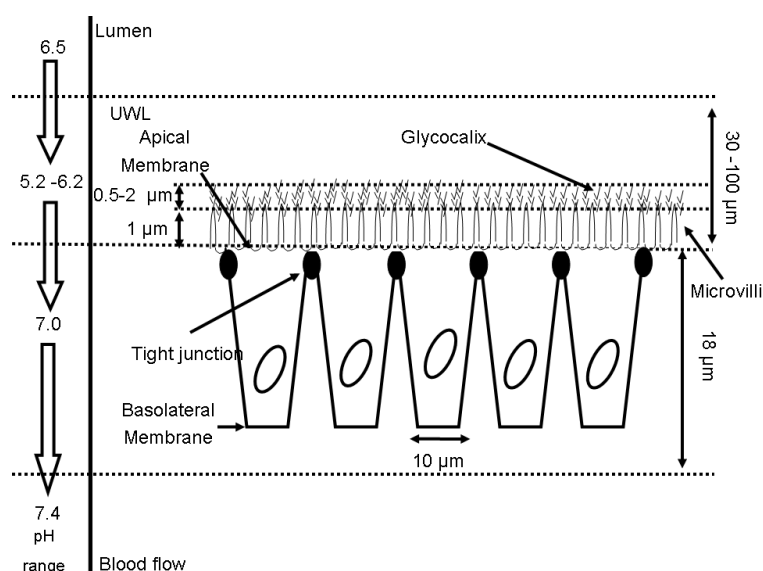


Figure I. 11 Pictorial description of enterocyte in intestinal endothelium highlighting the sizes of different compartments and also the changes of pH from lumen to blood flow (adapted from [19]).

One important aspect related with absorption is the effect of the unstirred water layer on the overall absorption process. From the Figure I. 11 it is noticed that UWL has a length 5 times the length of the gastrointestinal membrane and is the first structure that hydrophobic molecules need to cross before getting in contact with the membrane. For molecules like sterols which are very hydrophobic, presenting low solubility in aqueous phase, the diffusion through the UWL can be the limiting step for the overall absorption process [57]. The next Figure I. 12 shows the dependence of solubilization and passive permeability obtained for short chain FA, long chain FA and sterols with increasing hydrophobicity and also the rates of intestinal absorption observed considering the presence and absence of a diffusion barrier (UWL).

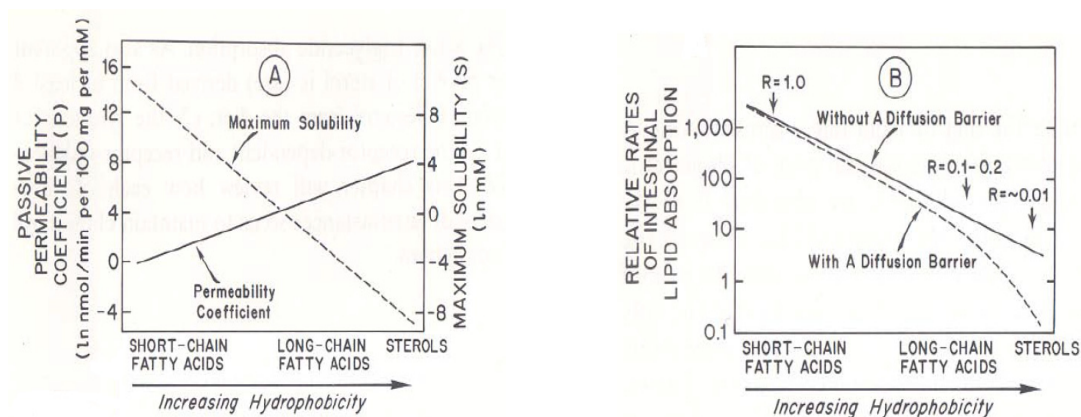


Figure I. 12 Panel A shows the logarithm of the maximum solubility and passive permeability coefficient for a series of FA and sterols of increasing hydrophobicity. The product of these two values for any given lipid yields the maximum rate of absorption of that lipid in the intestine, both in the absence and presence of a diffusion barrier, as shown in panel B. The values of R show the ratios of the maximum rates of absorption of different lipids in the presence and absence of the diffusion barrier [58].

If the lipid shows a high solubility in aqueous environment it can diffuse easily through the UWL. The key factor for absorption is then the permeability through the membrane, which is dependent on the partition to, diffusion through and length of the membrane. The concentration in the vicinity of the membrane will be similar to the one in the bulk solution in the lumen, although the partition coefficient will be low due to the higher affinity for aqueous solution. On another hand if the permeating molecule is very hydrophobic the diffusion through UWL is the limiting step, limiting the availability of the hydrophobic molecule to the membrane. As sterols have a very low solubility in an aqueous environment, a wider concentration gradient between lumen and membrane

vicinity is formed, being in this case the UWL the limiting step for absorption to occur. Once molecules permeate the UWL they are absorbed by the membrane because of their higher partition coefficient to membrane. The same occurs with longer chain FA while in the case of short chain FA, due to their solubility in aqueous environment, the limiting step is the permeation through the membrane. Increasing hydrophobicity enhances partition to the membrane because all the molecules able to cross the UWL can partition to the membrane due to their high partition coefficient. However there is a decrease in the availability of these molecules at the membrane due to their low solubility in the aqueous environment. Another major aspect is that increasing the size of the molecule affects the diffusion through the UWL and also through the membrane. Decreasing of the hydrophobicity favours solubility and diffusion through the UWL to the membrane, but partition to the membrane is limited due to the lower affinity of these molecules for the membrane (lower partition).

Having explored the solubility and diffusion phenomena in the overall process of absorption, through two different barriers UWL and the apical membrane, we will describe one of the major role of BS in this process, and how significant it is in the cholesterol absorption process.

The solubilization of hydrophobic molecules is done in mixed vesicles and mixed micelles. Although diffusion of these aggregates is slower than the diffusion of the molecule as a monomer, the advantage of using the micelles as vehicles of transport is due to the enhancement of solubility achieved. For FA, the efficiency of their transport in micelles can be as large as 150 times higher [59]. Permeation depends on the delivery of molecules to be permeated and this delivery depends on the equilibrium defined by the vehicle that transports the molecule and the concentration of this molecule as a monomer in aqueous solution.

Another important aspect in BS micelles is their size. The micelles of GDCA and GCDCA show an aggregation number of 16-18 aggregates per molecule and GCA about 6 [23]. Although it is known that hydrophilic BS solubilizes less cholesterol, which can be related to the size of the aggregates, the fact of having a smaller size can be an advantage to deliver cholesterol to the membrane due to the higher diffusion of this micelle when compared with the larger micelles of more hydrophobic BS. The next Figure I. 13 shows the different equilibrium established in the intestinal lumen and at interface with the gastrointestinal membrane.

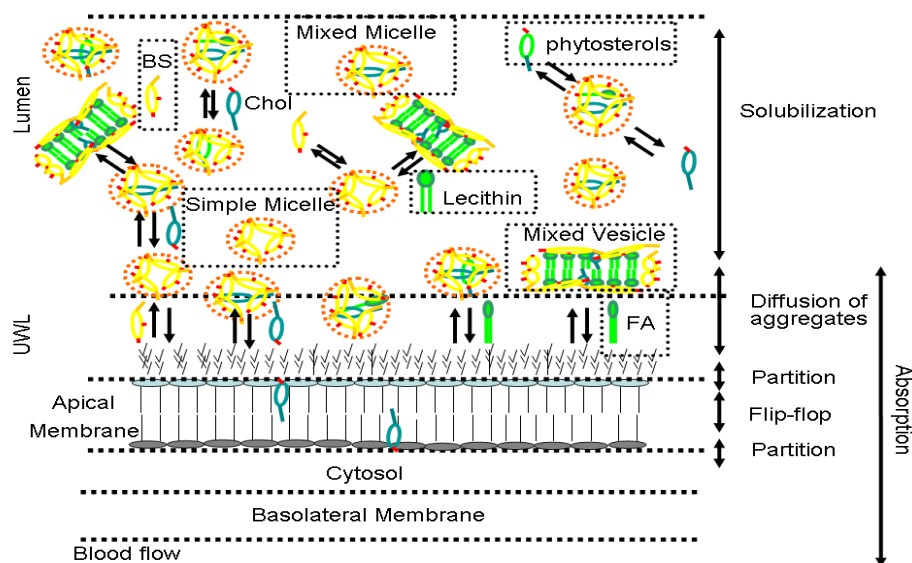


Figure I. 13 Simple model representing passive diffusion of hydrophobic molecules (cholesterol) through apical membrane. The solubilization process is achieved by different kinds of aggregates: namely micelles and vesicles and several equilibriums are shown (composed of BS, Lecithin, FA, and Chol). Phytosterols are also shown to reinforce the possibility of physicochemical mechanisms (co-solubilization and/or co-precipitation) in the solubilization process that inhibit cholesterol solubilization. The absorption process of cholesterol involves the diffusion to near the membrane, partition of the monomer to the external leaflet, translocation to the inner leaflet and partition to the cytosol and all the events until the diffusing molecule is delivered to the blood flow.

At this point we could argue why molecules are absorbed as a monomer and not as a fusion of micelles or lipid aggregates. An interesting inverse relation has been observed between the solubilization capacity and cholesterol absorption enhancement of bile salt micelles. The most hydrophilic taurine conjugates lead to a higher absorption of cholesterol in humans [60] and a higher efficiency in cholesterol absorption was obtained when it was solubilized in taurocholic instead of taurodeoxycholic BS [34]. Those results are important for the understanding and control of cholesterol absorption in two ways: *i*) they indicate that cholesterol delivery to the epithelial membrane does not occur through fusion of the mixed micelles with the membrane but rather *via* cholesterol in the aqueous phase; *ii*) increasing the affinity of cholesterol to the micellar aggregates in the intestine decreases its aqueous concentration and may inhibit cholesterol absorption. A simplistic interpretation of the system would be that BS

micelles are monomerizing agents supplying molecular cholesterol, and other hydrophobic molecules, for partition into the membrane via aqueous solution. Another important question would be whether BS are crucial for absorption of cholesterol and other hydrophobic molecules in the intestine. The solubility of cholesterol and FA in the presence and absence of BS micelles showed different behaviours. Cholesterol absorption decreased completely in the absence of BS, highlighting their crucial role in cholesterol solubilization. However FA were able to be absorbed even in the absence of BS, although a decrease of 10 to 20 % was observed [58]. In another study another surfactant, Pluronic F68, was also used but no cholesterol absorption process occurred, reinforcing the singular role of BS for absorption [61]. BS seem to have a particular influence in the cholesterol absorption and are requested to promote solubilization and absorption of cholesterol [62]. This is a surprising system and although a lot of studies were made on cholesterol solubility in BS micelles, in the presence and absence of lecithin, the focus was mainly on the topic of gallstone disease. This is a disease developing due to cholesterol precipitation in the gallbladder and efforts were addressed to solubilize gallstones by the action of BS which were more potent. Ursodeoxycholate, named after the major BS present in bears, was an efficient solubilizer of gallstones [51; 63]. The increase or decrease of molecules absorption can be a useful tool to control some diseases in humans. Due to the important function of BS in these processes, we decided to study the effects of several BS with physiological relevance but with different hydrophobicities.

The next section will describe briefly some known cholesterol transporters and non passive transport strategies for cholesterol in gastrointestinal membrane and also at liver.

I. 10 - Cholesterol transporters

I. 10. 1 - Nieman Peak C1 L1 (NPC1L1) (absorption of cholesterol in intestine and liver)

NPC1L1 is a transmembrane protein highly expressed in the enterocyte (epithelial cells) of intestine, more specifically in jejunum and proximal ileum. It is also found in the human liver hepatocytes in the canalicular membrane [64]. This protein has been implicated in the transport of cholesterol. It has a sterol sensing domain (SSD), 13 transmembrane regions, 3 large loops protruding into the extracellular space, several cytoplasmic loops and a C-terminal cytoplasmic tail. Evidences for action of NPC1L1 in the transport of cholesterol were demonstrated in mice genetically altered with no NPC1L1 protein leading to a 70% reduction of cholesterol absorption. They also did not show a further decrease upon using Ezetemibe, a known inhibitor of this protein. These mice subjected to large doses of cholesterol were resistant to hypercholesteremia and showed similar results to those obtained with normal mice treated with Ezetemibe. From a physicochemical perspective Ezetemibe is a molecule partitioning easily in the membranes, changing their elastic properties. There is no detailed study on the effect of this drug on the fluidity of membranes. If membrane properties would be altered this would compromise not only the absorption of cholesterol but also of other nutrients essential to life.

NPC1L1 is also been involved on the selectivity towards phytosterols. Although phytosterols are very similar to cholesterol, they seem not internalized by this protein. However in terms of effectiveness to bind cholesterol, it has a higher binding affinity to this protein. Evidences also come from mice treated with Ezetemibe showing also a deficit in absorption of phytosterols [11]. The same question should also be addressed to other essentially hydrophobic molecules.

I. 10. 2 - Regulation by ABC transporters (efflux of cholesterol and phytosterols from apical membrane)

ATP binding cassette (ABC) transporters are membrane proteins that are localized in the brush border membrane at the intestine. These proteins limit cholesterol absorption by regurgitating cholesterol back to the intestinal lumen. Once cholesterol is inside of the apical membrane of the enterocyte it is usually esterified, namely with oleic acid (60%) [65]. The cholesterol and phytosterols not esterified are effluxed back to the lumen by ABC transporters. Phytosterols, although very similar to cholesterol, are much less esterified than cholesterol; the reason why this happens is still unknown. Transporters are ATP dependent and there are divided in several classes. The most commonly found in apical membrane in the intestine are ABCG5 and ABCG8.

Sitosterolemia disease was found to be related with defects in these transporters and was characterized by high absorption of cholesterol and phytosterols.

I. 10. 3 - LDL receptor pathway (transporter of cholesterol from blood to cells)

The LDL receptor pathway is the known mechanism by which mammalian cells acquire exogenous cholesterol. Briefly, LDL carrying cholesterol or cholesterol esters bind to the LDL receptor in the plasma membrane and they join with other receptors in localized regions of the plasma membrane, called clathrin-coated pits. The coated pits are composed of clathrin and other proteins invaginating into vesicles expelling it out from the plasma membrane to the cytosol. These vesicles eventually merge with early endosomes, losing the clathrin coat, and form larger vesicles called endosomes. The LDL receptors are not degraded during this process and they are recycled again to the plasma membrane. This process is used by several other molecules. The endosomes can suffer maturation and be delivered to the trans Golgi network where they receive other proteins and become lysosomes (the most acidic organelles with degradative function). The LDL-chol in the endosomes can migrate to the plasma membrane again or can go to the endoplasmic reticulum. Once there, they are esterified by ACAT (acyl-coenzyme A: cholesterol acyltransferase).

The efflux of LDL-cholesterol from endosomes seems to be related with Nieman Pick enzymes type C1 and type C2. The first type C1 is associated with both

Chapter I

internal membranes and delimiting membranes of endosomes. The type C2 is a glycosylated soluble protein, localized in the lumen of endosomes. The mechanism is not understood, but it is known that a malfunction of these enzymes causes a lipid storage and trafficking disorder with accumulation of unesterified cholesterol.

Summarizing, cholesterol can be absorbed through the intestine by two mechanisms. It is fundamental to determine the contributions of each of the mechanisms considering the cholesterol passive diffusion and mediated transport. The full understanding of absorption, namely the passive diffusion view, should be pursued because it can give simple answers from physicochemistry principles that can help the understanding of better and more efficient strategies to decrease cholesterol absorption.

**Chapter II A Good Choice of
Experimental Technique Can Help to Solve a
Scientific Problem: NMR and ITC Theoretical
Background.**

II. 1 - The NMR spectroscopy

Like any other kind of spectroscopy, Nuclear Magnetic Resonance spectroscopy (NMR) relies on the absorption of a quantum of radiation, involving transition between energy levels in a molecule or atom [66; 67; 68]. In NMR spectroscopy the energy levels involved are those of a spinning nucleus under an applied magnetic field. Some nuclei show magnetic properties associated with their spin, which under a magnetic field tends to align with the field.

When the external magnetic field is applied to a spinning magnetic nucleus, the spin axis precesses around the direction of the magnetic field (vertical Z axis), as we can see in Figure II. 1

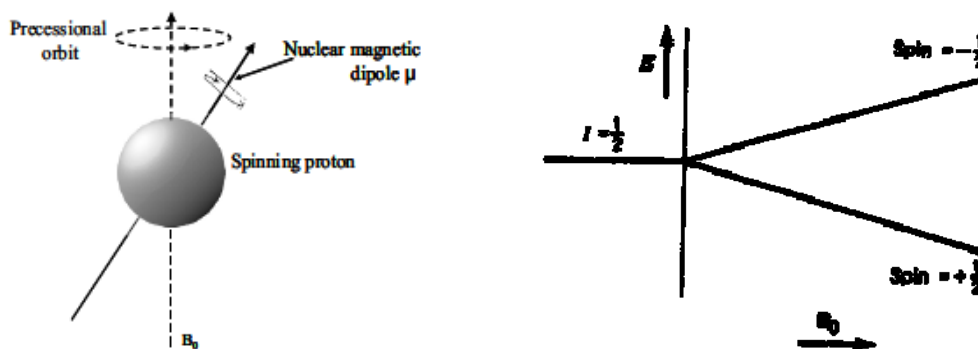


Figure II. 1 Precession orbit defined by the nuclear magnetic moment under an applied field B (left). Energy levels of proton nucleus, $I = \frac{1}{2}$, in a magnetic field B . The lower energy state has magnetic number $m_l = \frac{1}{2}$, and is designated by α . The higher energy level has the magnetic number $m_l = -\frac{1}{2}$ and is designated by β .

The nuclear magnetic moment (μ) is directly proportional to the spin quantum number I , and is given by $\mu = \frac{\gamma h}{2\pi}$. The precession frequency (ν), also called Larmor frequency, is directly proportional to the strength of the applied magnetic field (B), $\nu = \frac{\gamma B}{2\pi}$. The γ value is the nucleus gyromagnetic ratio, which has a characteristic

Chapter II

value for each nucleus. The energy of interaction (nuclear Zeeman interaction) is proportional to the nuclear moment and the applied field $E = -\frac{\gamma h m_I}{2\pi} B$.

A nucleus of spin I has $2I+1$ possible orientations relative to B , given by the magnetic spin quantum number (m_I). The m_I can take the following values defined by the interval, $-I, -I+1, \dots, I-1, I$. Taking the example of proton we will have two possible orientations $-\frac{1}{2}$ and $\frac{1}{2}$. Quantum restrictions limit the number of orientations that the magnetic moments can show under the influence of a magnetic field. In the case of a proton ^1H , it can be either aligned with or opposed to the external magnetic field, corresponding to high and low energy states, respectively. In a macroscopic system in equilibrium in the presence of B , there will be a difference in population distribution between the two states that is given by the Boltzmann distribution, $\frac{N_\beta}{N_\alpha} = \exp\left(\frac{\Delta E}{kT}\right)$, where N_α and N_β are the respective populations in each state. The energy difference, ΔE , between these two states is very small, and the excess of population in the low energy level is around 1 in a total of 10^6 , being this the main reason for the low sensitivity in NMR spectroscopy.

If the adequate energy is supplied to the spin systems, with the frequency ν , such the resonance condition, $\Delta E = h\nu$ is fulfilled, transitions between the two spins states will occur. Supply of electromagnetic radiation is then able of reversing the spin, by the absorption of energy. However, there are other mechanisms occurring, as the exciting energy is dissipated through the surrounding environment in a process described as nuclear relaxation. In relaxation the population of spin states returns to the equilibrium.

The magnetic fields usually used in NMR range from 1.4 to 18.79 T, or even higher nowadays. The resonance condition for protons requires radiofrequencies of 60 to 800 MHz, in the case of the above fields. Protons have a magnetic spin of $I = \frac{1}{2}$. All other nuclei with non-zero values of I are also magnetic, although only those with $I = \frac{1}{2}$ (ex. ^3H , ^{13}C , ^{31}P) provide NMR signals free from broadening due to quadrupolar relaxation. This is the case of ^2H nuclei and others with $I > \frac{1}{2}$. Nuclei with even mass

number and charge number have zero spin and are NMR silent and therefore not observable. An example of this is the ^{12}C isotope. The ^{13}C isotope is observable but its natural abundance is low (1.103%). Also the resonance frequency of ^{13}C is around $\frac{1}{4}$ of ^1H , which makes it a less sensitive nucleus.

An NMR spectrum can be of valuable information, not only because it provides qualitative data about the nature and structure of the molecular studies but also because it can be quantitative. The main features that can be addressed from a NMR spectrum are the chemical shift, peak integrals, multiplicities, couplings and the widths of peaks. These features will be quickly described using ^1H as an example but also apply for other nuclei.

As mentioned before, NMR requires the application of an external magnetic field to promote the differential distributions of spins in the nucleus. However the effective field sensed by the nucleus is affected by the presence of the electron cloud surrounding the nucleus. The more electrons are present around the nucleus the weaker is the field sensed, i.e. the more it is shielded. In molecules nuclei have particular electronic clouds around them which configure them a specific electronic environment. Depending on the position and the electronegativity of the vicinal atoms, each nucleus will experience different levels of shielding. So the effective field felt by a nucleus will be lower for the more protected nuclei (higher shielding). In conditions of fixed frequency and variable field this would mean that higher shielding would need a higher field for attaining resonance. The field (B_0) applied will not be equal to the field noticed by the nuclei (B_N) and results from shielding of the nucleus by the amount σB_0 . The field on the nuclei will be equal to, $B_N = B_0(1 - \sigma)$, where σ is called the shielding constant. Also, instead of using absolute values of shielding constant, it is normally used the difference from a reference compound ($\delta = \sigma_{\text{ref}} - \sigma$), given by,

$$\delta_i = \frac{\nu_i - \nu_{\text{ref}}}{\nu_0} \quad \text{Equation II. 1}$$

where ν_0 is the spectrometer frequency. The position of a signal relative to a standard gives the chemical shift (δ_i).

Another property of an NMR spectrum is the fact that the area of the different peaks is directly proportional to the number of chemically equivalent nuclei originating that peak. Provided that some care is taken to prepare the NMR experiment, namely

Chapter II

using an adequate relaxation delay for a full relaxation of the nuclei, NMR will be both qualitative and quantitative.

Each proton in the molecule can feel the magnetic effects of other protons nearby, causing local modifications on the magnetic field felt by the nuclei. This effect is transferred through the covalent bonds between atoms via a mechanism called scalar coupling and results in characteristic resonance patterns. They depend on a number of factors, including the number and the nature of chemical bonds between the spins. They can be differentiated from chemical shift namely by two properties: 1- the value of splittings (which depend on the coupling constants between the nuclei) are independent of the magnetic field at which the spectrum is acquired; 2- if the spectrum of one family of spins i is observed, then it will manifest the coupling to another spin family of spins j to which it is coupled. As an example, considering two neighbouring ^1H , the multiplicity of multiplet obtained arises from the spin coupling between them, and that is only observed between non-equivalent ^1H , resonating at different frequencies. In this situation the pattern is given by the $(n+1)$ rule stating that when a particular ^1H has n neighbours that are equivalent to each other then signal multiplicity of the first will be given by the value $n+1$. Vicinal protons will give two duplets.

II. 1. 1 - The NMR experiment

A basic NMR experiment can be divided in three steps: 1- preparation, 2- excitation (pulse) and 3- acquisition. In the first step, called preparation step, time is given for the spins to come to equilibrium and usually is referred as relaxation delay. In the second step, the radio frequency pulse is applied for a short (μsec) time to promote the excitation of the spins and finally in the third step the signal is acquired during a defined acquisition time. In order to increase the signal to noise ratio, this sequence is repeated several times and the corresponding signals are summed up until a sufficient time averaging is recorded.

The signal obtained from this basic experiment is called free induction decay (FID) which contains the information of the magnetization in function of time. A Fourier transform gives this information in frequencies dimension.

The behaviour of the bulk magnetization M (the sum of the individual spins) immediately after subjected to a pulse of angle θ , is given by the components:

$$\begin{cases} M_{x'} = 0 \\ M_{y'} = M_0 \sin \theta \\ M_{z'} = M_0 \cos \theta \end{cases}$$

The magnetization can be selectively manipulated by using defined radio frequency pulses to acquire different kinds of information. Figure II. 2 shows the effect of different pulse widths placing the magnetization in various planes. A 90° pulse place the M vector in the xy plane and 180° pulse inverts the magnetization.

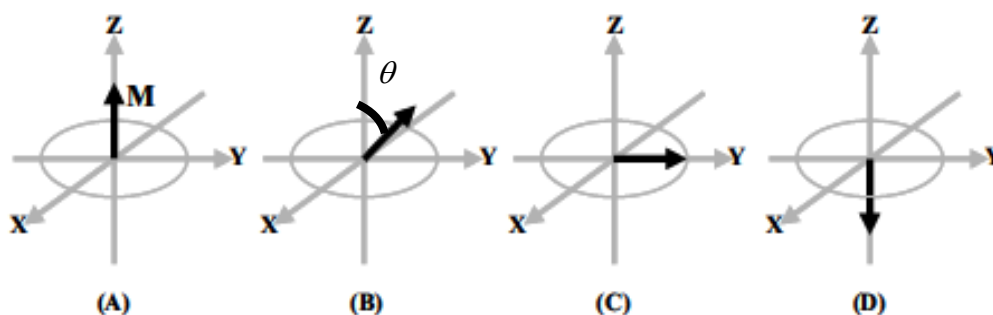


Figure II. 2 Diagram showing the magnetization evolution with several pulses: a) overall magnetization vector is aligned with the field (parallel to z axis) b) pulse with an angle $< 90^\circ$ c) pulse with an angle of 90° transferring the magnetization vector to the xy plane d) pulse with an angle of 180° inverting the magnetization vector.

Chapter II

After the pulse is switched off, the perturbed system will return to its equilibrium position, where M is back parallel to the applied field. This occurs through two separate processes. In one of the processes relaxation is achieved by loss of energy from excited nuclear spins to the surrounding molecular lattice, and is designated as spin-lattice relaxation or most commonly as T1 relaxation. In this case the longitudinal M'_z value returns to M_0 . The second process is related with the nuclear spin interchanging energy with other spins and, as a consequence, some spins start to precess at higher rates relative to others, resulting in loss of phase coherence. This relaxation process is designated by spin-spin relaxation or T2 relaxation. In this process transverse magnetization M'_y and M'_x values returns to zero. Relaxation is then the process by which the bulk magnetization returns to its equilibrium value. In NMR the typical values of T1 and T2, relaxation times, can go from microseconds to minutes and the rate of relaxation is sensitive to the physical environment in which nuclei are and also to the nature of the motion which the molecule is undergoing. The equilibrium state has no transverse magnetization but there is a Z component along the direction of the applied field. The size of this component depends of the number of spins, their gyromagnetic ratio and strength of the applied field. The relaxation is an extremely important characteristic to keep in mind in NMR. Full relaxation of spins must be accomplished; otherwise the signal will not truly recover in time. Due to the spin-spin interaction, some couplings can occur leading to a more complicated spectrum due to the transfer of magnetization between spins. Considering a simple example, a ^{13}C - ^1H system, both nuclei are NMR sensitive and would be influenced by each other. In this way they will be coupled giving rise to two resonances in the carbon spectrum and also in the proton spectrum. In the ^{13}C NMR spectrum the carbon will be coupled with the proton and in the ^1H NMR spectrum the proton will be coupled with the carbon. In simple molecules this could be easily interpreted but in molecules with higher number of atoms, these couplings would lead to a quite complex spectrum. To avoid the coupling effect, one strategy is to decouple the nuclei. Making use of the characteristic magnetization of each nucleus it is possible to manipulate them in such a way that we can saturate one of the nuclei. The saturation is a process by which equal populations of spins in the aligned and anti-aligned state can be achieved. This methodology makes the saturated nucleus (e.g. ^1H) invisible to the adjacent nuclei (^{13}C), resulting in a spectrum respecting only to this nucleus. The ^{13}C spectrum of a molecule having the ^{13}C - ^1H bond and acquired with

^1H decoupling will present a single peak, as there is no longer coupling between ^{13}C and ^1H . The intensity of this single peak will result from the collapse of the doublet and from the so-called Nuclear Overhauser Effect (NOE). The NOE effect is the change of intensity of resonances (e.g. ^{13}C) upon the saturation of another resonance (e.g. ^1H) close to it, and to which it is magnetically coupled through space. The NOE effect can be rationalized as follows. In the case of two coupled spins we can draw the expected spin states and transitions, as can be seen in the Figure II. 3.

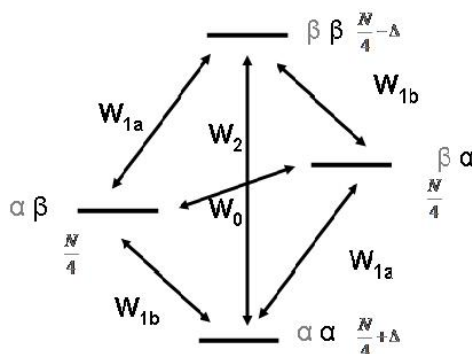


Figure II. 3 Spins states and transition probabilities (w_i) for a coupled two spin system.

The spin states and the transitions probabilities (w_i) are shown in Figure II.3, being w_i the probability of transition between two connected states and i is the change in the spin number during the transition. W_{1a} and W_{1b} are the allowed single quantum, $\Delta m_l = \pm \frac{1}{2}$, transitions for spin A and spin B assuming a total number of spins N distributed by the four energy levels. The Boltzmann distribution tells us that an excess of population should be present in the lowest energy level ($+\Delta$) and a deficit of population in the highest energy level ($-\Delta$). After spins being perturbed they tend to relax and the relaxation path is the same that the one took for excitation. Although other possible mechanism for relaxation could be the transitions of double quantum or zero quantum, they are forbidden by quantum mechanics. However other methods enable relaxation the so called non-radiative. If decoupling is applied to spin B this will approach the energy levels $\alpha\alpha$ and $\alpha\beta$ (Figure II. 3). At the same time it will also approach energy levels $\beta\alpha$ and $\beta\beta$. The relaxation between $\alpha\alpha$ and $\beta\beta$ is no longer forbidden because it became single quantum, but the difference in populations is now 2Δ , which is double of what would be obtained without decoupling. To determine the effect of NOE (η) in a system we can use the information of a spectrum recorded with decoupling and without

decoupling, which will be given by $\eta = \frac{M_A - M_A^0}{M_A^0}$, where M_A and M_A^0 are the magnetization in the presence and absence of saturation of spin A, respectively. Figure II. 4 shows the pulse sequence used in both channels (^{13}C and ^1H). The decoupling effect is active instantaneously after applying the decoupling radiofrequency, while the NOE effect build up and decay depends on the T1 values. This difference in time scales can be used to separate the two effects. To obtain spectra proton decoupled with the NOE effect, the saturation should be done during the whole sequence in the proton channel. To get the ^{13}C spectra without NOE, decoupling is done only during the acquisition step and this way a decoupled carbon spectrum is obtained without signal enhancement due to the NOE effect. In order ensure that full relaxation enables the restoration of equilibrium populations, the relaxation delay is defined as at least 5 times the T1 value (spin lattice relaxation time).

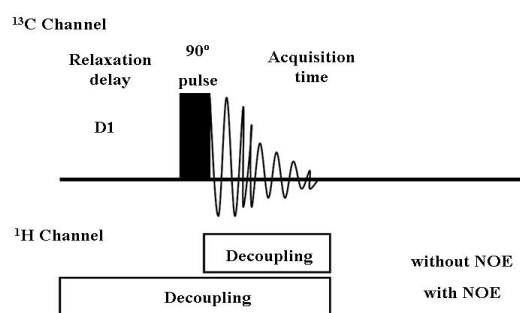


Figure II. 4 Scheme sequence of the parameters to define in a NMR experiment to have a ^{13}C NMR spectrum decoupled with NOE and without NOE.

The enhancement of ^{13}C NMR by the NOE effect due to the non-radiative transitions is useful due to the gain of signal intensity (sensitivity) obtained that could go up to two times. This has a large effect on the time requested to acquire spectra. This effect was used in our studies for quantification of cholesterol enriched in ^{13}C in BS micelles.

II. 2 - Isothermal Titration Calorimetry (ITC)

Almost any chemical reaction or physical change involves a change in heat. A measure of the heat transferred to or from the surroundings, exothermic or endothermic reaction respectively, is given by the chemical quantity involved in the reaction (mol) times the change in enthalpy (ΔH kJ/mol).

A measure of the rate of heat transfer to the surroundings is simply equal to the rate of the reaction ($\frac{\partial n}{\partial t}$, mol/sec) times the enthalpy change. Therefore, calorimetric measurements can tell us about the extension of the reaction that has taken place (e.g. partition coefficient between two phases) and also how fast this process occurs. This type of measurements has some advantages relatively to some optical techniques namely, there is no concern with the turbidity of the solutions, it does not depend on the presence of a fluorophore probe tag and it can be done in a broader range of conditions (pH, temperature, ionic strength, etc). There are several ways through which calorimetric measurements can be done. In the present study we use a power compensation instrument. This system was designed to have two cells, being one the reference cell usually filled with water kept at constant temperature and another one where the reaction takes place, called sample cell. As the chemical reaction takes place in the sample cell and heat is released or absorbed, a temperature controller feedback system supplies or receives heat in order to maintain the isothermal conditions. The raw signal obtained in this kind of instrument is given by the power applied to keep the temperature constant as a function of time ($\mu\text{cal/sec}$). The heat change is given by the integral of the heat power during the time of the measurement, which basically lasts until the value comes to the baseline. Figure II. 5 show a typical scheme of the power compensation ITC. From a single experiment we can obtain the enthalpy change, the partition coefficient and also the free energy and entropy at the temperature of the experiment. ITC was for a long time used to determine binding constants of ligands with proteins [69]. However due to its high sensitivity and after some important changes in previous protocols, it has been used to follow the interaction of some amphiphilic molecules with lipid bilayers [70; 71]. The reason behind the adaptation of the previous protocols was lipid vesicles do not have well defined binding sites, and upon interaction with amphiphilic molecules, their structures can change when too high local concentrations of ligands are achieved.

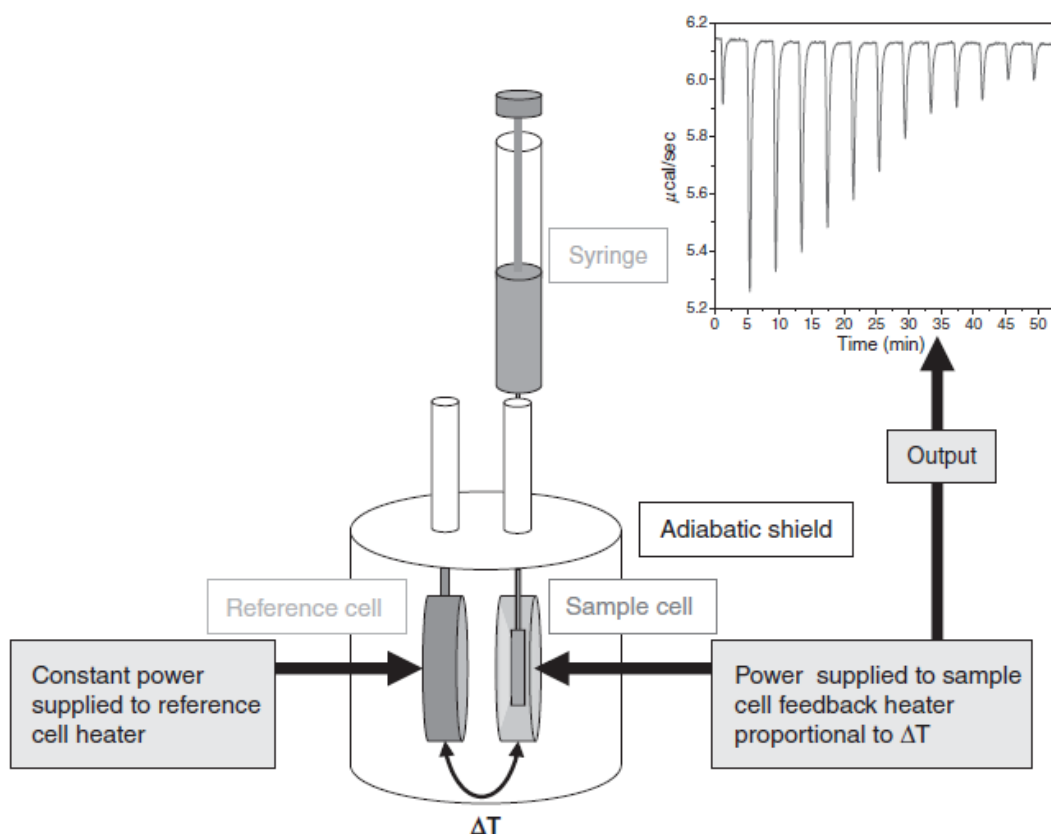


Figure II. 5 Representative diagram of a typical ITC experiment with power compensation. Major features of this type of instrument such as reference and sample cells, syringe for adding titrant, and the adiabatic shield are noted in the figure. This diagram shows an oversimplification of how the power is applied by the instrument to maintain temperature constant between the reference and sample cells is measured, resulting in the output signal [72; 73].

From a measurement of ITC we can collect, for each titration step, the heat that is integrated which is proportional to the enthalpy change times the number of moles that interact with the lipid membrane. The heat (q) involved can be calculated using the following expression,

$$q(i) = \Delta H \left(n_{\text{amphiphile-Lipid}}(i) - n_{\text{amphiphile-Lipid}}(i-1) \left(1 - \frac{V(i)}{V_{\text{cell}}} \right) \right) + q_{\text{dil}} \quad \text{Equation II. 2}$$

where $V(i)$ is the injection volume, V_{cell} is the volume of the calorimetric cell, and q_{dil} is the “heat of dilution” (residual heat due to nonbinding phenomena). The amount of amphiphile associated with the lipid bilayer is determined assuming a given model for the interaction. When

an amphiphile is interacting with a membrane, this can be characterized by a simple partition using the partition model which will be explored in the next section.

II. 2. 1 - Partition Model

Considering membrane and water as two separate phases, equilibrium is reached between them when the chemical potential of the solute in the lipid bilayer and in the aqueous phase are equal. In these conditions the mole fraction coefficient is defined by

$$K_X = \frac{X_{amphiphile}^{bilayer}}{X_{amphiphile}^{water}} = \frac{\frac{n_{amphiphile}^{bilayer}}{n_{amphiphile}^{bilayer} + n_{lipid}}}{\frac{n_{amphiphile}^{aqueous}}{n_{amphiphile}^{aqueous} + n_{water}}} = \frac{n_{amphiphile}^{bilayer} \times (n_{amphiphile}^{aqueous} + n_{water})}{n_{amphiphile}^{aqueous} \times (n_{amphiphile}^{bilayer} + n_{lipid})} \approx \frac{X_{amphiphile}^{bilayer} \times C_{Water}}{C_{amphiphile}^{aqueous}} \quad \text{Equation II. 3}$$

where $X_{amphiphile}^{bilayer}$ is the molar fraction of amphiphiles in the lipid bilayer, and $X_{amphiphile}^{water}$ is the molar fraction of the amphiphiles in the aqueous environment. Because the amphiphile has a very low solubility in water, $n_{amphiphile}^{aqueous} + n_{water} \approx n_{water}$, and then if we divide the chemical amount by the volume of solution we will get concentration of water C_{water} (55.5 M) and concentration of aqueous amphiphiles $C_{amphiphile}^{aqueous}$. Other authors used a concentration based partition coefficient K_P^{obs} given by the concentrations ratio of amphiphiles in lipid phase and amphiphiles in the water phase.

$$K_P^{obs} = \frac{\frac{n_{amphiphile}^{bilayer}}{V_{lipid}}}{\frac{n_{amphiphile}^{aqueous}}{V_{water}}} = \frac{\frac{n_{amphiphile}^{bilayer}}{[POPC] \times \bar{V}_{POPC} \times V_{Total}}}{\frac{n_{amphiphile}^{aqueous}}{V_{Total}}} \quad \text{Equation II. 4}$$

V_T represents the total volume, which is approximately equal to the water volume. The molar volume of lipid can be obtained from the literature; for POPC it is around 0.76 dm³/mol [74]. K_X can be converted into K_P^{obs} by

$$K_X \approx K_P^{obs} \times V_{Lipid} \times C_{Water} \quad \text{Equation II. 5}$$

Using the partition model we can describe, in each step of titration, the amount of amphiphile associated with the lipid bilayer responsible for the observed change in heat. This is achieved by the following equation

$$n_{\text{amphiphile_Lipid}} = \frac{n_{\text{amphiphile}} K_p^{\text{obs}} [\text{Lipid}] \overline{V_L} \gamma}{1 + K_p^{\text{obs}} [\text{Lipid}] \overline{V_L} \gamma} \quad \text{Equation II. 6}$$

this introduces the equilibration factor, γ , which is a measure of the fraction of lipid accessible to the amphiphiles during the titration experiment, with values of 1 for fully permeable (fast translocation of ligand) and 0.5 for impermeable membranes (slow translocation of ligand).

Depending on the relative rates of translocation and insertion/ desorption, amphiphiles may or may not be equally distributed between the two bilayer leaflets. This requires the substitution of amphiphiles concentration by its effective concentration, $[A]^*$, which depends on the effective lipid concentration, $[L]^*$, according to the following equation.

$$[L]^*(i) = [L]^*(i-1) \left[1 - \frac{V(i)}{V_{\text{cell}}} \right] + \gamma \left[[L]^{\text{Syr}} \frac{V(i)}{V_{\text{cell}}} \right] \quad \text{Equation II. 7}$$

$$n_{A_T}^*(i) = n_{A_T}^*(i-1) \left[1 - \frac{V(i)}{V_{\text{cell}}} \right] + \left[\gamma \left[A_L^{\text{Syr}} \right] + \left[A_W^{\text{Syr}} \right] \right] V(i) \quad \text{Equation II. 8}$$

where index i refers to the injection number, superscript *Syr* indicates concentrations in the syringe and subscripts L and W indicate the phase where the amphiphile (A) is dissolved, being L for the lipid and W for water (T for the sum of both).

For experiments following the uptake protocol (addition of lipid to ligand in the aqueous phase) all ligands are accessible for partition, and the effective lipid concentration is either equal to its total concentration - case of fast translocation - or only respective to the lipid in the outer monolayer - case of slow translocation, according to equation II.2.5. In this type of experiments, if γ is unknown, the uncertainty is propagated to the partition coefficient but the calculated enthalpy variation is accurate. On the other hand, in experiments following the release protocol (addition of pre-incubated lipid and amphiphiles to buffer), both the lipid effective concentration and the available moles of ligand (amphiphiles) must be calculated from

equation II.2.6 and II.2.7. In this situation, both K_p^{obs} and ΔH are affected by the uncertainty in γ . The combination of both protocols allows the determination of the equilibration factor and, therefore, the accurate measurement of K_p , ΔH and a qualitative estimation of the translocation rate constant. For the case of charged ligands the partition coefficient obtained directly from the ratio of concentration of both phases, K_p^{obs} , is dependent on the concentration of ligand and is related to the intrinsic partition coefficient, K_p^{obs} , via the of the bilayer surface potential (ψ_0). This relation is given by the following equation,

$$K_p^{obs} = K_p e^{\frac{-z_i F \psi_0}{RT}} \quad \text{Equation II. 9}$$

If charged molecules are partitioning into the membrane a surface potential develops due to the imposition of charge in the bilayer, characterized by an enhancement of charge density at the surface of membrane (σ). These parameters can be calculated using the Gouy-Chapman theory. Charge density can be obtained by the following two equations,

$$\sigma^2 = 2000 \varepsilon RT \sum_i C_i \left(e^{\frac{-z_i F \psi_0}{RT}} - 1 \right) \quad \text{Equation II. 10}$$

$$\sigma = \frac{e_0 \sum z_i \left(\frac{n_i}{n_L} \right)}{\sum A_j \left(\frac{n_j}{n_L} \right)} \quad \text{Equation II. 11}$$

where ε is the dielectric constant. F is the Faraday constant, R is the ideal gas constant, T is the temperature of measurement, C_i is the concentration of charged species i with the charge Z_i , e_0 is the elemental electrostatic charge, A_j is the area of the j component of the lipid bilayer, n_j and n_i are the number of moles of the membrane component j and I, n_L is the number of moles of lipid. Equation II. 10 gives the charge density calculated from surface potential and Equation II. 11 gives the charge density calculated from the local concentration of the charged molecules in the membrane. The ratio of lipid to bound amphiphiles should be higher than 20 for small amphiphiles and the ionic strength higher than 100 mM to decrease charge influence in the partition obtained [75]. The use of uptake and release protocols can help to describe the accessible area of lipid

Chapter II

to ligand which allows knowing, during the time scale of each peak, if translocation is fast or slow.

The ITC technique was used for the determination of partition of conjugated and non conjugated BS to lipid membranes (Chapter V).

Chapter III *Direct Non-Invasive*

Quantification of Cholesterol Solubilized in Bile Salt Micellar Aqueous Solutions

This work was published at, F.M. Coreta-Gomes, W.L.C. Vaz, E. Wasielewski, C.F.G.C. Geraldes, and M.J. Moreno, Quantification of cholesterol solubilized in bile salt micellar aqueous solutions using C-13 nuclear magnetic resonance. *Analytical Biochemistry* 427 (2012)

III. 1 - Abstract

In this work we develop a methodology to quantitatively follow the solubilization of cholesterol on glycodeoxycholic acid (GDCA) micelles using ^{13}C NMR. The amount of solubilized cholesterol enriched in ^{13}C at position 4, [4- ^{13}C]cholesterol, was quantified from the area of its resonance, at 44.5 ppm, using the CH_2 groups from GDCA as an internal reference. The loading of the micelles with cholesterol leads to a quantitative high field shift of most carbons in the non-polar surface of GDCA and this was used to follow the solubilization of unlabeled cholesterol. The solubilization followed pseudo first-order kinetics with a characteristic time constant of 3.6 h and the maximum solubility in 50 mM GDCA is 3.0 ± 0.1 mM, corresponding to a mean occupation number per micelle ≥ 1 . The solubilization profile indicates that the affinity of cholesterol for the GDCA micelles is unaffected by the presence of the solute leading essentially to full solubilization up to the saturation limit. The relaxation times of GDCA carbons at 50 mM give information regarding its aggregation, and indicate that GDCA is associated in small micelles ($R_h=13$ Å) without any evidence for formation of larger secondary micelles.

III. 2 - Introduction

Cholesterol homeostasis is a matter of vital importance in animal physiology and perturbations in its normal levels have been associated with diseases from atherosclerosis to diabetes and Alzheimer's disease [76]. The amount of cholesterol in the cell membrane affects their mechanical properties and there is increased evidence for the presence of cholesterol dependent micro-heterogeneity with the coexistence of two immiscible liquid phases [3; 77]. This heterogeneity has been implicated in several cell functions from protein trafficking and signal transduction to infection and lipid homeostasis [3; 78; 79; 80; 81]. The total concentration of cholesterol in the body and its distribution between blood components and tissues is subject to sophisticated regulatory mechanisms [82]. Two major steps are considered critical in the maintenance of cholesterol total concentration [63; 83]: its synthesis in the liver; and the enterohepatic circulation with secretion of cholesterol into bile and its partial re-absorption, together with cholesterol from diet, at the upper intestine. It is now well

established that cholesterol absorption requires its emulsification in mixed bile salt/lipid micelles [2; 5; 60; 84; 85; 86; 87; 88; 89] and passive mechanisms are usually considered predominant based on the relatively fast equilibration of cholesterol between hydrophobic assemblies [90; 91; 92], on the incomplete reduction of cholesterol absorption in the presence of known protein inhibitors [83] and on the fact that humans are able to synthesize the required cholesterol [88]. Cholesterol solubilization in bile salt micelles is also strongly correlated with gallstone formation and this has been addressed by several authors during the last decades [32; 93; 94; 95; 96; 97]. Although much studied, several processes involved in cholesterol homeostasis are still unclear and some important questions still remain, this being true even for the physicochemical characterization of bile salt and lipid mixed micelles and their emulsification of sterols. Additionally, the established methodologies to follow sterol solubilization are based on the physical separation of sterol in the different phases or aggregates of different sizes [29; 30; 38; 41; 93; 98; 99; 100] and those invasive approaches may disturb the equilibrium distributions. In this work we develop methodology that allows the direct quantification of cholesterol emulsified in small micelles, in the presence of large aggregates such as excess cholesterol crystals or lipid vesicles and micro-emulsions. Cholesterol enriched in ^{13}C at carbon 4 was used which allows its detection in sub millimolar concentrations using modern NMR equipment. Small aggregates of emulsified lipid are easily quantified while large aggregates are invisible due to their slow tumbling rate [101]. NMR has been used previously in the study of sterol emulsification by bile salt micelles but it has been limited to qualitative information [102]. The development of NMR equipments with an improved sensitivity and resolution has allowed the quantitative characterization of the chemical commercial availability of ^{13}C enriched cholesterol made possible the work presented in this paper where the quantitative characterization of cholesterol solubilized in small micelles is performed without the need for sample processing.

In this work we establish the methodology with the characterization of the kinetics and maximum solubility of cholesterol in Glycodeoxycholic (GDCA) micelles. This bile salt was chosen because of its high concentration in human bile [16; 86; 99; 103; 104] and its relatively high efficiency in cholesterol emulsification [41; 98; 105]. The aggregation behaviour of the bile salt is critical for its cholesterol solubilizing capacity and it has been the subject of several studies. The critical micellar

concentration (CMC) of GDCA has been re-assessed at the conditions used (aqueous solution with 150 mM NaCl, 10 mM Tris-HCl buffer at pH=7.4, 37 °C) using a probe partition methodology [106] and by isothermal titration calorimetry [33]. The structures of GDCA and [4-¹³C]cholesterol are shown in Figure III. 1.

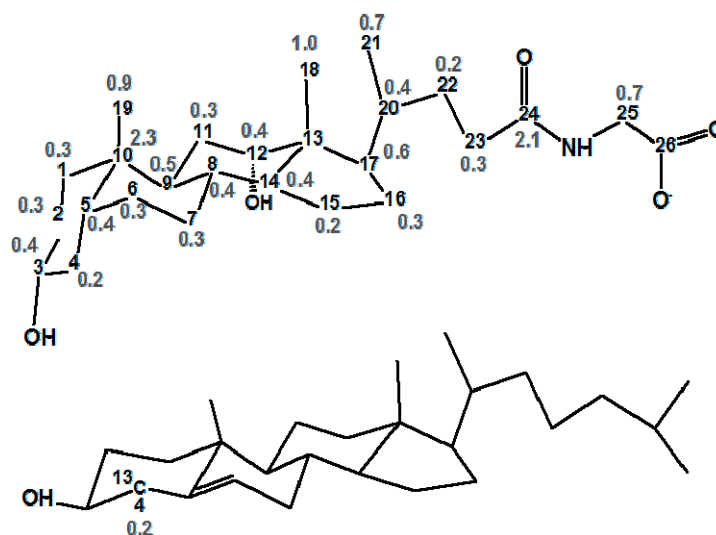


Figure III. 1 Molecular structures of GDCA (top) and [4-¹³C]cholesterol (bottom). The relaxation times (T_1 in s) obtained for each carbon of GDCA and for carbon 4 of cholesterol are also shown.

III. 3 - Materials and methods

III. 3. 1 - Materials

N-phenyl-1-naphthylamine (NPN) was obtained from Merck (Hohenbrunn, Germany), [4-¹³C]cholesterol and deuterium oxide (99.8%) for NMR experiments were obtained from Cortecnet (Paris, France) and sodium glycodeoxycholic acid (GDCA) was bought from Sigma (Steinheim, Germany). The non-aqueous solvents used for sample preparation (chloroform, methanol and acetone) were of spectroscopy grade and the aqueous buffer components (Triz-HCl, NaCl and NaN₃) were of high purity and purchased from Sigma, water was first distilled and further purified by activated charcoal and deionization.

III. 3. 2 - Methods

The Critical Micellar Concentration (CMC) of GDCA was determined using the method developed in [106], based on the increase in the fluorescence quantum yield and shift to smaller wavelengths of NPN upon association with preformed micelles. The total concentration of NPN was 1 μM and the concentrations of GDCA in the aqueous buffer were changed between 0 and 50 mM, at 37 °C. The fluorescent emission of NPN was followed using an excitation wavelength of 330 nm on a Cary Eclipse fluorescence spectrophotometer from Varian (Victoria, Australia) equipped with a thermostated multi-cell holder accessory. The aggregation of GDCA was also characterized by Isothermal Titration Calorimetry (ITC) using a VP-ITC instrument from MicroCal (Northampton, MA, USA) with a reaction cell volume of 1410.9 μL, at 37 °C. The injection speed was 0.5 μL s⁻¹, stirring speed was 199 rpm and the reference power was 10 μcal s⁻¹.

Proton-decoupled ¹³C NMR spectra acquisitions were performed with a Varian VNMRS 600 MHz NMR spectrometer, equipped with a high field "switchable" broadband 5 mm probe with z-gradient. Spectra were acquired at 37 °C with a 90° pulse angle sequence, a spectral width of 31250 Hz with an acquisition time of 2.3 s, a relaxation delay of 7 s and 1024 acquisition scans. Proton decoupling was achieved using a Waltz16 decoupling sequence. ¹³C-¹H} NOE effect was obtained by comparing ¹³C spectra with full proton decoupling to ¹³C spectra with proton decoupling only during acquisition

(spectra acquired with 3000 scans). Spectra were processed with MestreNova 6.1.1 (Mestrelab Research S.L., Santiago de Compostela, Spain).

Aqueous suspensions of [4-¹³C]cholesterol were prepared by evaporating the required volume of a solution in chloroform/methanol (87/13, v/v), blowing dry nitrogen over the heated (blowing hot air over the external surface of the tube) solution, and removal of organic solvent traces in a vacuum desiccator for 30 min at 23°C. The glass tube with the dry residue was then transferred to a thermostatic bath at 37 °C and hydrated with a preheated solution of GDCA in the aqueous buffer (Tris-HCl 10 mM at pH 7.4, 0.15 M NaCl, 1 mM EDTA and 0.02% NaN₃ in D₂O), and was continuously stirred at 100 rpm. The molar concentration of bile salt plus sterol was maintained at 50 mM along all the experiments. The samples were left in the bath with continuous stirring during the specified period (experiments on the kinetics of emulsification) or up to 24 to 36 h (experiments on the maximum solubilization) and then characterized by ¹³C NMR to obtain the amount of solubilized cholesterol using the GDCA signal as an internal standard.

The solubilization of cholesterol in GDCA micelles may proceed via interaction of cholesterol solubilized in the aqueous phase with the micelles or by direct interaction of GDCA (as monomer or in micelles) with the cholesterol film. The mechanism is not known but both processes are expected to occur. For simplicity, in the kinetic scheme used, Equation III. 1, we have considered only direct interaction between the micelles (M) and solid cholesterol (C_S, which may be as a film or in crystals suspended in the aqueous phase) to generate cholesterol emulsified in the micelles (C_M).



The rate constants k_1 and k_{-1} are the forward and reverse rate constants for solubilization in the micelles.

From the kinetic scheme shown in Equation III. 1 one may obtain the rate equation for the amount of cholesterol solubilized in the micelles, Equation III. 2.

$$[C_M]_{(t)} = [C_M]_{(\infty)} + \left([C_M]_{(0)} - [C_M]_{(\infty)} \right) \times e^{-k_d t} \quad \text{Equation III. 2}$$

Chapter III

The solubilization rate constant (k_d) is a function of the forward and reverse rate constants ($k_d = k_1[M] + k_{-1}$), $[C_M]_{(0)}$ and $[C_M]_{(\infty)}$ are the concentration of cholesterol solubilized immediately after the addition of the micelles and at equilibrium, respectively. The best fit of Equation III. 2 to the experimental results, using Excel and Solver (Microsoft, Seattle, WA), allowed the calculation of the characteristic rate constant for cholesterol dissolution in the micelles (k_d) and the maximum amount of cholesterol solubilized $[C_M]_{(\infty)}$.

III. 4 - Results and discussion

III. 4. 1 - Determination of GDCA Critical Micelle Concentration

For the solubilization of cholesterol the bile salt must be associated in micelles and therefore the characterization of GDCA critical micellar concentration is an important parameter for the rationalization of the maximum amount of solubilized cholesterol. This parameter has been previously measured by other authors [25; 29; 30] and it was found to depend strongly on the properties of the aqueous solution namely its ionic strength [25] and temperature [33]. We have therefore measured the CMC of GDCA in the aqueous buffer solution and temperature used in this work from the variation of N-phenyl-1-naphthylamine (NPN) fluorescence quantum yield and maximum wavelength when in the presence of GDCA micelles [106].

The value obtained for GDCA CMC, 1.7 mM, is similar to those reported in the literature for the same value of pH and ionic strength being somewhat larger than the first CMC observed by pyrene fluorescence and light scattering, 1.2 mM, [30] and smaller than the mid transition observed by isothermal titration calorimetry (ITC), 2 mM, [29]. Roda and co-workers have also followed the micelization of GDCA by surface tension and probe solubilization and found similar values for the CMC at pH=8, 2.0 mM and 2-3 mM respectively, [25]. The different values reported are dependent on the techniques used to follow the formation of the micelles which have different relative sensibilities for smaller and larger aggregates. We have also followed the process of demicelization of GDCA by ITC and the results obtained are shown in Figure III. 2 plot B. A broad transition was observed from 1.2 to 3.5 mM with a maximal heat variation at 2.2 mM. The heat variation as a function of the concentration of GDCA was analyzed using the same procedure as for NPN fluorescence to obtain the CMC – intercept of the two linear regimes – leading to 1.6 mM, in very good agreement with the results obtained from NPN partition.

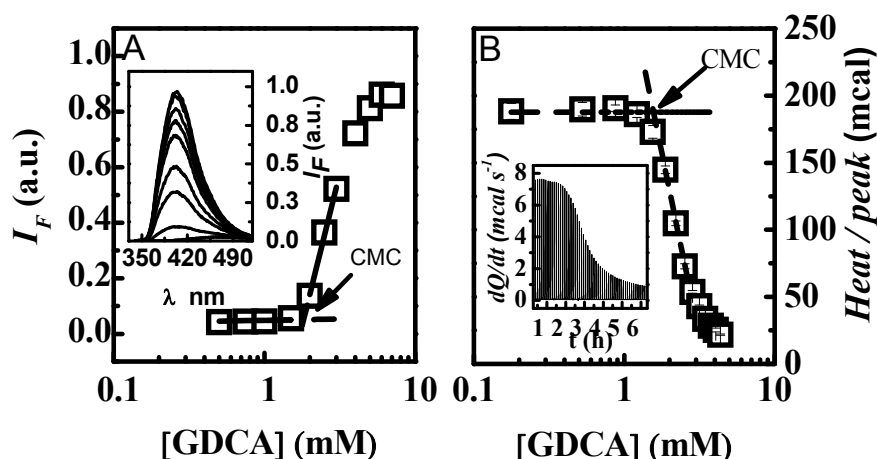


Figure III. 2 Plot A: Fluorescence emission spectra (insert) and integrated intensity (350 - 500 nm) of NPN in the presence of different concentrations of GDCA (\square) in aqueous buffer at 37 °C. Plot B: Thermogram obtained due to the addition of 5 μ L aliquots of GDCA 25 mM into aqueous buffer at 37 °C (insert) and heat evolved as a function of the concentration of GDCA in the ITC cell. The linear best fit to the two regimes is also shown and the CMC is obtained from the intercept of the two lines leading to 1.7 mM (plot A) and 1.6 mM (plot B).

III. 4. 2 - Solubilization of [4-¹³C]cholesterol in GDCA micelles

We have followed the solubilization of cholesterol in GDCA micelles by ¹³C NMR using cholesterol enriched in ¹³C at position 4, [4-¹³C]cholesterol. The solubilization of cholesterol in bile salt micelles was previously attempted using ¹H NMR but only qualitative information could be obtained due to the complexity of the NMR spectra [102]. The approach followed in the present work results in a carbon resonance from cholesterol well isolated from GDCA resonances that allows its accurate quantification. The slow tumbling of the excess cholesterol in crystals generates very broad peaks that are included in the baseline being invisible by NMR. This property, previously used by other authors [107; 108] to qualitatively follow emulsification of cholesterol and/or lecithin in bile salt micelles, allows the quantification of emulsified cholesterol in the presence of large aggregates without the need to perform any sample processing such as the filtration or size exclusion chromatography required in previous work [29; 30; 38; 41; 93; 98; 99; 100]

In Figure III. 3 are shown typical ¹³C NMR spectra obtained for GDCA in D₂O buffer. The insert shows the absorption spectra near the resonance from [4-¹³C]cholesterol for

GDCA alone (A), and in the presence of 1mM (B) and 3 mM (C) cholesterol, at a total concentration of lipid (GDCA+cholesterol) equal to 50 mM. The resonances from GDCA were attributed according to previous work [99].

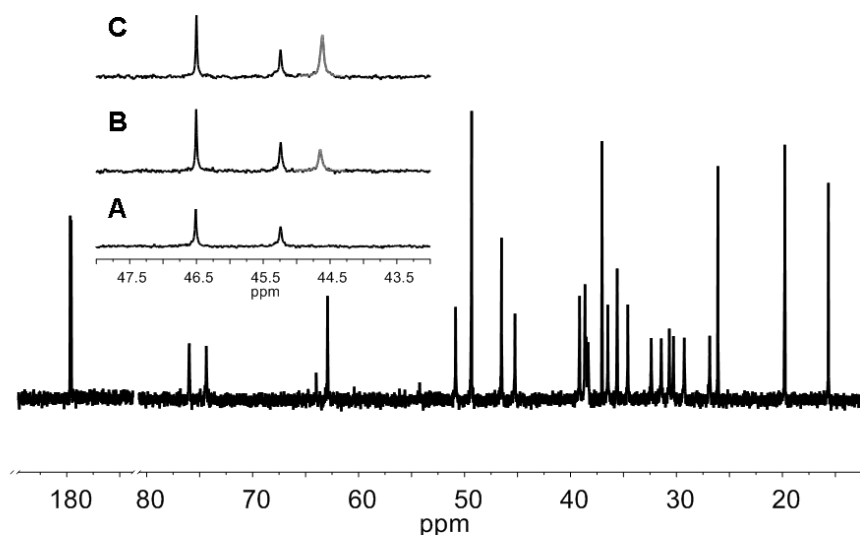


Figure III. 3 ^{13}C NMR spectra of GDCA in D_2O aqueous buffer solution at 37°C , obtained on a Varian 600 MHz spectrometer (—), with ^1H decoupling and NOE. GDCA assignments were compared with those obtained elsewhere [109]. The insert plots are expansions of the spectra of GDCA in absence (A) and in the presence of $[4\text{-}^{13}\text{C}]$ cholesterol 1 mM (B) or 3 mM (C). The resonance of carbon 4 from cholesterol is fitted with the gray line (—).

Those results clearly show that the resonance from carbon 4 of cholesterol is easily distinguished from those of GDCA and that the method has enough sensitivity to allow the quantification of solubilized cholesterol. The spectra in Fig.III.3 were obtained using a 90° pulse, with $^{13}\text{C}\text{-}\{^1\text{H}\}$ Nuclear Overhauser Enhancement (NOE), to improve the method sensitivity, and with a relaxation delay (D_1) of 7 s that allows the full relaxation of all nuclei with the exception of the carbonyl and quaternary carbons, see Table III. S 1 in the supplementary material and Figure III. 1. The presence of the NOE has the inconvenience that the areas are no longer proportional to the concentration of the resonant carbon. To re-establish the quantitative value of the NMR spectra, the NOE factor must be calculated for each carbon. Those factors have been calculated through the comparison between the areas obtained with (^1H decoupling throughout the entire experiment) and without NOE (^1H decoupling only during the acquisition step) after

3000 scans and are given in Table III. S 2 of the supplementary material. This information allow us to take advantage of the NOE improvement in sensitivity (that allowed running a well defined spectra with only 1024 scans) while retaining quantitative power. The concentration of solubilized cholesterol was calculated using the CH₂ groups of GDCA as internal standard and taking into account the natural enrichment in ¹³C of GDCA and full enrichment for cholesterol carbon 4, as explained in detail in Table III. S 3 of the supplementary material.

The kinetics of cholesterol solubilization by GDCA micelles was obtained from the analysis of samples with 47 mM GDCA added to a cholesterol film that would lead to a total cholesterol concentration of 3 mM if completely dissolved. Several independent samples were prepared and their NMR spectrum was measured at given times after addition of GDCA to the cholesterol film. Typical results are shown in Figure III. 4 showing that equilibrium is essentially achieved after 10 h and that the amount of solubilized cholesterol remains unchanged up to 60 h. Some additional experiments were performed at different total concentrations of cholesterol and the values obtained for the characteristic solubilization time were similar (data not shown).

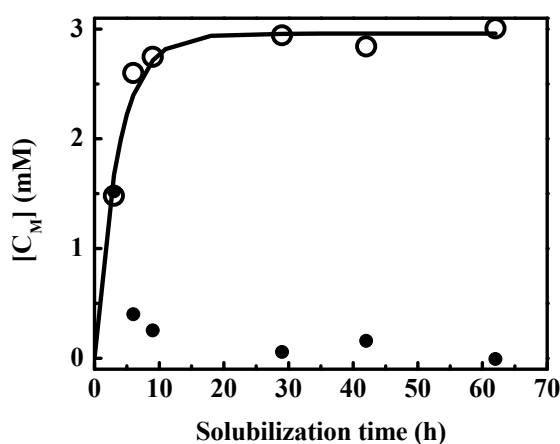


Figure III. 4 Typical kinetic profile obtained for the solubilization of a [4-¹³C]cholesterol film (3 mM) by 47 mM GDCA micelles at 37 °C (○). The line is the best fit of Equation III. 2 with $k_d = 1.6 \times 10^{-3} \text{ s}^{-1}$ (leading to a characteristic solubilization time, τ_d , equal to 3.6 h), $[C_M]_{(\infty)} = 3 \text{ mM}$ and $[C_M]_{(0)} = 0 \text{ mM}$. The amount of cholesterol not solubilized (●) is also shown.

After knowing the characteristic time for solubilization, the cholesterol film of several samples with increasing concentrations of cholesterol (from 0.5 up to 5 mM) were prepared. An aqueous solution of GDCA (giving a total lipid concentration of 50 mM) was added and the NMR spectrum was measured 24 to 36 h after. Typical results obtained are shown in Figure III. 5 which allows the calculation of the maximum value for cholesterol solubilization (Cholesterol Saturation Index, CSI) in GDCA micelles at 50 mM total lipid concentration. The CSI value considered in GDCA micelles was obtained from the intercept of both regimes and is equal to 3.0 ± 0.1 mM.

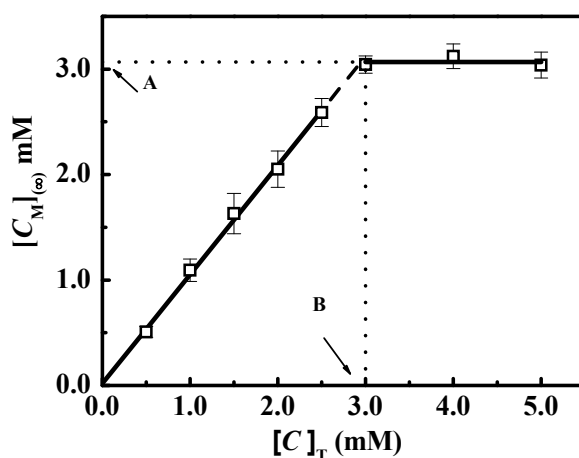


Figure III. 5 Concentration of $[4-^{13}\text{C}]$ cholesterol solubilized by GDCA micelles ($[C_M]_{(\infty)}$) as a function of the total concentrations of cholesterol ($[C]_T$) for a total concentration of lipid equal to 50 mM at 37 °C. The CSI value may be obtained from the maximum $[C_M]_{(\infty)}$ (3.1 mM, point A), or from the intersection of the best fit to both regimes in cholesterol solubilization (3.0 mM, point B). The values shown are the average and standard deviation of at least three independent experiments.

The results obtained show a complete solubilization of cholesterol up to a total concentration of 3.0 mM above which no further cholesterol may be solubilized by the GDCA micelles. This indicates that the partition coefficient of cholesterol between the aqueous solution and the GDCA micelles remains unchanged up to the maximum amount of cholesterol solubilized. Micelles saturated with cholesterol are therefore expected to retain their ability to solubilize other solutes structurally unrelated with cholesterol.

Chapter III

Solubilization of cholesterol by bile salts in general, and by GDCA in particular, has been previously studied by other authors where micelles and small aggregates were physically separated from cholesterol crystals and large aggregates followed by quantification of cholesterol in the solubilized fraction (see for example references [29; 30; 38; 41; 93; 98; 99; 100]). The cholesterol saturation index obtained in this work for GDCA micelles is significantly higher than the values obtained previously at the same concentration of GDCA: 2.0 mM in water at pH~7 [98], 2.2 mM in 50 mM carbonate buffer at pH=10 with 100 mM NaCl [41], and 2.5 mM in 10 mM Tris-HCl buffer at pH=7.5 with 150 mM NaCl [30] this last work at experimental conditions equivalent to the current ones.

The much smaller emulsification efficiencies encountered [41; 98] are partially due to the use of cholesterol monohydrate crystals, whose increased stability leads to a shift in the equilibrium towards the crystalline form [32]. Cholesterol films prepared from organic solvents usually lead to anhydrous cholesterol crystal [32] and in fact, the shape of the crystals obtained in this work at conditions of excess [4-¹³C]cholesterol indicate that anhydrous crystals are formed. This effect explains the small increase observed in the later work [30] as compared with previous reports [41; 98], but cannot justify the larger solubilization efficiency found in this work. The higher value now obtained must be related with the elimination of the step of physical separation between the different cholesterol phases indicating that some solubilized cholesterol was lost during the separation process. We note additionally that for some cholesterol samples the amount of solubilized cholesterol was somewhat smaller with the presence of crystals with the morphology of the hydrated form. This was interpreted as being the result of small amounts of water in the cholesterol powder and/or in the organic solvent used to prepare the film.

From the maximum amount of solubilized cholesterol and the aggregation parameters of GDCA the average occupation number of cholesterol in the micelles could be calculated giving important information regarding the local concentration of cholesterol in the micelles. The value obtained by us for the CMC (1.6 to 1.7 mM), as well as those reported in the literature (1.2 to 2 mM) [25; 29; 30], indicates that most GDCA is associated in micelles at the total concentration used in this work, ~50 mM. The second parameter required, the aggregation number, is however not well defined making the calculation of the micelle concentration a difficult task. The size of bile salt micelles has

been characterized by ultracentrifugation [23], static light scattering [28; 30; 37; 110; 111; 112; 113; 114], dynamic light scattering [110; 113] and by freezing point depression [115]. Those measurements give the average molecular weight or hydrodynamic radius of the aggregates from which the mean aggregation number may be calculated. It is usually considered that bile salts have complex aggregation behaviour with the formation of primary and secondary micelles depending on their total concentration [23]. From the techniques used for the characterization of bile salt aggregation, the only one that could give a detailed description of this behaviour is dynamic light scattering with quantitative information of all scattering species. This was however not performed in the indicated references where only the average aggregation parameters were reported. The mean aggregation number reported for GDCA at neutral or alkaline pH, with 150 mM NaCl, ranges from 15 [114] to 22 [41]. The dependence of the size of the micelles on the total concentration of bile salt was somewhat better characterized for the taurine conjugate (TDCA) where an increase in the mean occupation number was clearly shown at high ionic strength [113] and no significant effects were observed without added salts [115].

Given the poor definition of the aggregation number of GDCA micelles, and in particular at a total concentration of 50 mM, it is not possible to calculate accurately the mean occupation number of cholesterol. If the extreme values reported are used the calculated mean occupation number varies from 1.0 to 1.4.

III. 4. 3 - Effects of solubilized cholesterol in GDCA NMR spectra

Despite the large uncertainty in the mean occupation number of cholesterol in the GDCA micelles at saturation, most micelles have at least one cholesterol molecule and some effect of the solubilize on the surfactant properties is anticipated. In fact, we have observed a frequency shift of the resonances from most GDCA carbons in direct proportion to the amount of cholesterol solubilized, Figure III. 6 and Table III. S 4.

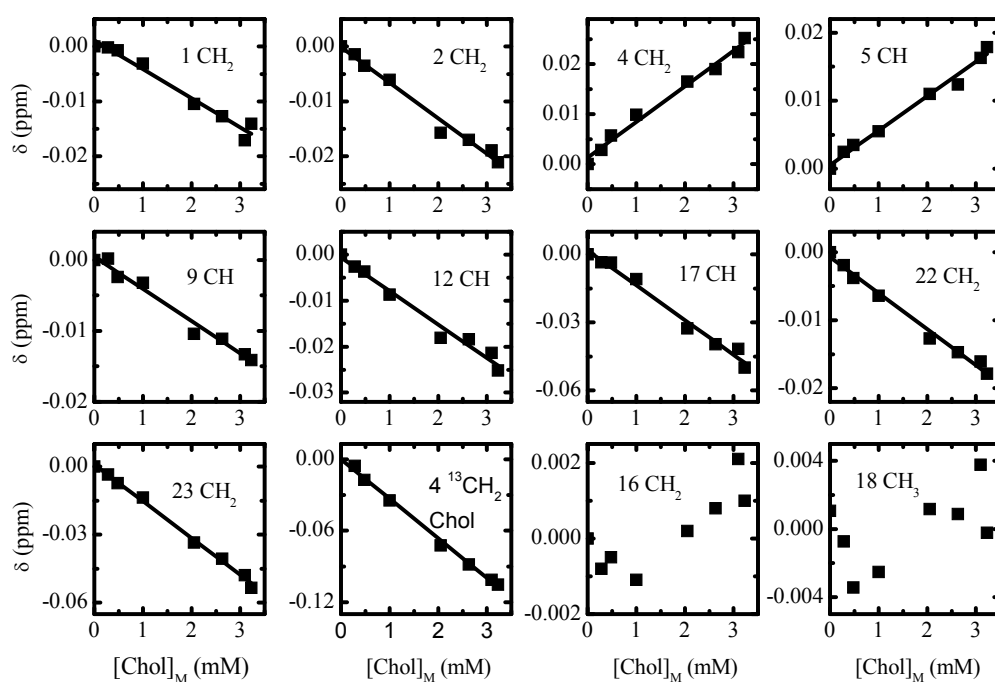


Figure III. 6 Resonance shifts observed for GDCA carbons 1, 2, 4, 5, 9, 12, 17, 22 and 23, as a function of the concentration of solubilized $[4-^{13}\text{C}]$ cholesterol, after using the resonance of GDCA carbon 18 as an internal reference to reduce uncertainty. The resonance shift of carbon 4 of $[4-^{13}\text{C}]$ cholesterol and carbon 16 of GDCA is also shown, as well as raw data obtained for GDCA carbon 18.

Those shifts are a result of an altered environment around the nuclei [24] and allow the quantification of solubilized solute, Figure III. 7. A single resonance was always observed for each nucleus indicating that cholesterol exchange between micelles is faster than the time scale of the NMR technique.

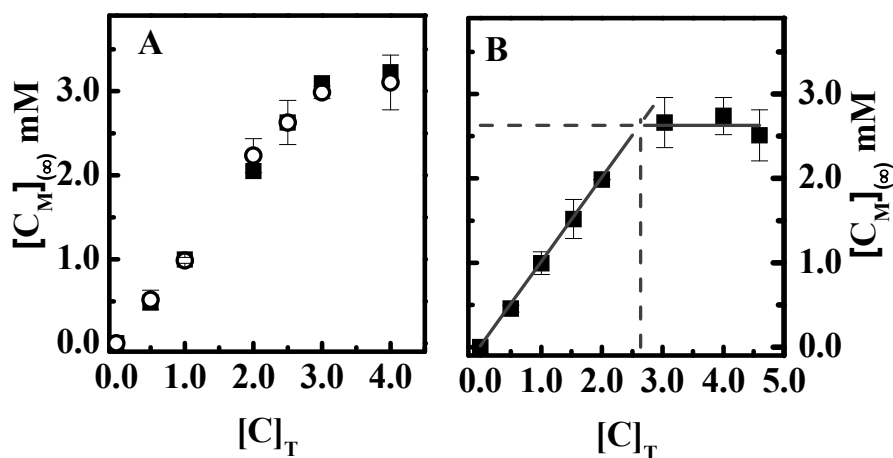


Figure III. 7 Solubilization of $[4-^{13}\text{C}]$ cholesterol (plot A) and cholesterol (plot B) by GDCA micelles ($[C]_{M(\infty)}$) as a function of the total concentration of cholesterol ($[C]_T$) for a total lipid concentration equal to 50 mM at 37 °C. The amount of cholesterol solubilized was obtained from the area of its resonance for $[4-^{13}\text{C}]$ cholesterol (○) or from the shift observed on the bile salt resonances (■) (plot A and B). The lines are the best fit to the two regimes for unlabeled cholesterol solubilization and their intersection gives the cholesterol Saturation Index 2.7 ± 0.1 mM.

The resonance frequency from most carbons was affected by the presence of cholesterol. To improve the reproducibility in the resonance frequencies between different experiments, we have used the methyl resonance from GDCA carbon 18 as an internal reference and it was fixed at 15.37 ppm. This reference was chosen because its chemical shift was not dependent on the concentration of solubilized cholesterol and showed a relatively small standard deviation, lower right panel of Figure III. 6. The carbons which showed a significant shift in their resonances due to the presence of solubilized cholesterol (> 0.005 ppm *per* mM cholesterol) and with a correlation coefficient (R^2) for a linear dependence ≥ 0.97 are carbons 1, 2, 4, 5, 9, 12, 17, 22 and 23, see Figure III. 6 and Figure III. S 4 in the supplementary materials for details. The resonance shift for most carbons – with the exception of 6, 11, 15, 16 and 18 (this last one used as reference) - showed a linear dependence with the amount of solubilized cholesterol with $R^2 \geq 0.9$ and the resonance from $[4-^{13}\text{C}]$ cholesterol itself was strongly correlated with the concentration of cholesterol solubilized with a slope equal to -0.033

ppm/mM and $R^2 = 0.996$. The shift encountered for the nuclei that showed strong correlation is given in Figure III. 6 (together with the results obtained for 16 C as an example of one nucleus not significantly affected, and with the raw data obtained for 18C). The slope obtained from the linear fit was used to calculate the amount of [4- ^{13}C]cholesterol solubilized in the micelles and this is shown in Figure III. 7 plot A. This dependence was also used to calculate the amount of unlabeled cholesterol solubilized in GDCA micelles, the results are shown in Figure III. 7 plot B. The solubilization profile obtained for cholesterol is similar to that obtained for [4- ^{13}C]cholesterol as expected from the similar properties of both molecules. The value obtained for the saturation index (2.7 mM) is however significantly smaller than that obtained for [4- ^{13}C]cholesterol. This highlights the influence of the solute powder characteristics on the type of crystals formed and consequently on the maximal amount solubilized.

The distinct sensibility of GDCA carbons on the presence of solubilized cholesterol allow us to speculate regarding the localization of cholesterol in the micelles. Bile salt aggregation is usually considered to depend on its total concentration with the formation of small micelles (primary micelles, up to 10 molecules) at concentrations close to the CMC, and larger micelles (secondary micelles, formed by the association of primary micelles) at higher concentrations [23]. The observation that cholesterol solubilization by bile salt micelles is more efficient at higher concentrations lead to the suggestion that solubilized cholesterol may be located preferentially at secondary micelles, between the outer surfaces of the primary micelles in the larger aggregates [28]. It is also usually considered that the most hydrophobic surface of the bile salt is hidden from the aqueous solution when primary micelles are formed [107] while the formation of the secondary micelles is driven by the remaining hydrophobicity of the more polar surface and by hydrogen bonding between bile salt hydroxyl groups [23]. Within this picture, the results obtained in this work (significant shift proportional to solubilized cholesterol, for carbons 1, 2, 4, 5, 9, 12, 17, 22 and 23) indicate that cholesterol is preferentially located in the core of primary micelles, near the most hydrophobic surface of GDCA.

III. 4. 4 - GDCA dynamics

From the ^{13}C T_1 relaxation times obtained, Figure III. 1, one can obtain some information regarding the dynamics of GDCA in micelles and solubilized cholesterol. Within the CH_2 groups, T_1 varies between 0.2 and 0.3 s for atoms in the fused ring and up to C 23 being 0.7 s for C 25 in the glycine head group. This indicates that C 25 experiences internal mobility while the atoms in the sterol moiety can only move as a whole. The relaxation time observed for the ^{13}C labelled methylene carbon of cholesterol (0.2 s) indicates that the mobility of the solute is similar to that of the host micelle. An inspection of the results obtained for the CH_3 groups of GDCA reveals that the micelle is most compact at the interface between the fused ring and the GDCA carbonyl group in agreement with the low mobility obtained for C 22 and C 23.

The relaxation times observed for the less mobile groups may be used to calculate a micelle correlation time [66], this being ≥ 1.5 ns. This can in turn be used to estimate the minimum size of GDCA micelles, using the Perrin equation for a sphere [116], leading to an hydrodynamic radius of 13 Å, for $\eta = 0.7195$ cp [117]. The calculated radius is similar, although somewhat smaller, than the one reported by light scattering $R_h = 22$ Å [114].

III. 5 - Conclusions

Cholesterol, enriched in ^{13}C at carbon 4, solubilized in GDCA micelles was quantitatively measured by ^{13}C NMR indicating an efficient solubilization with a pseudo first order characteristic time constant of 3.6 h and a mean occupation number above 1 at saturation. In spite of the high mean occupation number obtained, the solubilization profile shows that the affinity of cholesterol for the micelles is unchanged up to the saturation point and this indicates that GDCA micelles retain their ability to solubilize other solutes structurally unrelated to cholesterol. This explains the non-competitive solubilization of cholesterol and aromatic hydrocarbons, or small chain alkyl benzenes, by bile salt micelles [118]. Conversely, the maximum solubility of cholesterol in bile salt micelles is expected to decrease due to the presence of solutes that co-crystallize with cholesterol [29; 118] as a result of the decreased aqueous solubility [119].

Solubilized cholesterol affects significantly the chemical shift of most GDCA carbons in the non-polar surface indicating that it is preferentially located in the hydrophobic core of primary micelles. This shift in GDCA resonances may be used to quantitatively follow solubilization of NMR silent solutes and this was shown for the case of unlabeled cholesterol.

The critical micelle concentration of GDCA measured by probe partition and heat of demicelization indicates that most bile salt is aggregated in micelles at the concentrations used, in agreement with previous results. Some information regarding the size of the micelles was obtained from the ^{13}C T_1 relaxation times of GDCA and no evidence was encountered for the formation of large secondary micelles at a total concentration of bile salt equal to 50 mM.

III. 6 - Supplementary material

Table III. S 1 ^{13}C Longitudinal relaxation times (T_1) for GDCA carbons and carbon 4 of $[4\text{-}^{13}\text{C}]$ cholesterol. The T_1 values from C26 and C13 where not obtained due the use of time interval smaller than the necessary to measure the T_1 for this carbons.

Resonances	p.p.m.	T_1 (s)
C 24	179.67	2.1
C 26	179.53	
CH 12	75.95	0.4
CH 3	74.32	0.4
CH 14	50.78	0.4
CH 17	49.30	0.6
C 13	49.26	
CH ₂ 25	46.44	0.7
CH 5	45.18	0.4
CH ₂ [4- ^{13}C]cholesterol	44.51	0.2
CH 8	39.08	0.4
CH 20	38.56	0.4
CH ₂ 1	38.44	0.3
CH ₂ 4	38.27	0.2
C 10	36.97	2.3
CH 9	36.42	0.5
CH ₂ 23	35.52	0.3
CH ₂ 22	34.52	0.2
CH ₂ 2	32.29	0.3
CH ₂ 11	31.36	0.3
CH ₂ 16	30.59	0.3
CH ₂ 6	30.21	0.3
CH ₂ 7	29.17	0.3
CH ₂ 15	26.80	0.2
CH ₃ 19	26.02	0.9
CH ₃ 21	19.71	0.7
CH ₃ 18	15.60	1

Table III. S 2 $^{13}\text{C}\{-^1\text{H}\}$ Nuclear Overhauser Effect (NOE) on a solution of GDCA 49 mM with 1 mM of $[4\text{-}^{13}\text{C}]$ cholesterol, in D_2O buffer at 37 °C, obtained on a Varian 600 MHz spectrometer, with 90° pulse, D1=7 s, gain of 40, 3000 scans. The NOE effect (η^1) and correction factor (C.F.) were obtained via comparison of the spectra with ^1H decoupling along all the pulse (with NOE) and decoupling only along the acquisition time (without NOE). The table shows the average and standard deviation of two independent experiments for each resonance of GDCA and for carbon 4 of $[4\text{-}^{13}\text{C}]$ cholesterol.

Carbon number	Carbon type	p.p.m.	η	C.F.	Error (%)	Average	Error(%)
10	C	36.77	0.40	0.71	1.4	Quaternary	
13	C	49.06	0.52	0.76	19.4		
24	C	179.67	0.21	0.81	3.2		
26	C	179.44	0.23	0.81	0.8		
3	CH	74.21	0.45	0.69	8.3	Tertiary	
5	CH	44.93	0.55	0.73	0.1		
8	CH	38.87	0.46	0.70	7.7		
9	CH	36.22	0.64	0.65	1.7		
12	CH	75.85	0.38	0.64	11.1		
14	CH	50.60	0.52	0.66	6.8		
17	CH	49.13	0.38	0.90	4.2		
20	CH	38.36	0.08	0.67	11.8		
1	CH ₂	38.17	1.03	0.65	17.2	Methylene	
2	CH ₂	32.02	0.69	0.68	12.9		
4	CH ₂	37.98	0.60	0.70	13.7		
6	CH ₂	30.00	0.76	0.65	13.4		
7	CH ₂	28.99	0.46	0.66	4.8		
11	CH ₂	31.14	0.40	0.72	2.2		
15	CH ₂	26.60	0.46	0.67	10.5		
16	CH ₂	30.42	0.61	0.64	2.5		
22	CH ₂	34.37	0.62	0.65	7.4		
23	CH ₂	35.33	0.59	0.59	0.9		
25	CH ₂	46.19	0.42	0.51	5.7		
18	CH ₃	15.42	1.35	0.52	4.9	Methyl	
19	CH ₃	25.83	1.03	0.49	0.4		
21	CH ₃	19.47	0.87	0.44	4.0		
$[4\text{-}^{13}\text{C}]$ chol	CH ₂	44.50	0.27	0.77	3.1		

$^1\eta = \frac{I - I_0}{I_0}$ where I is the area with NOE and I_0 the area without NOE. The correction factor is

given by $\frac{1}{1 - \eta}$

Table III. S 3 Chemical shifts assignments, peak area, and quantification results from a ^{13}C NMR spectra obtained for an aqueous solution of GDCA 47 mM with [120]cholesterol 3 mM in a D_2O buffer, without NOE (correction factor times area with NOE) at 37 °C, obtained on a Varian 600 MHz spectrometer. The methylene carbons (gray) where the resonances from the bile salt that were used for the quantification.

Carbon number	Carbon Type	ppm	Area With NOE	Area Without
24	C	179.67	354.1	286.3
26	C	179.53	299.5	242.3
12	CH	75.95	386.3	246.5
3	CH	74.32	344.1	236.3
14	CH	50.78	358.0	234.5
17	CH	49.30	236.9	213.9
13	C	49.26	541.9	413.5
25	CH ₂	46.44	443.7	228.3
5	CH	45.18	322.8	234.4
[4- ^{13}C]chol	CH ₂	44.51	1918.9	1476.4
8	CH	39.08	362.8	252.4
20	CH	38.56	358.3	238.3
1	CH ₂	38.44	407.8	263.4
4	CH ₂	38.27	404.5	281.3
10	C	36.97	385.8	272.8
9	CH	36.42	383.6	251.2
23	CH ₂	35.52	438.1	257.7
22	CH ₂	34.52	380.9	247.6
2	CH ₂	32.29	314.6	214.1
11	CH ₂	31.36	382.1	274.2
16	CH ₂	30.59	350.8	222.9
6	CH ₂	30.21	379.5	247.0
7	CH ₂	29.17	341.5	226.1
15	CH ₂	26.80	377.5	253.2
19	CH ₃	26.02	546.8	268.3
21	CH ₃	19.71	571.7	250.4
18	CH ₃	15.60	537.6	277.2

$[C_M]$	s.d.
3.0	0.1

$$[C_M] = [BS] \frac{A_{Chol} (\text{without NOE})}{A_{BS} (\text{without NOE})} \frac{1.103}{100} \quad \text{Equation III. 3}$$

The concentration of emulsified cholesterol considered was the average of the different values obtained using Equation III. 3 for each BS CH₂ resonance.

Table III. S 4 Chemical shifts of GDCA carbon resonances as a function of solubilized [4-¹³C]cholesterol. The ¹³C NMR spectra were obtained on D₂O buffer at 37 °C using a Varian 600 MHz spectrometer. The carbon resonances in bold gray show a significant shift (slope ≥ 0.005 ppm and R² ≥ 0.97), proportional to the amount of the solubilized cholesterol as measured by the area of [4-¹³C]cholesterol.

GDCA		[C _T] (mM)								
Carbon number	Carbon type	0.3	0.5	1.0	2.0	2.6	3.1	3.2	Slope (m _i)	R ²
24	C	-0.001	0.001	0.003	0.006	0.012	0.013	0.012	0.004	0.94
26	C	0.000	0.002	0.003	0.007	0.012	0.012	0.013	0.004	0.98
12	CH	-0.003	-0.004	-0.009	-0.018	-0.018	-0.021	-0.025	-0.007	0.98
3	CH	-0.001	-0.002	-0.003	-0.009	-0.009	-0.013	-0.015	-0.004	0.97
14	CH	-0.001	-0.005	-0.008	-0.015	-0.016	-0.014	-0.017	-0.005	0.92
17	CH	-0.003	-0.004	-0.011	-0.033	-0.040	-0.042	-0.050	-0.015	0.98
13	C	0.000	-0.001	-0.002	-0.007	-0.008	-0.009	-0.010	-0.003	0.98
25	CH ₂	0.001	-0.001	-0.002	-0.007	-0.006	-0.007	-0.007	-0.002	0.94
5	CH	0.003	0.004	0.005	0.011	0.012	0.016	0.018	0.005	0.99
8	CH	0.000	-0.002	-0.003	-0.006	-0.009	-0.008	-0.011	-0.003	0.96
20	CH	0.003	0.004	0.005	0.009	0.009	0.009	0.010	0.003	0.88
1	CH ₂	0.000	-0.001	-0.003	-0.010	-0.013	-0.017	-0.014	-0.005	0.97
4	CH ₂	0.003	0.006	0.010	0.017	0.019	0.022	0.025	0.007	0.99
10	C	0.001	0.002	0.003	0.003	0.005	0.004	0.004	0.001	0.84
9	CH	0.000	-0.002	-0.003	-0.010	-0.011	-0.013	-0.014	-0.005	0.98
23	CH ₂	-0.003	-0.007	-0.014	-0.033	-0.041	-0.048	-0.053	-0.016	1.00
22	CH ₂	-0.002	-0.004	-0.006	-0.013	-0.015	-0.016	-0.018	-0.005	0.99
2	CH ₂	-0.001	-0.004	-0.006	-0.016	-0.017	-0.019	-0.021	-0.006	0.99
11	CH ₂	0.004	0.002	0.003	0.002	0.002	0.004	0.004	0.000	0.19
16	CH ₂	-0.001	0.000	-0.001	0.000	0.001	0.002	0.001	0.001	0.67
6	CH ₂	0.004	0.002	0.000	-0.001	-0.001	-0.001	-0.001	-0.001	0.47
7	CH ₂	-0.001	-0.002	-0.004	-0.008	-0.012	-0.012	-0.011	-0.004	0.97
15	CH ₂	0.003	0.001	0.004	0.002	0.003	0.003	0.003	0.001	0.24
19	CH ₃	0.001	0.001	0.002	0.004	0.005	0.004	0.005	0.002	0.95
21	CH ₃	-0.001	-0.002	-0.004	-0.010	-0.011	-0.013	-0.013	-0.004	0.99
18	CH ₃	The chemical shift of this resonance showed the smaller dependence on the concentration of solubilized cholesterol and was used as internal reference.								

Steps required in to calculate the concentration of solubilized cholesterol from the shift observed on the resonances of the GDCA carbons.

The resonances from the GDCA carbons indicated in gray in Table III. S 4 were linearly dependent on the concentration of cholesterol solubilized by the micelles (when measured by the intensity of [4-¹³C]cholesterol signal) and were used to calculate the concentration of unlabeled cholesterol solubilized in the micelles.

The slope was calculated from the best fit of Equation III. 5 to the experimental results, where $\Delta\delta_i$ is the variation in the chemical shift of carbon i when the amount of [4-¹³C]cholesterol solubilized was equal to $[^{13}C_M]$ as quantified by Equation III. 4, and is given in Table III. S. 4 together with the correlation coefficient.

$$\Delta\delta_i = m_i [^{13}C_M] \quad \text{Equation III. 4}$$

The concentration of unlabeled cholesterol solubilized in the GDCA micelles was calculated from the value observed for $\Delta\delta_i$ and the slope given in Table III. S 4. The values shown in the manuscript are the average ($\overline{[C_M]}$) and standard deviation ($\sigma_{[C_M]}$) of the concentration of cholesterol calculated from the slopes of each GDCA carbon shown in gray in Table III. S 4 ($[C_M]_i$), Equation III. 5.

$$[C_M]_i = \frac{\Delta\delta_i}{m_i}; \quad \overline{[C_M]} = \frac{1}{n} \sum_{i=1}^n [C_M]_i; \quad \sigma_{[C_M]} = \sqrt{\frac{\sum_{i=1}^n ([C_M]_i - \overline{[C_M]})^2}{(n-1)}} \quad \text{Equation III. 5}$$

An example is given in Table III. S 5.

Table III. S 5 Concentration of cholesterol solubilized in GDCA micelles calculated from the variation observed in the resonance of GDCA carbons, for the case where 1.5 mM total unlabeled cholesterol was equilibrated with 48.5 mM GDCA. Only the carbons shown in gray in Table III. S 4 were considered.

GDCA		Conversion of BS resonances shift into solubilized cholesterol concentration on BS micelles							
Carbon number	Carbon type	Chemical Shift Variation	Slope (m_i)	δ_{GDCA} GDCA 50 mM	$\delta_{GDCA+chol}$ GDCA 48.5 mM Chol _{unlabelled} 1.5 mM	$\Delta\delta$	$[C_M] \text{ (mM)} = \frac{\Delta\delta}{m_i}$	$[C_M] \text{ (mM)}$	s.d.
12	CH		-0.007	75.728	75.716	-0.012	1.6	1.5	0.2
17	CH		-0.015	49.113	49.092	-0.021	1.4		
5	CH		0.005	44.984	44.993	0.008	1.6		
1	CH ₂		-0.005	38.278	38.268	-0.009	1.7		
4	CH ₂		0.007	38.079	38.093	0.014	1.9		
9	CH		-0.005	36.224	36.218	-0.005	1.2		
23	CH ₂		-0.016	35.340	35.318	-0.022	1.3		
22	CH ₂		-0.005	34.333	34.325	-0.008	1.4		
2	CH ₂		-0.006	32.125	32.116	-0.009	1.3		

Chapter IV Cholesterol Solubility in Bile

***Salt Micellar Solutions: Dependence on Bile Salt
Composition and Competition Effects by
Phytosterols, Fatty Acids and Tocopherol***

IV. 1 - Abstract

Solubility of cholesterol in BS micelles is important to understand the availability of cholesterol for absorption in the intestinal epithelium and to develop strategies to decrease cholesterol intake from the intestinal lumen. The cholesterol saturation limit in different simple, binary and ternary BS micelle mixtures in relevant physiological conditions was determined. The effect of phytosterols (stigmasterol and stigmasterol), palmitic and oleic acids (saturated and unsaturated FA, respectively) and α -tocopherol (vitamin) in cholesterol solubility by the BS micelles was studied. The results showed that, depending on the constitution of the BS micelles, the average value of sterol *per* micelle was equal or lower than one. The solubility profile for the different BS mixtures used showed a linear dependence on the total concentration of sterol used until the solubility limit was reached. This was interpreted as a partition rather than a binding mechanism.

The effect of studied competitors showed that stigmasterol had the highest effect in the decrease of cholesterol solubility followed by stigmasterol, tocopherol and oleic acid. Palmitic acid slightly increased the solubility of cholesterol. From our studies, we can suggest two possible mechanisms to explain the effect of these compounds in cholesterol solubilization by BS micelles: A) co-solubilization, where we include tocopherol and oleic acid, that decreases cholesterol solubility, and palmitic acid that increases cholesterol solubility; and B) co-solubilization and co-precipitation, where we include stigmasterol and stigmasterol, which presented the most effective decrease on cholesterol solubility.

IV. 2 - Introduction

Of the 1800 mg of cholesterol absorbed *per* day by an average human, 600 mg are supplied by the diet and the remaining is due to the endogenous production [2; 87]. Although cholesterol is a vital molecule for human beings, it became lately known by its lethal properties. Indeed, high cholesterol levels in blood are responsible for atherosclerosis, one of the most deadly and incapacitating diseases in humans [121]. It is therefore crucial to make all the efforts to clarify the mechanisms underlying the development of this disease and the mechanisms that can potentially avoid it or clearly diminish its effects.

The solubilization of cholesterol in the intestine can be a key research target for this task and is strongly dependent on the diet. Prior to absorption cholesterol needs to be solubilized due to its low solubility in water [55]. This is achieved with the help of several molecules present in the duodenum content, namely BS, being the most representative the ones conjugated with glycine, PL and FA [16]. This mixture of components self-aggregates and forms either intermixed micelles or vesicles depending on the BS/Lipid ratio. These structures solubilize cholesterol and other hydrophobic nutrients and carry them to the apical membrane of the brush border membrane located in the intestinal epithelium [11; 26].

BS are crucial for cholesterol absorption [62]. Cholesterol solubilization by BS has been extensively studied in the past, focusing mainly in the therapeutic potentialities for gallstone disease [93]. A substantial mapping of ternary and binary phase diagrams of PL, BS and cholesterol was determined [104]. The size of the micelles, mixed micelles and vesicles formed with the different proportions of these components is known [59; 122]. The solubility of cholesterol in BS micelles and in the presence of PL was also addressed [34]. Looking carefully at the results obtained by different research groups, clear differences on the CSI were observed although similar approaches were implemented [8; 28; 30; 32; 34; 93; 123] (see Table I. 6, Chapter I). There are also some discrepancies between results obtained at different pH values because solubility of BS is affected by pH. At lower pH there is an increase in the least soluble protonated specie in solution, which will be solubilized in the micelle, decreasing the solubility capacity for other hydrophobic molecules such as cholesterol.

Although conjugated glycine BS have a higher prevalence in humans, most of the studies were done with taurine conjugates. Probably because of their low pKa they do not change ionization state during their presence in the duodenum [23]. At the typical duodenum pH (around 6 to 8), glycine conjugated BS species are mostly in their ionized form. To have a quantitative answer on the solubilization of cholesterol by BS we developed a method using ^{13}C NMR spectroscopy [120] which enables to follow cholesterol solubilization in the micelle. The determination of the cholesterol saturation limit in GDCA micelles was achieved and the ratio of cholesterol per micelle obtained was equal to one [120]. The main advantage of this method is that we can follow cholesterol solubilization in the micelle in a non-invasive way, i.e., without using any technique that could disrupt the equilibrium, such as filtration or chromatography used in previous studies [8; 34; 40; 123; 124]. One important observation was that different

hydrophobic BS have different capacities to deliver cholesterol to membranes [60] and that they were required for solubilization of cholesterol [7]. Cholesterol delivered didn't occur by a merging event (fusion) between the micelle and the membrane but instead it was delivered as an aqueous monomer [61].

In this work the approach was to reduce the complexity of the system (duodenum content) to two major class components only (BS and cholesterol). First we addressed the possibility of synergistic effects between the most representative BS present in the intestinal duodenum and how they affect the sterol solubilization. We used different compositions of BS, namely single, binary and a ternary relevant physiological composition, at the duodenal characteristic concentration. This would give valuable information regarding the decrease in cholesterol absorption through the intestinal epithelium as a direct result of the solubilization phenomena occurring in intestinal lumen.

One of the most used strategies to reduce cholesterol absorption in the intestine is to include in the diet sterols from vegetal origin [29; 125]. They are known to reduce cholesterol absorption and therefore cholesterol intake, although the mechanism is not yet completely understood. There are two possible mechanisms by which phytosterols can prevent cholesterol absorption: co-precipitation or/and co-solubilization [29; 125]. The most common phytosterols present in vegetables and added to margarines are sitosterol, stigmasterol and stigmastanol and their respective esters [110; 111; 112; 113]. Mixing these phytosterols with cholesterol in different proportions in the presence of BS can help to clarify the mechanisms behind phytosterol action, which can give hints to develop better and more effective strategies to reduce cholesterol absorption. As our method allows us to follow cholesterol solubilization in micelles, we can also get a quantitative answer on the decreasing effect of phytosterols on cholesterol solubility. The phytosterols studied here are the stigmasterol and stigmastanol.

The study also addressed the influence of saturated palmitic acid (PA) and unsaturated oleic acid (OA) FA on cholesterol solubilization by BS micelles. It is known that unsaturated FA can decrease cholesterol intake, while saturated FA seem to increase cholesterol absorption [126]. In this regard we addressed also the quantitative effect of these two components in the solubilization of cholesterol in BS micelles. Finally we also studied the effect of α -tocopherol, a component of vitamin E, in the solubilization of cholesterol as a model of a lipophilic vitamin. The following Figure IV. 1 shows the different BS and molecules used as competitors in this work.

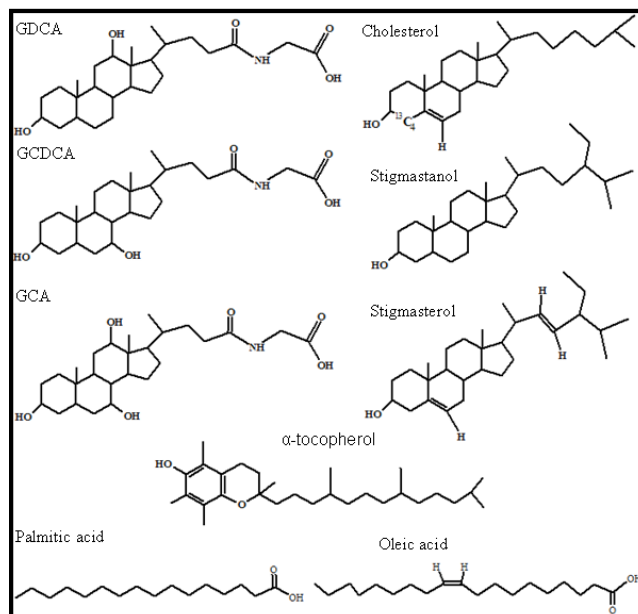


Figure IV. 1 Molecular structures of BS (GDCA, GCDCA and GCA); Cholesterol (enriched in ^{13}C in position 4); phytosterols (stigmastanol and stigmasterol), Vitamin (α -tocopherol) and FA (saturated–palmitic acid, unsaturated–oleic acid). For cholesterol, stigmasterol and oleic acid, the protons bounded to double bonds were discriminated to help in the interpretation of results.

IV. 3 - Materials and methods

N-Phenyl-1-naphthylamine (NPN) was obtained from Merck (Hohenbrunn, Germany), [4-¹³C]cholesterol and deuterium oxide (99.8%) for NMR experiments were obtained from CortecNet (Paris, France), and the BS sodium glycochenodeoxycholic acid (GCDCA), sodium glycocholic acid (GCA), sodium glycodeoxycholic acid (GDCA), α -tocopherol, stigmastanol and stigmasterol were bought from Sigma (Steinheim, Germany). Oleic acid and palmitic acid were bought from Avanti. The non-aqueous solvents used for sample preparation (chloroform, methanol, and acetone) were of spectroscopy grade, and the aqueous buffer components (Tris-HCl, NaCl, and NaN₃) were of high purity and purchased from Sigma; water was first distilled and further purified by activated charcoal and deionization.

The CMC of single, binary and ternary BS mixtures used were determined using the method developed in reference [44], based on the increase in fluorescence quantum yield and blue shift of the fluorescence emission spectra of NPN on association with preformed micelles. The total concentration of NPN was 1 μ M, and the concentrations of simple, binary and ternary BS mixtures in the aqueous buffer were changed between 0 and 50 mM at 37 °C. The fluorescent emission of NPN was followed using an excitation wavelength of 330 nm on a Cary Eclipse fluorescence spectrophotometer obtained from Varian (Victoria, Australia) equipped with a thermostated multi-cell holder accessory. Tocopherol solubility was followed by absorption spectroscopy due to its absorptivity ($3.2 \times 10^3 \text{ cm}^{-1} \text{ M}^{-1}$, $\lambda = 292 \text{ nm}$). A calibration curve was done at a range of tocopherol concentrations going from 0.5 to 5 mM in GDCA 50 mM solution using a cuvette of 0.1 cm width, showing to be linear in this range. Whenever a separate phase is formed the absorptivity is no longer linear.

The size of the micelles present at a concentration of 50 mM, with and without cholesterol solubilized, was also characterized by dynamic light scattering (DLS) using a Beckman Coulter N4 Plus apparatus operating with a He neon laser at 632.8 nm as light source and a scattering angle of 90°. The autocorrelation curves were analyzed with the PSC control software provided with the equipment. The refraction index considered for the samples was 1.33, and the viscosity was 1.127 cp [46]. The experiments were done at 37 °C, up to six measurements were run for each sample, and two independent samples were analyzed.

The solids obtained were characterized by Polarized Light Thermal Microscopy (PLTM) using a hot stage Linkam system, model DSC600, with a Leica DMRB microscope and a Sony CCD-IRIS/RGB video camera. Real Time Video Measurement System software by Linkam was used for image analysis. The images were obtained by the combined use of polarized light and wave compensators, using a 200 magnification.

Proton-decoupled ^{13}C NMR spectra acquisitions were performed on a Varian VNMRs 600 NMR spectrometer equipped with a high field “switchable” broadband 5-mm probe with z-gradient operating at a frequency for ^1H spectra (599.72 MHz) and for ^{13}C spectra (150.8 MHz). ^{13}C NMR spectra were acquired at 37 °C with a 90° pulse angle sequence, a spectral width of 31,250 Hz with an acquisition time of 2.3 s, a relaxation delay of 7 s, and 1024 acquisition scans. Proton decoupling was achieved using a WALTZ-16 decoupling sequence. ^{13}C - $\{^1\text{H}\}$ nuclear Overhauser enhancement (NOE) was obtained by comparing ^{13}C spectra with full proton decoupling and ^{13}C spectra with proton decoupling only during acquisition (spectra acquired with 3000 scans). The values used for correcting the NOE effect are shown in Figure IV. S1 and Figure IV. S2. Spectra were processed with MestreNova 6.1.1 (Mestrelab Research, Santiago de Compostela, Spain). The relaxation delay used ensured that the ^{13}C signals are quantitative for carbons with a relaxation time equal to 1.4 s or shorter. This is the case for C_4 of cholesterol and for all BS carbons except the carbonyl and quaternary carbons [120]. ^1H NMR spectra of stigmasterol and oleic acid were obtained at 37 °C with a 90° pulse angle sequence, a spectral width of 7225 Hz, acquisition time of 1.5 s, a relaxation delay of 2.5 s, and 512 acquisition scans.

Aqueous suspensions of $[4\text{-}^{13}\text{C}]$ cholesterol with and without different competitors (phytosterols, FA, tocopherol) were prepared by evaporating the required volume of a solution in chloroform/methanol (87:13, v/v), blowing dry nitrogen over the heated solution (blowing hot air over the external surface of the tube), and removing organic solvent traces in a vacuum desiccator for 30 min at 23 °C. The glass tube with the dry residue was then transferred to a thermostatic bath at 37 °C and hydrated with a preheated solution of BS in the aqueous buffer (10 mM Tris-HCl (pH 7.4), 0.15 M NaCl, 1 mM ethylenediaminetetraacetic acid (EDTA), and 0.02% NaN_3 in D_2O) and was continuously stirred at 100 rpm. In the case of FA another assay was done solubilizing first the FA in BS solution wait 24 h and then added to a film of cholesterol. The total concentration of BS plus sterol was maintained at 50 mM in all experiments of solubilization. In the experiments of competition using phytosterols, FA

and tocopherol the total concentration of GDCA BS used was 50 mM. The samples were left in the bath with continuous stirring during 24 to 48 h (experiments on the maximum solubilization) and then characterized by ^{13}C NMR to obtain the amount of solubilized cholesterol using the BS CH_2 resonances (similar to the resonance followed in cholesterol) as an internal standard or by the addition of TSP (trimethylsilyl propionate, used as an internal standard) to the sample or both.

IV. 4 - Results and discussion**IV. 4. 1 - Determination of CMC of glycine conjugated BS**

The concentration at which BS form micelles is very important because it states the concentration at which the BS are soluble as a monomer, and this information, together with the aggregation number, gives the concentration of micelles in solution. The CMC determination of GDCA was addressed in a previous work by our research group using two independent methods, isothermal calorimetric titration and dye solubilization (NPN). The results obtained agreed within the experimental error [120].

In this work we have determined the CMC of different simple BS, GCA and GCDCA, binary mixtures, GDCA/GCA; GDCA/GCDCA and GCA/GCDCA, in proportion (50:50) and one ternary mixture physiologically relevant, GCA/GCDCA/GDCA, in proportion (37.5:37.5:25), using the fluorescence properties of NPN. The normalized fluorescence intensity maximum dependence on the concentration for the several BS and their mixtures is shown in Figure IV. 2. CMC values and standard deviations errors obtained are shown in Table IV. 1.

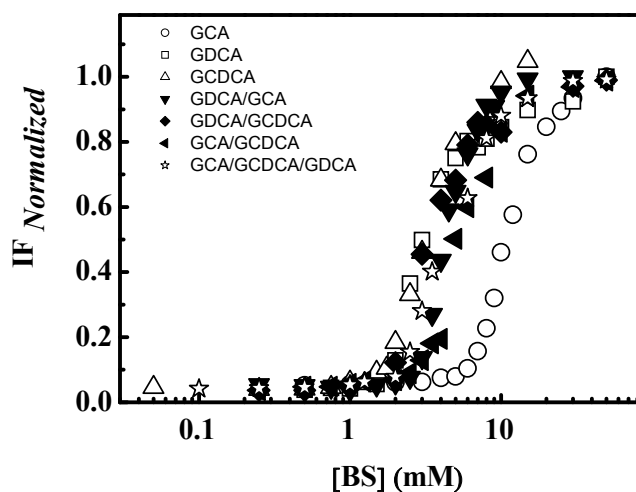


Figure IV. 2 Dependence of NPN fluorescence intensity maximum (1 μ M) in different concentrations of single, binary (50:50) and ternary BS mixtures (37.5:37.5:25) (shown in the figure) in aqueous buffer pH=7.4 and I=150 mM at 37 $^{\circ}$ C. The values obtained for the CMC and standard deviations are shown in Table IV. 1 (page 113).

From the results it was observed that the BS showing the highest CMC is GCA. This BS has three hydroxyl groups, one more than the others BS studied (see Figure IV. 1), being soluble in water in the monomeric state up to a higher concentration than the

others. Both dihydroxy BS show a similar CMC, within the error of the measurement having a much lower CMC than GCA.

The results obtained in this work for the simple mixtures, are smaller than the available data obtained by ITC, using similar conditions (GDCA, 2.0 mM, GCDCA, 2.2 mM, and GCA, 8.5 mM) [29]. The observed difference between the results is not due to the measurement itself but to the approach used to determine the CMC value. CMC by definition is the concentration at which micelles start to form. The values above reported for the CMC using ITC correspond to the BS concentration at which the first derivative is null, this approach leads to higher values of the CMC and is not in agreement with its definition because at this concentration 50% of the BS are already aggregated in micelles. In our measurements the approach was to define two linear regimes, one in the beginning where no changes are observed in the parameter measured (at low BS concentration) and another where there is a sharp transition. The CMC value is calculated from the intersection of both regimes, the point where micelles start to form. The CMC obtained for the binary mixtures, GDCA/GCA (50:50), GCA/GCDCA (50:50) and GDCA/GCDCA (50:50) was equal to the ones predicted considering that the mixture of surfactants was ideal (see Chapter I, section I. 5 page 21). By ideal mixture we mean that there is no net interaction between the species in the mixture and that the free energy associated to the mixing is equal to the sum of free energies of each surfactant. The CMC obtained for the ternary mixture GCA/GCDCA/GDCA (37.5:37.5:25) showed lower value of CMC than the one predicted considering an ideal solution. This would mean that this mixture of BS shows some interaction that cannot be described by the average behaviour of each BS.

After the determination of BS CMC we carried the study of solubilization of cholesterol in BS micelles.

IV. 4. 2 - Determination of Cholesterol Solubilization Index

The determination of sterol solubilized in BS micelles was obtained using the method developed by this group and described in Chapter III [120]. Briefly, labelled [4-¹³C]cholesterol solubilized in the micelles was followed by ¹³C NMR spectroscopy and also by the chemical shift analysis (CSA) of BS resonances that were most sensitive to the presence of cholesterol. Figure IV. 3 shows the results obtained for the CSI for the several mixtures, the average values and standard deviations are shown in Table IV. 1.

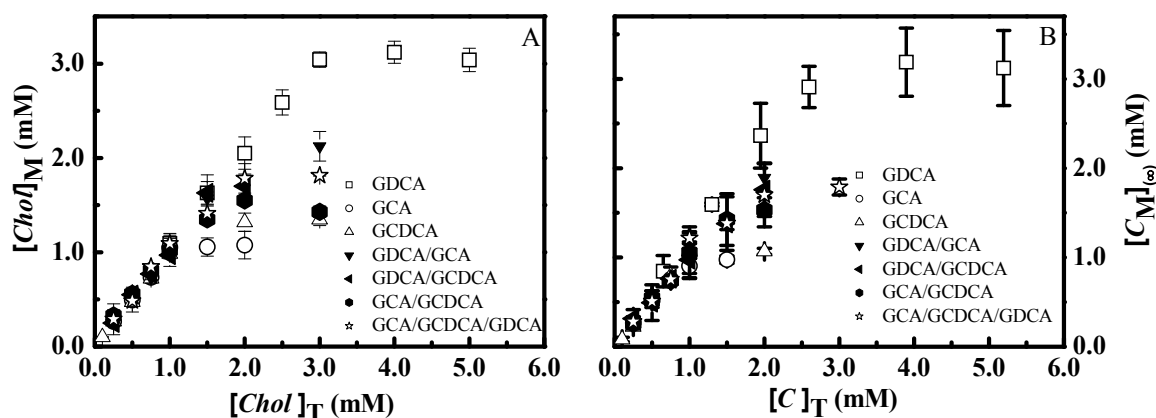


Figure IV. 3 Concentration of [4-¹³C]cholesterol solubilized by BS micelles ($[Chol]_M$) as a function of the total concentrations of cholesterol ($[Chol]_T$) for a total concentration of lipid (BS+ Chol) equal to 50 mM. The experiments were performed at 37 °C. The amount of solubilized cholesterol was obtained from the area of its resonance for [4-¹³C]cholesterol (plot A) or from the chemical shift observed on the bile salt resonances (plot B). The CSI value can be obtained from the maximum $[Chol]_M$, or from the intersection of the best fit to both regimes in cholesterol solubilization (see Chapter III, Figure III. 5 and III. 7). The average and standard errors associated with the CSI obtained are shown in Table IV. 1. They are the average of at least three independent experiments.

The same values for CSI were obtained from both methods, showing that the chemical shift of BS resonances is a reliable method to quantify solubilization of cholesterol even for more complex mixtures (binary and ternary) of BS. Figure IV. 3 show that GDCA was the BS solubilizing more cholesterol, it has the lowest solubility in water (lowest CMC) and the highest hydrophobicity [101]. The most hydrophilic BS (GCA) showed the lowest solubilizing capacity for cholesterol. Surprisingly, although GCDCA has a similar CMC to GDCA, its cholesterol solubilizing capacity is more

similar to GCA. Similar qualitative results, but not quantitatively were obtained before by other authors for the same BS [32]. This emphasizes that the hydroxyl position change between the structures of GDCA and GCDCA is not affecting its solubility in water as monomer but considerably modifies the capacity of the hydrophobic core of the micelles to accommodate cholesterol. The studied BS mixtures showed a solubilizing capacity equal to the one obtained using the average of solubility capacities of each BS weighted by their molar fraction. The exception to this result was the mixture GDCA/GCDCA which showed a lower capacity to solubilize cholesterol than the expected from the average of each BS. This mixture in terms of CMC behaves ideally but regarding solubilization it was observed that it reduces cholesterol solubility, suggesting that the core of the micelles is more disturbed. The disturbing effect has the same magnitude as the one observed for the mixture of BS showing the lowest solubility for cholesterol, reinforcing that the presence of the hydroxyl group at that position has a particular destabilizing effect regarding cholesterol solubility. This mixture showed to be one of the best to reduce cholesterol solubility. To the best of our knowledge, this is the first time that this effect among different compositions of BS has been evaluated. Looking carefully to the mixtures of BS it is clear that the mixture of BS solubilizing the less cholesterol is GCA/GCDCA. The addition of GDCA to this mixture decreases the CMC without a significant increase in solubility of cholesterol. The biologically relevant mixture shows a trade off between the lowest CMC, which leads to the formation of micelles at a lower concentration, with a mean capacity of solubilization of cholesterol. To better compare the results of cholesterol solubilization obtained by us and the results of others groups, we will use the ratio of concentration of cholesterol solubilized in the micelles by concentration of micelles ($[\text{Chol}]_M/[\text{Micelles}]$). The aggregation number for GDCA, GCA and GCDCA reported in the literature in similar conditions than the ones used in this work are shown in Table IV. 1 [122].

Table IV. 1 Values of CSI and CMC determined for single, binary and ternary mixtures of BS. The predicted values for CSI and CMC are also shown assuming that the mixtures of BS behave as an ideal solution. The values of aggregation number obtained for micelles in similar conditions obtained by others are also given.

BS compositions	CSI (mM)	CSI ^{a)} (mM)	CMC (mM)	CMC ^{b)} (mM)	Size (nm)	\bar{A} ^{c)}	[Micelles] (mM)	$\frac{[Chol]_M}{[Micelles]}$
GDCA	3.0 ± 0.1		1.7 ± 0.1		2.6 ± 0.2	16	3.0	1.0
GCA	1.0 ± 0.1		6.5 ± 0.1		2.4 ± 0.4	6	7.8	0.1
GCDCA	1.3 ± 0.1		1.6 ± 0.1		2.9 ± 0.1	18	2.7	0.5
GDCA/GCA	1.9 ± 0.1	2.0	2.7 ± 0.1	2.7	2.4 ± 0.2			
GDCA/GCDCA	1.6 ± 0.2	2.2	1.8 ± 0.1	1.6	2.4 ± 0.2			
GCA/GCDCA	1.4 ± 0.1	1.2	2.7 ± 0.2	2.6	2.3 ± 0.1			
GCA/GCDCA/ GDCA	1.8 ± 0.2	1.6	1.9 ± 0.2	2.3	2.4 ± 0.2			

a) CSI predicted for the complex BS mixtures using the average value of cholesterol solubilization obtained for each single BS weighted by their molar fraction.

b) CMC predicted values were obtained as explaining in Chapter I, section I.5, page 20.

c) Aggregation number per micelle, values obtained from the reference [122].

These results allow us to calculate the quantity of sterol *per* micelle. The values obtained for CSI and CMC for the different BS and their mixtures are also shown. The results obtained showed that GDCA micelles contain an average of one molecule of cholesterol per micelle, being these micelles that best accommodate cholesterol. The other dihydroxy BS, GCDCA, shows half of the solubilizing capacity of GDCA. GCA shows even less affinity for cholesterol with a mean occupancy of 0.1. The results are consistent with the available literature on cholesterol solubilization, where GDCA shows an average cholesterol solubilization per micelle of 0.9, GCDCA 0.4 and GCA 0.2 [28; 30; 34].

This solubilization capacity from the various BS can be interpreted using the Poisson distribution which enables the determination of the probability (p) of observing the most probable discrete events (x) considering the average mean occupancy (λ) of cholesterol for each BS which is given by the following Equation IV. 1,

$$p(x, \lambda) = \frac{e^{-\lambda} \lambda^x}{x!} \quad \text{Equation IV. 1}$$

Table IV. 2 show the probability results for several discrete events to occur for the single BS micelles.

Table IV. 2 Poisson distribution of cholesterol per micelle of BS, considering the average solubility of cholesterol per micelle (λ) and x discrete possible events.

Events	GDCA	GCDCA	GCA
x	$\lambda = 1$	$\lambda = 0.5$	$\lambda = 0.1$
0	0.37	0.61	0.90
1	0.37	0.30	0.09
2	0.18	0.08	0.00
3	0.06	0.01	0.00

The Poisson distribution results show that the events considering micelles without any sterol and micelles with one sterol are the events having the highest probability of occurrence. For the BS solubilizing higher quantities of cholesterol as GDCA, there is also a significant probability of having micelles with two, or even three, molecules of cholesterol.

From the profile of the curves obtained from Figure IV. 3 there is a linear increase of the amount of cholesterol solubilized with the increase in the total concentration of cholesterol until the saturation limit is reached. This is compatible with the partition of cholesterol between cholesterol in aqueous solution and cholesterol in micelles. This also discards the possibility of binding phenomena where the variation of free binding sites available in the micelles would lead to a non-linear dependence with the total concentration of cholesterol in the system. A possible interpretation from the results would be as follows: a higher solubilization means that a higher partition occurs between the aqueous phase and the GDCA micelles. This would mean that the free energy associated with the solubilization of cholesterol in those micelles is more favourable than with the other BS micelles, including the binary and ternary mixtures and the chemical potential for the solubilization process associated with GDCA is the smallest for all the studied micelles. The ternary mixture of BS showed an intermediary solubilizing capacity, showing that the system is not optimized for a maximum of cholesterol solubility. Instead it behaves as an average of the solubilities of the different BS. If the main function was only the solubilization of hydrophobic molecules it would be expected that the solubilization capacity of micelles would be the highest possible,

Chapter IV

which from the results would be the one from GDCA micelles. However absorption process should be thought as a trade off between solubilization in intestinal lumen and partition to the gastrointestinal membrane. This reinforces the commitment between a micelle having a mean solubilizing capacity allowing hydrophobic drugs to be solubilized at a small concentration of solubilizer but at the same time it should be an efficient supplier of monomers to the aqueous phase for the partition into the membrane.

IV. 4. 3 - Effect of phytosterols in cholesterol solubilization in GDCA micelles

Several compounds are known to affect cholesterol absorption in the intestine and have been implicated in changes in the solubilization capacity of the dietary mixed micelles (DMM) in the intestinal lumen. Phytosterols are probably one of the most studied families of molecules studied with this purpose [29; 39; 127]. FA, namely the unsaturated ones, and some vitamins (α -tocopherol) are also involved in the decrease of cholesterol absorption [128]. To understand whether these compounds affect the solubility of cholesterol in BS micelles and, most importantly, to determine quantitatively their effect we used a pre-established method that follows the cholesterol solubilized in the micelle [120]. Figure IV. 4 shows an expansion of a typical ^{13}C NMR spectrum of GDCA micelles acquired in the presence of various molecules considered and of labelled $[4-^{13}\text{C}]$ cholesterol. The resonance at 44 ppm belongs to the carbon four (C_4) of labelled $[4-^{13}\text{C}]$ cholesterol and allows the determination of the cholesterol solubilized in the micelles.

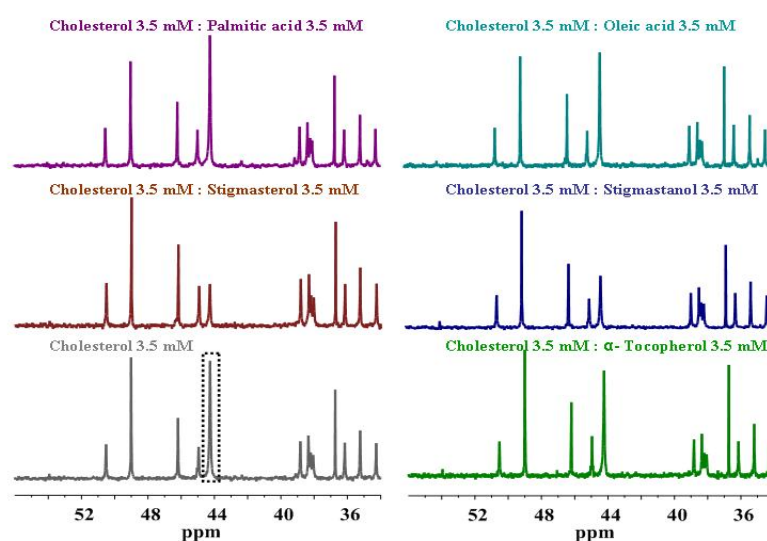


Figure IV. 4 ^{13}C NMR expanded spectra (from 56 to 34 ppm) of 50 mM GDCA with 3.5 mM $[4-^{13}\text{C}]$ cholesterol:3.5 mM competitor in D_2O aqueous buffer solution at 37 °C, acquired in a Varian 600 MHz NMR spectrometer, with ^1H decoupling and NOE. The peak of $^{13}\text{C}_4$ enriched cholesterol appears at 44 ppm (dotted box). It is noticeable the decrease in peak height in the presence of the phytosterols, tocopherol, oleic acid and an increase in the case of palmitic acid.

Results clearly showed stigmasterol and stigmastanol induced the highest effect on cholesterol solubility decrease. They belong to two classes of phytosterols of vegetal origin designated as sterols and stanols, respectively, known as inhibitors of cholesterol absorption. Two mechanisms can explain the decreasing of cholesterol solubility through the action of phytosterols [29; 129]. On the one hand, phytosterols and cholesterol can compete for the hydrophobic core inside the micelle in a process called co-solubilization. On the other hand, cholesterol can have its solubilization decreased in the presence of phytosterols due to a co-precipitation of both sterols, in a mechanism called co-precipitation. A last possibility is a combination of both processes.

Figure IV. 5 shows bar graphs of the effect of stigmastanol at the different phytosterol/cholesterol ratios of 0, 0.5 and 1 with constant total cholesterol concentration of 3.5 mM.

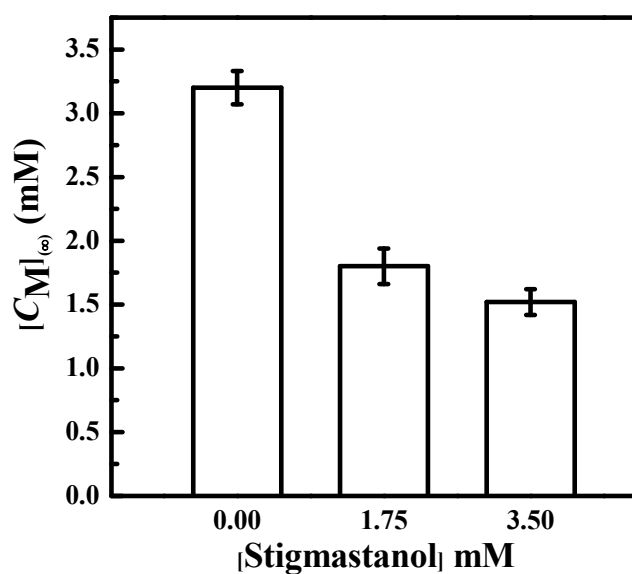


Figure IV. 5 Effect of stigmastanol on cholesterol solubilization in GDCA BS micelles. The values shown respect to phytosterol/cholesterol ratios of 0, 0.5 and 1. BS were composed of GDCA 50 mM and the cholesterol content used in every experiment was 3.5 mM. The values of solubilization of cholesterol at equilibrium ($[Chol]_M$) are the average of at least three independent experiments and the standard deviation is shown.

In the absence of competitor the solubility of cholesterol in a GDCA 50 mM solution is 3.2 mM. This value is higher than the CSI obtained for micelles of GDCA shown in Table IV. 1 because in the study of competition with co-solutes we use a total concentration of BS equal to 50 mM; and in the previous measurements the total concentration was 50 mM including cholesterol and BS.

The presence of stigmastanol in the solution shows a decreasing cholesterol solubility effect. Assuming the affinities of both sterols for the micelle are the same, what is a reasonable assumption given the similarities of their molecular structures, it would be expected that when both sterols were in equal proportion, cholesterol solubilization would decrease to half of its value in the absence of stigmastanol. This seems to explain what is observed when the cholesterol/stigmastanol proportion is 1. However, when this proportion is 0.5, being stigmastanol concentration half of cholesterol, the observed decrease in cholesterol solubilization is also around half of its value in the absence of stigmastanol. This represents a much higher effect than it would be expected considering the above mentioned similar interaction of both sterols with the BS micelles.

One possible way to clarify the mechanism behind the action of stigmastanol in decreasing cholesterol solubility in BS micelles could be the assessment of stigmastanol solubility in the micelle. Unfortunately our method was not able to follow stigmastanol solubility in the micelle due to the absence of a proton or carbon resonance, which would allow the quantification of its micellar solubilization. Another possibility would be to follow the sterol emulsified by chemical shift analysis similar to the one done with cholesterol [120].

In the case of the effect of stigmasterol, it was possible to quantitatively determine the solubilization of both sterols in the BS micelles. The molecular structures of cholesterol and stigmasterol are very similar as they have the same sterol backbone. The major difference is in the side chain (see Figure IV. 1) where stigmasterol has an additional double bond. The proton spectrum of cholesterol in BS micelles (shown in the Figure IV. 6) has a peak at 5.3 ppm which is characteristic of alkene protons. Stigmasterol has a proton near the double bond which resonates at this same frequency of cholesterol alkene proton (gray arrow in Figure IV. 6). The two additional protons of the double bond in the side chain resonate close to water frequency at 4.6 ppm (black arrows in Figure IV. 6). Although these two latter signals could not be used due to distortions caused by the proximity to water resonance, the signal of the protons located

in the cholesterol and stigmasterol backbone could be informative of the solubilization of both sterols.

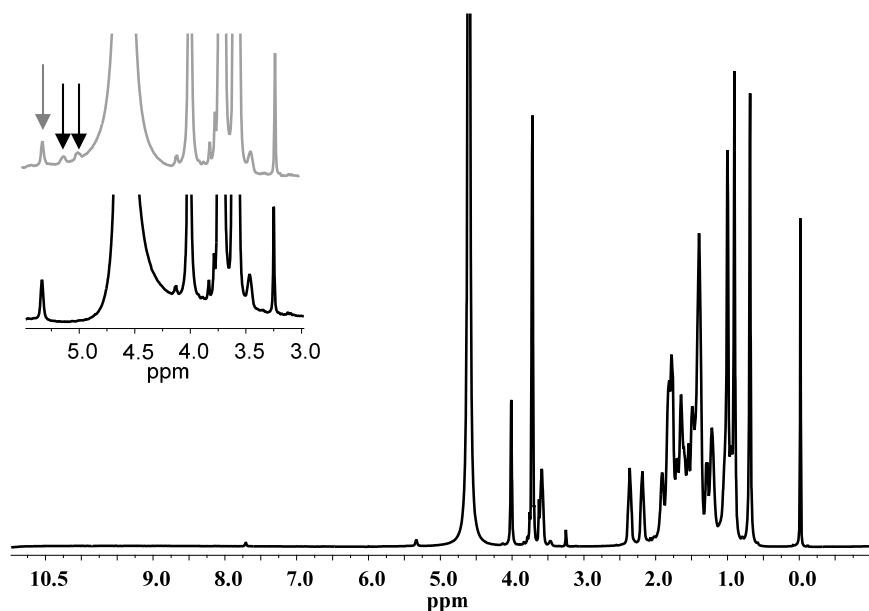


Figure IV. 6 ^1H NMR spectra of 50 mM GDCA BS micelles in D_2O buffer Tris-HCL pH=7.4 with 3.5 mM $[4\text{-}^{13}\text{C}]$ cholesterol. The inserts present an expansion from 5.5 to 3.0 ppm showing the peak of cholesterol solubilized in micelles (black line) and the peaks from cholesterol and stigmasterol (gray line).

Using a known quantity of TSP as internal reference it was possible to quantitatively determine the concentration of solubilized sterols from the peak area of the above mentioned proton. Concentration of cholesterol in the same solution was obtained by quantitative ^{13}C NMR spectroscopy. While in the proton spectrum the area of the signal at 5.3 ppm corresponds to both of the sterols solubilized in the micelle, in the ^{13}C NMR spectrum only cholesterol is quantified because only it, and not stigmasterol, is enriched in ^{13}C . Referring to TSP signal we defined a corresponding area for the cholesterol concentration. Therefore, subtracting it to the overall sterols area, the corresponding area for the stigmasterol solubilized in the micelle was determined. Figure IV. 7 shows the results obtained for the effect of the presence of stigmasterol on cholesterol solubilization in GDCA BS micelles, the sterol solubilization in the micelles and the sum of both sterols solubilized in the micelle.

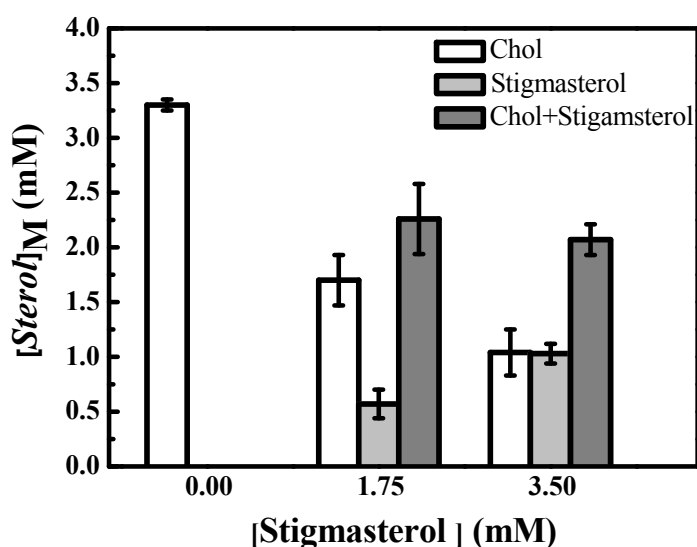


Figure IV. 7 Effect of stigmasterol on cholesterol solubilization by GDCA BS micelles. The values shown respect to ratios of phytosterol/cholesterol 0, 0.5 and 1. The BS composition is GDCA 50 mM and the total cholesterol content used in every experiment was 3.5 mM. The values of solubilization at equilibrium for both cholesterol and stigmasterol in the GDCA micelles ($[Sterol]_M$) are the average of at least three independent experiments. The standard deviation associated with the amount of sterol solubilized is also shown.

The results show that the increase in the proportion of stigmasterol/ cholesterol from 0.5 to 1 leads to a decrease in the solubility of cholesterol in the GDCA micelles, an increase of stigmasterol solubilized in the micelle and to a decrease of the total sterol (cholesterol plus stigmasterol) solubilized relatively to the total amount solubilized by the micelles in the absence of phytosterol.

The methodology used in this work allows to show that co-solubilization of both sterols is occurring. To the best of our knowledge this is the first time solubilized cholesterol and phytosterol are measured directly in the same micelle solution with non-invasive techniques like filtration or chromatography. The overall solubilizing capacity of GDCA micelles in the presence of both sterols decreases with the increase in the proportion of stigmasterol. This was interpreted as an indication of co-precipitation mechanism and is compatible with a lower aqueous solubility for the mixture cholesterol plus stigmasterol than that of cholesterol. The decrease in cholesterol solubility is significantly larger in the presence of stigmasterol than of stigmasterol for the GDCA micelles. However, this difference is only observed for the ratio 1:1. The

reduction in cholesterol solubilized was very similar for both phytosterols at the ratio phytosterol/cholesterol equal to 0.5.

The literature about solubilization of phytosterols and their quantitative effects on decreasing cholesterol solubility in BS micelles and/or dietary models are not consensual. Cholesterol and stigmasterol solubility in non conjugated BS was studied as a function of BS concentration. Results showed that the presence of stigmasterol in deoxycholic acid micelles, at similar concentration to the one used in our work, induced a mild decreasing effect on cholesterol solubility [130]. In the same work, cholestanol (a stanol similar to stigmastanol) showed a strong decrease in the amount of solubilized cholesterol. The total sterol (cholestanol plus cholesterol) solubilized at the BS micelle was lower than the cholesterol solubilized in absence of phytosterols. This was also observed for the competition of sitostanol in taurine conjugated BS, TCA, although in this work other phytosterols studied showed similar decreasing effects for cholesterol solubility (sitosterol and campesterol) [124].

In systems mimicking intestinal lumen like DMM, published results show that sitosterol (from sterol family, similar to stigmasterol) leads to a decrease of cholesterol solubility to half. They also show that the total amount of sterol (phytosterol plus cholesterol) solubilized by the micelles decreases when compared with the amount of cholesterol solubilized by the micelles in the absence of competitor [40].

However, another study using the same DMM reported different solubility limits for both sterols. It showed also that the solubility of cholesterol decreased to half in the presence of competitor, but that the solubility of both sterols in the micelle was equal to the cholesterol solubility when in absence of competitor [29; 40].

Using a dietary model different than the previous ones, other studies investigated the effects of several phytosterols. They showed that stigmasterol has the highest effect on the decrease of cholesterol though the sum of both sterols solubilized in the micelle was equal to the cholesterol solubilized in absence of competitor [42].

The results for dietary models can show some variability due to the complexity of the mixtures precluding the information obtained. In this work the strategy was to use a simple mixture of GDCA micelles changing the proportion of competitor/cholesterol ratio evaluating its effects on cholesterol solubilization. This gives some hints about the mechanisms of action of phytosterols. On the one hand, as the ratio of stigmasterol/cholesterol increases cholesterol solubility decreases due to a co-solubilization mechanism. The solubility of stigmasterol also increases with the increase

of stigmasterol present in the system when stigmasterol/cholesterol ratio is increased. On the other hand, the solubilizing capacity of the micelle for both sterols decreases when compared to the solubility capacity for cholesterol in absence of phytosterol. This can be explained by a co-precipitation mechanism leading to a decrease in available sterol to be solubilized in the micelle.

Our results point to the existence of co-solubilization and co-precipitation mechanisms to describe the action of phytosterols in the decrease of cholesterol solubility in the GDCA micelles. In equal proportion of phytosterol/cholesterol, stigmasterol shows to be the phytosterol with highest capacity to decrease cholesterol solubility when compared with stigmastanol.

Significant information came from the chemical shift analysis similar to the one done in section IV. 4. 2 and already published [120]. Because stigmastanol solubilization in the GDCA micelles could not be determined, we address whether chemical shift analysis could be a robust method to determine phytosterol solubilization in the micelle. The initial assumption was that as phytosterols and cholesterol have similar chemical structures they would show similar chemical shift when inserted in the micelle. Making use of the quantitative NMR information obtained for both stigmasterol and cholesterol solubilized in the micelle and the observed chemical shift variation in BS resonances, a correlation between chemical shift and solubilized sterol was obtained. Table IV. S 3 shows the chemical shift variation and the slopes obtained for the micelles in presence of cholesterol or cholesterol plus stigmasterol. Slopes relating chemical shift with sterol solubilization in the two situations show similar values. This allows the determination of the total solubilized sterol following the chemical shift of the most sensitive BS resonances [120]. The determined value of solubility was equal to the value of solubilized sterol in the micelle determined by quantitative ^{13}C NMR. This demonstrates the robustness of the method and the validity of the initial assumption. Therefore using the same strategy for the stigmastanol it was possible to determine the solubility of stigmastanol in the micelle in presence of cholesterol.

Table IV. S 4 shows an example of the determination of both sterols solubilization (cholesterol and stigmastanol) by chemical shift analysis of the BS resonances. After the complete analysis of all the chemical shifts we could post the different results obtained for both sterols and cholesterol solubilized in the micelle (Table IV. 3).

Table IV. 3 Comparison between total sterol (cholesterol+ stigmasterol) solubilized in GDCA micelles determined by quantitative ^{13}C and ^1H NMR spectroscopy and the total sterol determined from quantitative chemical shift analysis (qCSA). Determination of stigmastanol solubilized in the micelle using similar chemical shift analysis as for stigmasterol. The total cholesterol present in the solutions was 3.5 mM and the concentration of GDCA was always 50 mM.

	mM	Cholesterol	Chol/Stigmasterol 2:1	Chol/Stigmasterol 1:1	Chol/Stigmastanol 2:1	Chol/Stigmastanol 1:1
Quantitative NMR	$[\text{Chol}]_M$	3.2 ± 0.1	1.6 ± 0.2	1.0 ± 0.2	1.8 ± 0.1	1.6 ± 0.1
	$[\text{Stigmasterol}]_M$		0.6 ± 0.2	1.0 ± 0.1		
	$[\text{Total Sterol}]_M$		2.2 ± 0.3	2.0 ± 0.1		
qCSA NMR	$[\text{Total Sterol}]_M$		2.1 ± 0.3	2.0 ± 0.1	2.5 ± 0.1	2.9 ± 0.2
	$[\text{Stigmastanol}]_M^{\text{a)}}$				0.7 ± 0.3	1.3 ± 0.1
	$[\text{Stigmasterol}]_M^{\text{a)}}$		0.5 ± 0.1	1.0 ± 0.1		

^{a)} The concentration of stigmasterol and stigmastanol was obtained by the difference between the total sterol obtained by chemical shift analysis and the concentration of cholesterol determined by ^{13}C NMR quantification for at least three independent experiments.

The results obtained show that both stigmastanol and stigmasterol are solubilized in the micelle. Moreover they indicate that the total sterol solubilizing capacity of the micelles decreases in the presence of phytosterols. The decrease in sterol solubility is more pronounced in the presence of stigmasterol than stigmastanol. However, the values of solubilization of each phytosterols determined for the two considered proportions are similar. These results suggest that stigmasterol promote more efficiently the co-precipitation mechanism than stigmastanol, this being reflected in the observed decrease of cholesterol solubility.

IV. 4. 4 - Effect of saturated and unsaturated fatty acids in cholesterol solubilization in GDCA micelles

To study the effect of saturated and unsaturated FA on cholesterol solubilization, we used palmitic and oleic acid as competitors for cholesterol. The results obtained are shown in Figure IV.8.

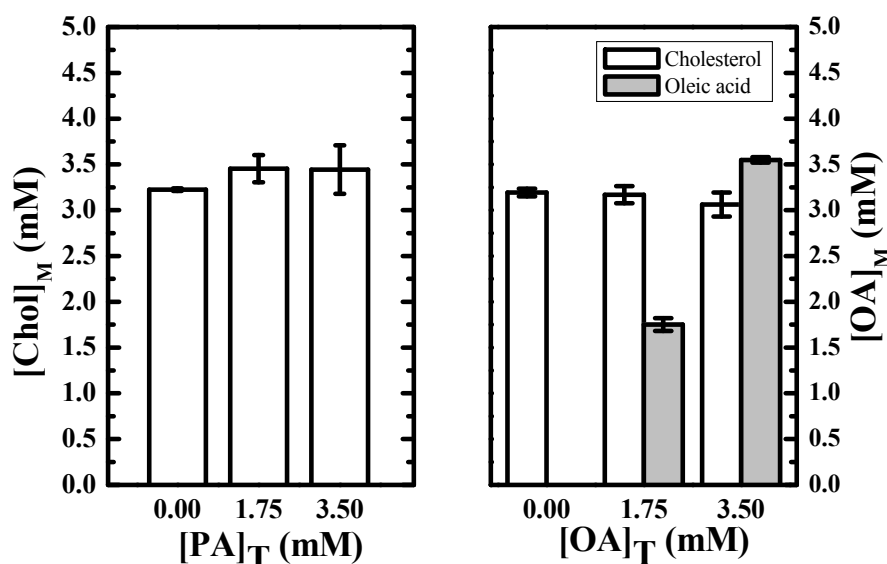


Figure IV. 8 Effect of saturated (palmitic acid-left panel) and unsaturated fatty acids (oleic acid-right panel) on cholesterol solubilization. Values shown are for fatty acids/cholesterol ratios in the absence of fatty acids and with ratios of cholesterol/fatty acids equal to 0.5 and 1. BS composition is 50 mM GDCA and the cholesterol content used in each experiment is 3.5 mM. The values indicated for the solubility are the average and standard deviation of at least three independent experiments. The solubility of oleic acid by the BS micelles, in the presence of sterol is shown, was obtained by ¹H NMR quantification and is also shown.

The saturated palmitic acid shows a small increase in the solubility of cholesterol for the different proportions used. For these experiments two different assays were performed. In the first one a film of cholesterol and FA and the system was allowed to equilibrate for 24 h was prepared, following the methodology described in Chapter III, to which the BS solution was added to which BS are joined. In the other assay, a pre-equilibrated solution of BS with FA was added to the cholesterol film. The results obtained from the two experiments were similar and are part of the results of Figure IV. 8. In the absence of FA, GDCA micelles solubilize 3.2 mM out of a total cholesterol concentration of 3.5 mM. Addition of PA 1.75 mM to the BS micelles leads

to a slight increase of cholesterol solubility. Doubling the concentration of PA in the system leads to the total solubilization of cholesterol present in solution. To clarify whether the cholesterol solubility limit was achieved, a higher cholesterol concentration (5 mM) was studied for both PA concentrations (1.75 and 3.5 mM). Results showed that PA has a low increasing effect on the solubility of cholesterol. But the limit of solubility was achieved when 3.5 mM was solubilized in the micelle for each concentration of PA. DLS measurements did not show any increase on aggregate average size in the presence of PA (2 - 3 nm) for both proportions used.

The analysis of the chemical shift from the different resonances of BS with cholesterol and FA showed that several resonances were sensitive to the increase of FA in the system and could be used to quantify solubilized FA. Table IV. S 4 (supplementary material) shows a typical example of the quantitative determination of the solubilized PA in the BS micelles followed by the chemical shift analysis. This result demonstrates that PA was completely solubilized by BS micelles at both concentrations used.

Results obtained for cholesterol solubility in the presence of OA presented in Figure IV. 8 (right panel) showed another trend when compared with PA. The unsaturated OA leads to a slight decrease on cholesterol solubility although it is very small when compared with the effect of phytosterols with the same proportions. Solubility of OA in the micelles was also followed by quantitative NMR; which demonstrated they were completely soluble in both concentrations used (1.75 and 3.5 mM). This result is different than the observed for phytosterols, where the competitor was not completely solubilized by the micelles and showed a defined solubility limit. The result was also confirmed by chemical shift analysis (Table IV. S 5 supplementary material). This was consistent with observations done with DMM where oleic acid showed to decrease cholesterol solubility when high OA/ cholesterol ratios were used [29].

DLS measurements did not show a significant change in the size of the micelles (2-3 nm) in presence of the FA. Both palmitic and oleic acids can form micelles in aqueous solution, which could theoretically solubilize cholesterol. The resulting dependence of the BS chemical shift in presence of FA clearly shows that FA are being solubilized at the micelle, affecting several BS resonances by their presence with chemical shifts quite distinct between themselves and when compared with those in presence of cholesterol. At the highest content of FA used in this work (3.5 mM), on

average one molecule of FA is solubilized for each micelle of GDCA. This can explain why the size of BS micelles is not modified.

IV. 4. 5 - Effect of α -tocopherol in cholesterol solubilization in GDCA micelles

Vitamin E is one of the most abundant lipid-soluble antioxidants in higher mammals [128]. It can exist in two forms: tocopherols and tocotrienols. α -Tocopherol (molecular structure in Figure IV. 1) is one of the most representative forms of tocopherols. We will study their effect on cholesterol solubilization by BS micelles and compare its behaviour with the one of FA and phytosterols. Results obtained are shown in Figure IV. 9.

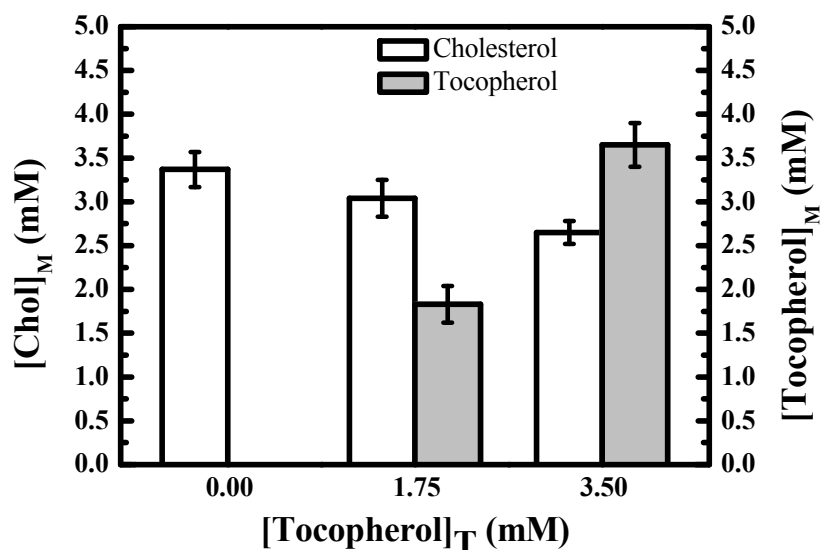


Figure IV. 9 Effect of tocopherol on cholesterol solubility by the BS micelles. The values shown are for tocopherol/ cholesterol ratios of 0, 0.5 and 1. The BS composition is 50 mM GDCA and the total cholesterol content used in each experiment is 3.5 mM. The values of solubility are the average of at least three independent experiments and the standard deviation are shown. The solubilization of tocopherol in the BS micelles in presence of sterol is also shown and measured by absorption.

From the solubilization profile a decrease of cholesterol solubility in the presence of α -tocopherol is noticed. Although this effect is clearly lower than the one observed for phytosterols, it is higher than the one observed for the oleic acid. Tocopherol solubility in GDCA micelles was followed by absorption and it was complete for both concentrations studied, like in the case of FA.

The analysis of chemical shift variation of BS resonances allows the determination of the solubility of tocopherol in the BS micelles (Table IV. S 6 supplementary material). Resulting values are similar to the ones obtained by the absorption assay.

IV. 5 - Conclusions

The solubilization of hydrophobic drugs in intestinal lumen by BS micelles is a process very important in drug delivery and pharmacokinetics. It is also of extreme importance for the understanding of cholesterol absorption in the intestine and the development of strategies to avoid atherosclerosis and gallstone disease.

There are several works in literature where the cholesterol solubility on BS micelles was addressed [8; 30; 34; 40; 41; 123; 131]. However most of the work was done with conjugated taurine and unconjugated BS, which are not the most prevalent in intestinal lumen [16]. Other works used more complex mixtures, DMM, in order to mimetize the intestinal content and determined cholesterol and other co-solubilizers solubility [29; 40; 42; 132]. The results obtained in these works showed different cholesterol and total sterol solubilization, being difficult to interpret them (see Chapter I section I. 7).

In this work we studied quantitatively cholesterol solubilization in several simple and complex mixtures of the most abundant and representative BS present in the intestinal lumen, using a NMR non-invasive method [120]. Our results clearly showed that BS micelles composition present *in vivo* are not optimized for the highest solubilizing capacity, instead they show a compromise between CMC (ability to solubilize hydrophobic compounds at determined concentration of BS, where micelles are formed) and the mean solubility limit for cholesterol. The results obtained for the solubility of cholesterol were interpreted as part of the dual physiological role of BS micelles at intestinal lumen; they not only help the solubilization of the hydrophobic molecules but also work as a vehicle of their delivery to the intestinal membrane.

In order to understand diet changing effect on cholesterol solubility by BS micelles in the intestinal lumen, we studied the effect of several hydrophobic molecules, such as phytosterols (stigmasterol and stigmastanol), fatty acids (saturated palmitic acid and unsaturated oleic acid) and vitamin E (tocopherol). These molecules, namely phytosterols, unsaturated FA and tocopherol are known to decrease cholesterol absorption in the intestine [87], although the mechanism is not fully understood [10; 29; 133; 134].

From the results obtained in this work two main mechanisms of action were observed. Co-solubilization where cholesterol and the other hydrophobic molecule are solubilized in the micelles, with two different behaviours: 1- decrease of cholesterol

solubility, like in the case of tocopherols and OA; 2- increase of cholesterol solubility, like in the case of PA. Co-solubilization and co-precipitation mechanism where is observed a decreasing effect in cholesterol solubility by the action of phytosterols (stigmastanol and stigmasterol). Phytosterols showed to be more effective in the decreasing of cholesterol solubility, being followed by tocopherol and OA.

This work clearly shows that cholesterol solubility can be reduced by different mechanisms which were quantitatively evaluated and characterized, showing the importance of the presence of sterols of vegetal origin, vitamins and unsaturated FA in intestinal lumen. These results can help to improve better strategies to decrease cholesterol absorption and also in the development of better models based on BS for drug delivery to the GIM.

IV. 6 Supplementary Material

Table IV. S 1 $^{13}\text{C}\{-^1\text{H}\}$ Nuclear Overhauser Effect (NOE) on a solution of 49 mM GCA with 1 mM of $[4\text{-}^{13}\text{C}]$ cholesterol, in D_2O buffer at 37 °C, obtained on a Varian 600 MHz NMR spectrometer, with 90° pulse, D1=7 s, gain of 40, 3000 scans. The NOE effect (η^2) and correction factor (C.F.) were obtained via comparison of the spectra with ^1H decoupling along all the pulse (with NOE) and decoupling only along the acquisition time (without NOE). The table shows the NOE values for each resonance of GCA and for carbon 4 of $[4\text{-}^{13}\text{C}]$ cholesterol.

GCA	Carbon type	assignments	NOE	c.f.	average	s.d.
10	C	37.18	0.52	0.66		
13	C	48.95	0.85	0.54		
24	C	180.02	0.34	0.74		
26	C	179.54	0.34	0.75	0.67	0.10
3	CH	74.43	0.58	0.63		
5	CH	43.9	0.74	0.58		
7	CH	71.13	0.91	0.52		
8	CH	42.06	0.67	0.60		
9	CH	29.18	0.73	0.58		
12	CH	75.94	0.68	0.60		
14	CH	44.36	0.63	0.61		
17	CH	49.21	0.38	0.72		
20	CH	37.95	0.78	0.56	0.62	0.07
1	CH ₂	37.66	0.61	0.62		
2	CH ₂	32.06	0.68	0.60		
4	CH ₂	41.2	0.57	0.64		
6	CH ₂	36.68	0.80	0.56		
11	CH ₂	30.54	0.63	0.61		
15	CH ₂	25.73	0.63	0.61		
16	CH ₂	30.04	0.64	0.61		
22	CH ₂	34.37	0.71	0.59		
23	CH ₂	35.29	0.97	0.51		
25	CH ₂	46.13	1.15	0.47	0.58	0.05
18	CH ₃	14.91	1.19	0.46		
19	CH ₃	24.9	1.03	0.49		
21	CH ₃	19.5	1.29	0.44	0.46	0.03
$[4\text{-}^{13}\text{C}]$ chol	CH ₂		0.35	0.74		

$^2\eta = \frac{I - I_0}{I_0}$ where I is the area with NOE and I_0 the area without NOE. The correction factor is

given by $\frac{1}{1 - \eta}$

Table IV. S 2 $^{13}\text{C}\{-^1\text{H}\}$ Nuclear Overhauser Effect (NOE) on a solution of 49 mM GCDCA with 1 mM of $[4\text{-}^{13}\text{C}]$ cholesterol, in D_2O buffer at 37 °C, obtained on a Varian 600 MHz NMR spectrometer, with 90° pulse, D1=7 s, gain of 40, 3000 scans. The NOE effect (η) and correction factor (C.F.) were obtained via comparison of the spectra with ^1H decoupling along all the pulse (with NOE) and decoupling only along the acquisition time (without NOE). The table shows the NOE values for each resonance of GCDCA and for carbon 4 of $[4\text{-}^{13}\text{C}]$ cholesterol.

GCDCA	Carbon type	assignments	NOE	c.f.	average	s.d.
24	C	179.36	0.28	0.78		
26	C	179.30	0.28	0.78		
13	C	45.15	0.36	0.73		
10	C	37.65	0.42	0.71	0.75	0.04
3	CH	74.32	0.44	0.70		
7	CH	70.87	0.62	0.62		
17	CH	57.72	0.62	0.62		
14	CH	52.76	0.48	0.68		
5	CH	44.25	0.32	0.76		
8	CH	42.24	0.08	0.93		
20	CH	38.20	0.79	0.56		
9	CH	35.37	0.52	0.66	0.69	0.12
25	CH ₂	46.27	1.00	0.50		
12	CH ₂	42.20	1.99	0.33		
4	CH ₂	41.35	0.39	0.72		
1	CH ₂	38.18	0.03	0.97		
6	CH ₂	37.06	0.69	0.59		
23	CH ₂	35.18	0.76	0.57		
22	CH ₂	34.40	0.61	0.62		
2	CH ₂	32.58	0.53	0.65		
16	CH ₂	30.71	0.66	0.60		
15	CH ₂	26.31	0.57	0.64		
11	CH ₂	23.51	0.56	0.64	0.62	0.16
19	CH ₃	25.62	1.00	0.50		
21	CH ₃	20.97	1.45	0.41		
18	CH ₃	14.49	1.04	0.49	0.47	0.05
$[4\text{-}^{13}\text{C}]$ chol	CH ₂	44.22	0.71	0.59		

Table IV. S 3 Chemical shift analysis dependence on the total concentration of sterol (stigmasterol+cholesterol) and cholesterol in the micelle. Resulting slope obtained for cholesterol (m_{chol}) and cholesterol plus sterol ($m_{chol+sitosterol}$) in the BS micelle are similar and was used to determine the total amount of sterol in the micelle ($[Total\ sterol]_M$). The total sterol amount determined by chemical shift analysis is equal to the total sterol ($[Sterol]_M$) amount determined by quantitative NMR (qNMR).

GDCA		Conversion of BS resonances shift into solubilized sterol concentration on BS micelles							
		qNMR	[Chol] _M mM	3.2	1.7			qCSA	[Total sterol] _M $= \frac{\Delta\delta}{m_i}$ mM
			[¹²³ M] mM		0.7				2.4 ± 0.2
			[Sterol] _M mM		2.4				
Carbon number r	Carbon type		δ_{GDCA} GDCA 50 mM	δ_{Chol} GDCA 50 mM Chol 3.5 mM	$\delta_{Chol+Stigmasterol}$ GDCA 50 mM Chol 3.5 mM Stigmasterol 1.75 mM	$\Delta(\delta_{Chol}-\delta_{GDCA})$	$\Delta(\delta_{chol+stigmasterol}-\delta_{GDCA})$	Slope (m_{chol})	Slope ($m_{chol+stigmasterol}$)
12	CH	Chemical Shift Variation	75.691	75.6562	75.666	-0.032	-0.025	-0.010	-0.010
17	CH		49.074	49.0414	49.034	-0.029	-0.040	-0.009	-0.017
5	CH		38.24	38.2128	38.228	-0.024	-0.012	0.004	0.005
1	CH ₂		38.047	38.0636	38.064	0.020	0.017	-0.008	-0.005
4	CH ₂		36.187	36.1627	36.173	-0.021	-0.014	0.006	0.007
9	CH		35.302	35.2395	35.26	-0.059	-0.042	-0.007	-0.006
23	CH ₂		34.298	34.2715	34.281	-0.023	-0.017	-0.019	-0.017
22	CH ₂		32.089	32.0591	32.068	-0.027	-0.021	-0.007	-0.007
2	CH ₂		75.691	75.6562	75.666	-0.032	-0.025	-0.008	-0.009

Table IV. S 4 Chemical shift analysis dependence on the total concentration of sterol (stigmastanol+cholesterol) and determination of stigmastanol solubilized in the micelle using the quantitative chemical shift analysis (qCSA) of the total sterol and the quantitative NMR (qNMR) solubilization of cholesterol in BS micelle.

GDCA		Conversion of BS resonances shift into solubilized sterol concentration on BS micelles							
		qNMR	[Chol] _M mM	3.2	1.7	1.6	qCSA		
[Stigmastanol] _M mM						0.7		1.3	
		[Total sterol] _M mM					2.5 ± 0.2	2.9 ± 0.2	
Carbon number	Carbon type	Chemical Shift Variation	δ_{GDCA} GDCA 50 mM	δ_{Chol} GDCA 50 mM Chol 3.5 mM	$\delta_{Chol+Stigmastanol}$ GDCA 50 mM Chol 3.5 mM Stigmastanol 1.75 mM	$\delta_{Chol+Stigmastanol}$ GDCA 50 mM Chol 3.5 mM Stigmastanol 3.5 mM	Slope (m_{chol})	$\Delta_{(\delta_{chol+stigmastanol} - \delta_{GDCA})}$ GDCA 50 mM Chol 3.5 mM Stigmastanol 1.75 mM	$\Delta_{(\delta_{chol+stigmastanol} - \delta_{GDCA})}$ GDCA 50 mM Chol 3.5 mM Stigmastanol 3.5 mM
								$\frac{\Delta\delta}{m_i}$ mM	
12	CH		75.688	75.659	75.666	75.666	-0.009	2.4	2.8
9	CH		36.188	36.166	36.172	36.169	-0.007	2.3	2.7
23	CH ₂		35.300	35.242	35.254	35.243	-0.018	2.5	2.9
22	CH ₂		34.300	34.275	34.279	34.275	-0.008	2.7	3.2
2	CH ₂		32.088	32.063	32.066	32.060	-0.008	2.8	2.9

Table IV. S 5 Concentration of palmitic acid solubilized in GDCA micelles calculated from the variation observed in the resonance of GDCA carbons, for the case where total palmitic acid ($[^{135}\text{T}]$) 1.75 mM was equilibrated with 50 mM GDCA and 3.5 mM of $[4\text{-}^{13}\text{C}]$ cholesterol .

GDCA		Conversion of BS resonances shift into solubilized PA concentration in BS micelles							
Carbon number	Carbon type	Chemical Shift Variation	Slope (m_{PA}) from BS resonances shift analysis in presence of PA	δ_{chol} $[^{120}] = 50$ mM $[^{135}\text{T}] = 1.75$ mM $[\text{Chol}]_{\text{M}} = 3.2$ mM	$\delta_{\text{chol+PA}}$ GDCA 50 mM $[\text{Chol}]_{\text{T}} = 3.5$ mM $[\text{Chol}]_{\text{M}} = 3.2$ mM	$\Delta\delta$	$[\text{PA}]_{\text{M}}$ (mM) $= \frac{\Delta\delta}{m_{PA}}$	$[\overline{\text{PA}}_{\text{M}}]$ (mM)	s.d.
9	CH		-0.011	36.170	36.153	-0.017	1.5	1.7	0.1
25	CH ₂		-0.012	46.204	46.184	-0.020	1.7		
7	CH ₂		-0.013	28.947	28.927	-0.020	1.5		
19	CH ₃		-0.018	25.793	25.761	-0.032	1.8		
21	CH ₃		-0.008	19.470	19.457	-0.013	1.6		
18	CH ₃		-0.011	15.361	15.341	-0.020	1.8		

The chemical shift analysis for the PA was done using the slope (m_{PA}) obtained for the solubilization of PA acid in BS micelles using the resonances showing the more sensitivity to the presence of the FA. The criterion was the use the BS resonances showing a higher correlation between the chemical shift variation and the PA solubilized ($R^2 > 0.98$). Cholesterol chemical shift contribution on the BS micelles composed of cholesterol and PA ($\delta_{\text{chol+PA}}$) was discounted using the chemical shift predicted considering the cholesterol concentration solubilized in the micelle determined by the ^{13}C NMR (δ_{chol}). After this discount the average PA concentration solubilized in the micelle ($[\overline{\text{PA}}_{\text{M}}]$) was determined using the average of the ratios obtained between the chemical shift variation ($\Delta\delta$) for the selected resonances and the slope obtained independently for the PA solubilization in GDCA micelles.

Table IV. S 6 Concentration of oleic acid solubilized in GDCA micelles calculated from the variation observed in the resonance of GDCA carbons, for the case where 3.5 mM total OA ($[^{136}]_T$) was equilibrated with 50 mM GDCA and 3.5 mM of $[4-^{13}C]$ cholesterol .

GDCA		Conversion of BS resonances shift into solubilized OA concentration on BS micelles						
Carbon number	Carbon type	Slope (m_{OA}) from BS resonances shift analysis in presence of OA	δ_{chol} $[^{120}] = 50$ mM $[Chol]_M = 3.2$ mM	$\delta_{chol+OA}$ GDCA 50 mM $[Chol]_T = 3.5$ mM $[^{136}]_T = 3.5$ mM $[^{136}]_M = 3.5$ mM $[Chol]_M = 3.2$ mM	$\Delta\delta$	$[OA_M]$ (mM) $= \frac{\Delta\delta}{m_{OA}}$	$\overline{[OA_M]}$ (mM)	s.d.
12	CH	-0.010	75.649	75.634	-0.015	3.2	3.5	0.2
9	CH	-0.011	36.150	36.133	-0.017	3.5		
25	CH ₂	-0.011	46.187	46.17	-0.017	3.5		
22	CH ₂	-0.009	34.258	34.243	-0.015	3.4		
2	CH ₂	-0.013	32.044	32.026	-0.018	3.2		
11	CH ₂	-0.007	31.132	31.115	-0.017	3.9		
19	CH ₃	-0.016	25.768	25.743	-0.025	3.4		
21	CH ₃	-0.008	19.459	19.445	-0.014	3.6		
18	CH ₃	-0.012	15.341	15.319	-0.022	3.8		

The chemical shift analysis for the OA acid was done using the slope (m_{OA}) obtained for the solubilization of OA acid in GDCA micelles using the resonances showing to be most sensitive to the presence of the FA. The criterion was the use of BS resonances showing higher correlation between the chemical shift variation and the OA solubilized ($R^2 > 0.98$). Cholesterol chemical shift contribution on the BS micelles composed of cholesterol and OA ($\delta_{chol+OA}$) was discounted using the chemical shift predicted considering the cholesterol concentration solubilized in the micelle determined by the ^{13}C NMR (δ_{chol}). After this discount the average OA concentration solubilized in the micelles ($\overline{[OA_M]}$) was determined using the average of the ratios obtained between the chemical shift variation ($\Delta\delta$) of the selected resonances and the slope obtained independently for the OA solubilization in GDCA micelles. The value obtained for the solubilization of OA by chemical shift analysis was equal to the one obtained by quantitative NMR ($[^{136}]_M$).

Table IV. S 7 Concentration of tocopherol solubilized in GDCA micelles calculated from the variation observed in some carbon selected resonances of GDCA, for the case where 1.75 mM total tocopherol was equilibrated with 50 mM GDCA and 3.5 mM of [4-¹³C]cholesterol .

GDCA		Conversion of BS resonances shift into solubilized tocopherol concentration on BS micelles							
Carbon number	Carbon type	Slope ($m_{tocopherol}$) from BS resonances shift analysis in presence of tocopherol	δ_{chol} [120] = 50 mM [Chol] _M = 2.8 mM	$\delta_{chol+OA}$ GDCA 50 mM [Chol] _T = 3.5 mM [tocopherol] _T = 1.75 mM [tocopherol] _M = 1.75 mM [Chol] _M = 2.8 mM	$\Delta\delta$	$\frac{[tocopherol]_M}{\Delta\delta} = \frac{1.75}{m_{tocopherol}}$ (mM)	$\overline{[tocopherol]_M}$ (mM)	s.d.	
10	C	Chemical Shift Variation	-0.0094	36.736	36.719	-0.016	1.7	1.7	0.1
8	CH		-0.0102	38.834	38.819	-0.014	1.4		
11	CH2		-0.0067	31.134	31.121	-0.013	1.9		
16	CH2		-0.0048	30.370	30.361	-0.008	1.7		
6	CH2		-0.0048	29.980	29.972	-0.008	1.7		
19	CH3		-0.0121	25.791	25.770	-0.021	1.7		
18	CH3		-0.0139	15.356	15.333	-0.024	1.7		

The chemical shift analysis for the tocopherol was done using the slope ($m_{tocopherol}$) obtained for the solubilization of tocopherol in GDCA micelles using the resonances showing to be the most sensitive to the presence of the vitamin. The criterion was the use BS carbon resonances showing the higher correlation between the chemical shift variation and the tocopherol solubilized ($R^2 > 0.98$). Cholesterol chemical shift contribution on the BS micelles composed of cholesterol and tocopherol ($\delta_{chol+tocopherol}$) was discounted using the chemical shift predicted considering the cholesterol concentration solubilized in the micelle determined by the ¹³C NMR (δ_{chol}). After this discount the average tocopherol concentration solubilized at the micelle ($\overline{[tocopherol]_M}$) was determined using the average ratios between the chemical shift variation ($\Delta\delta$) of the selected BS resonances and the slope obtained independently for the tocopherol solubilization in GDCA micelles. The average value obtained for the solubilization of tocopherol by chemical shift analysis was equal within the error to the one obtained by absorption quantification ($[tocopherol]_M$).

**Chapter V Isothermal Calorimetric Study
of the Interaction of Bile Salts with Lipid
Membranes**

V. 1 - Abstract

Bile salts (BS) are bio-surfactants responsible for the solubilization of hydrophobic compounds (e.g. cholesterol) in the intestinal lumen, which due to their low aqueous solubility would not be solubilized otherwise. Although they are known by their solubilization capacities, BS can also interact with membranes altering their physicochemical properties. One key parameter for the accurate understanding of how these properties are altered is the partition coefficient. This parameter can provide the local concentration of BS in the membrane.

In this work we determined the partition of several BS, non-conjugated and conjugated with glycine, to large unilamellar vesicles (LUV) composed of POPC and POPC/SpM/Cholesterol (1:1:1) by isothermal titration calorimetry (ITC).

The results showed that the most hydrophilic BS partition less to the membranes than the most hydrophobic, but the translocation follows the inverse trend. The presence of cholesterol and sphingomyelin leads to a decrease of partition of the non-conjugated BS (DCA, CDCA), exhibiting positive enthalpies and faster translocations when compared with less ordered membranes. This was interpreted as a possible manifestation of liquid order/liquid disordered phase coexistence in those membranes.

The intrinsic enthalpy of partition was calculated from the observed enthalpy in the presence of pH buffers with distinct ionization enthalpies. Results indicated that non-conjugated BS change their ionization state to a larger extent upon partition from water to the membrane.

V. 2 - Introduction

Cell membranes are continuously exposed to stimuli. Their function is ambivalent; on one hand they form a structured surface ensuring integrity between two separated aqueous media. On the other hand they are requested to be permeable enough to guarantee cell homeostasis. A good example of what have been said is gastrointestinal membrane (GIM).

In the intestine, prior to absorption, non-polar molecules (e.g. Cholesterol) need to be solubilized in the duodenum content (rich in BS, PL and FA [16]) and carried to the proximity of the GIM [16; 18]. Model membranes composed of POPC and POPC/SpM/Chol (1:1:1) can mimic the apical and basolateral membranes of the gastrointestinal epithelium [137]. Once near the GIM, cholesterol carried by the BS

micelles can be absorbed by diffusion, by a protein mediated process, or both [2]. The most representative BS present at intestinal lumen are those conjugated with glycine (GDCA, GCDCA and GCA) [18]. Micelles of BS are commonly seen merely as vehicles for the transport of hydrophobic molecules to the membrane, overcrossing the UWL, however, their interaction with the membrane can profoundly alter its elastic properties [47; 48]. These interactions will depend on the local concentration of BS in the membrane. Upon the addition of cholic acid to POPC membranes the order parameters for palmitoyl chain decrease [44] unlike the well known condensing effect of cholesterol which increases the order of acyl chains of POPC [46].

Available literature shows that some attempts to determine the partition coefficient of BS into membranes of physiological relevance were made under the goal of understanding the membrane solubilization by BS [36; 49; 50; 113; 138]. Most data on partition of BS to model membranes were obtained using lipid to bound ligand ratio quite low (see Chapter I Section I. 8). This ratio is a critical parameter because a too low ratio leads to high perturbation in the membrane due to aggregation phenomena. The partition obtained is not the intrinsic partition coefficient and is characteristic of that particular concentration used, being useless to predict the partition coefficient at other different concentration. To guarantee the absence of these effects, the lipid to bound ligand ratio should be higher than 20 at 50% of the titration, otherwise more complex partition models are requested [75; 139].

The qualitative evaluation of kinetics of ligand translocation across bilayers, translocation factor (γ) can be determined using both the uptake and release protocols [140; 141]. This determination allow to know the amount of lipid available (only the outer monolayer or both monolayers) to the association with the ligand.

The enthalpy of partition observed from the interaction of amphiphiles with membranes can also help to characterize their phase polymorphism. The increase of membrane order usually leads to characteristic enthalpic changes, showing a transition that goes from exothermic (into less ordered membranes like POPC) to endothermic for partition into more ordered membrane like SpM/Chol (6:4) [142; 143; 144; 145].

POPC membranes are known to be in a liquid disordered state, however the POPC/SpM/Chol (1:1:1) membrane state is not consensual. Some reports suggest it is in a liquid order state [146; 147] and other describe it as being in liquid order/liquid disordered phase coexistence state [1].

The observed enthalpy directly obtained from partition of an amphiphile into a membrane assessed by ITC gathers several contributions, namely the intrinsic enthalpy, the contribution from the heat of dilution and the buffer ionization enthalpy. The enthalpic contributions due to the proton dissociation of different buffers can be used to discount its contribution from the observed enthalpy. This is done determining the partition enthalpy as a function of the enthalpies of ionization of different buffers [148]. Due to that contribution some buffers are less suitable for ITC measurements as their ionization enthalpy affect strongly the observed enthalpy. However when the intrinsic partition enthalpy is very low, the use of a buffer with a high enthalpic contribution can help in the enhancement of the observed heat, allowing the measurement that would be impossible otherwise. This strategy is commonly used for protein-ligand [72; 149] but can also be applied to lipid membrane-amphiphile systems.

Results from the presented work show a decrease in the partition of conjugated and non-conjugated BS with the increase of hydrophilicity of the BS to POPC membranes. The translocation obtained varies in the opposite direction. Partition of DCA and CDCA to POPC/SpM/Chol (1:1:1) membranes was lower whereas the translocation was higher than the obtained for POPC membranes. This result together with the high endothermic enthalpy observed from the partition to the POPC/SpM/Chol (1:1:1) membrane were interpreted as a manifestation of liquid ordered/liquid disordered phase coexistence state.

V. 3 - Materials and methods

Sodium salt of glycochenodeoxycholic (GCDCA), glycocholic (GCA), glycodeoxycholic (GDCA), cholic acid (CA), chenodeoxycholic acid (CDCA), cholic (CA) were purchased from Sigma. The conjugated and non-conjugated BS were weighted and solubilized in the respective buffer and whenever necessary the pH was adjusted with NaOH.

The lipids 1-palmitoyl-2-oleoyl-sn-glycero-3-phosphocholine (POPC), Cholesterol (Chol) and egg Sphingomyelin (SpM) were purchased from Avanti Polar Lipids (Alabaster, AL, USA). The required aqueous suspensions of lipids were prepared by evaporating a solution of the necessary lipid mixture in chloroform/methanol (87:13, v/v) azeotropic solution, blowing dry nitrogen over the heated solution and leaving the residuum in a vacuum desiccator for at least 8 h at 23°C. The solvent free residue was then hydrated with Hepes (10 mM, pH 7.4), Phosphate (10 mM, pH 7.4) or Tris-HCl buffer (10 mM, pH 7.4) containing 150 mM sodium chloride (NaCl), 1 mM ethylenediaminetetraacetic acid (EDTA), and 0.02% of sodium azide (NaN₃) aqueous solution. The hydrated lipid was subject to several cycles of vortex/incubation at a specified temperature (room temperature for POPC and 60°C for POPC/CHOL/SpM) for at least 1 hour to produce a suspension of multilamellar vesicles. These vesicles were then extruded at the same temperature, using a minimum of 10 steps, through two stacked polycarbonate filters (Nucleophore) with a pore diameter of 0.1 μm. For the lipid vesicles containing BS (release experiments), the methodology used was incubating a concentrated solution of BS with the lipid vesicles, with an equilibration time of 24 h at 37 °C.

The final phospholipid concentration was determined using a modified version of the Bartlett phosphate assay [150]. The final cholesterol concentration was determined by the Lieberman–Burchard method [151].

Titration were performed on a VP-ITC instrument from MicroCal (Northampton, MA) with a reaction cell volume of 1410.9 μL, at 37 °C. The injection speed was 0.5 μL s⁻¹; the stirring speed was 296 rpm (to avoid formation of foam) and reference power was 10 μcal s⁻¹. As recommended by the manufacturer, a first injection of 4 μL was performed before starting the experiment to account for diffusion from/into the syringe during the equilibration period. However the injected amount was taken into

account in the calculations. The titration proceeded with additions of 10 μL per injection. Amphiphilic ligands like BS may adsorb to some equipment parts, particularly to the filling syringe, reducing the amount of ligand available. To overcome this drawback, after cleaning thoroughly with water and before it was filled up with the required titration solution, the equipment cell was rinsed with a solution having the same composition of the one to be used in the experiment. All solutions were previously degassed for 15 min.

Two protocols for the ITC experiments were used in this work: (I) uptake, in which liposomes were injected into a BS solution in the cell, and (II) release, in which a liposome solution containing BS was injected into the cell containing buffer. The purpose of the uptake and release protocols was to obtain thermodynamic parameters for the reaction as well as a qualitative evaluation of the translocation rate constant [71; 140]. The thermograms were integrated using the data analysis software Origin 7.0 as modified by MicroCal to handle ITC experiments. The resulting differential titration curves were fitted with the appropriate equations using Microsoft Excel and the Add-In Solver.

Concentrations in the cell were calculated from the volume overflowed from the cell due to the addition of the solution with the syringe, considering overflow faster than mixing and therefore the composition of the leaving solution to be the equilibrium composition before the addition [72; 149].

The predicted heat involved in titration step (i), $q(i)$, is calculated by Equation V. 1, and the best fit of the model to experimental values was obtained by least square minimization between the experimental and the predicted heat per injection for all of the titration steps, as previously described [139]:

$$q(i) = \Delta H \left(n_{BS-L}(i) - n_{BS-L}(i-1) \left(1 - \frac{V(i)}{V_{cell}} \right) \right) + q_{dill} \quad \text{Equation V. 1}$$

Where the $V(i)$ is the injection volume, V_{cell} the volume of the calorimetric cell, and q_{dill} the “heat of dilution” (residual heat due to nonbinding phenomena). The amount of BS associated with the lipid bilayer is calculated assuming simple partition between the aqueous and the lipid phase,



observed partition coefficient (K_p^{obs}) is given by the ratio of the concentrations of BS in each phase calculated with respect to the volume of the respective phase. It is provided by the equation V. 4, where n_{BS_T} is the total chemical amount of BS from which n_{BS_W} are in the aqueous and n_{BS_Lipid} are in the lipid phases.

$$K_p^{obs} = \frac{n_{BS_Lipid}/V_L}{n_{BS_W}/V_W} = \frac{n_{BS_Lipid}/[L] \times \overline{V}_L \times V_T}{n_{BS_W}/V_T} \quad \text{Equation V. 3}$$

$$n_{BS_Lipid} = n_{BS_T} \times \frac{K_p^{obs} \times [L] \times \overline{V}_L}{1 + K_p^{obs} \times [L] \times \overline{V}_L} \quad \text{Equation V. 4}$$

In the equation V. 3, V_T is the total volume, and V_L and V_W are the volumes of the lipid and aqueous phases, respectively. The molar volumes, \overline{V}_L considered for the lipids used in this work were $0.76 \text{ dm}^3 \text{ mol}^{-1}$ for POPC and SpM and $0.34 \text{ dm}^3 \text{ mol}^{-1}$ for cholesterol [74]. For the mixture POPC/Chol/SpM (1:1:1) a weighted average value was used. Values of the adjustable parameters, K_p^{obs} and ΔH , are generated by the Microsoft Excel Add-In Solver. The corresponding heat evolved at each injection is calculated using equation V. 1 and V. 4. They are compared to the experimental values obtained in the titration, and the square difference is minimized. In the above mentioned equations it is implicitly assumed that the entire lipid is available to the ligand. Depending on the relative rates of translocation and insertion/desorption, BS may or may not be able to equilibrate between the two bilayer leaflets. This requires the substitution of BS concentration by its effective concentration, $[BS]^*$, which depends on the effective lipid concentration, $[L]^*$, according to Equation V. 5 and V. 6.

$$[L]^*(i) = [L]^*(i-1) \left[1 - \frac{V(i)}{V_{cell}} \right] + \gamma \left[[L]^{Syr} \frac{V(i)}{V_{cell}} \right] \quad \text{Equation V. 5}$$

$$n_{BS_T}^*(i) = n_{BS_T}^*(i-1) \left[1 - \frac{V(i)}{V_{cell}} \right] + \left[\gamma [BS_L^{Syr}] + [BS_W^{Syr}] \right] V(i) \quad \text{Equation V. 6}$$

where the index i refers to the injection number, the superscript *Syr* indicates concentrations in the syringe, and the subscripts L and W indicate the phase where BS are dissolved (L for the lipid, W for water and T for the sum of both). This introduces

the equilibration factor, γ , which is a measure of the fraction of lipid accessible to BS during the titration experiment, with values of 1 for fully permeable (fast translocation of ligand) and 0.5 for impermeable membranes (slow translocation of ligand). For experiments following the uptake protocol (addition of lipid to ligand in the aqueous phase), the whole amount of ligand is accessible for partition, and the effective lipid concentration is either equal to its total concentration (case of fast translocation) or is reduced to the lipid in the outer monolayer (case of slow translocation). In this type of experiments, if γ is unknown, the uncertainty is propagated to the partition coefficient, but the calculated enthalpy variation is accurate. On the other hand, in experiments following the release protocol, both the lipid effective concentration and the available chemical quantity of ligand must be calculated from equation V. 4. In this situation, both K_p^{obs} and ΔH are affected by the uncertainty in γ . The combination of both protocols allows the calculation of the equilibration factor and therefore, the accurate measurement of K_p^{obs} , ΔH and a qualitative estimation of the translocation rate constant.

V. 4 - Results and discussion

V. 4. 1 - Partition of BS into bilayers in the liquid disordered phase (POPC) using the uptake protocol

The partition of non conjugated BS (CA, DCA and CDCA) and their glycine conjugates to LUV of POPC was investigated by ITC. BS concentrations used in these experiments were always much lower than their CMC and the ratio of lipid to bound ligand was always above 20.

In a typical experiment of the uptake protocol, 10 mM of lipid was loaded in the syringe to titrate a solution of BS with a concentration in the cell of 10 μ M. Figure V. 1 shows the raw data (Plot A) and the differential heat due to DCA titration with LUV composed of POPC (Plot B), assuming slow translocation ($\gamma=0.5$).

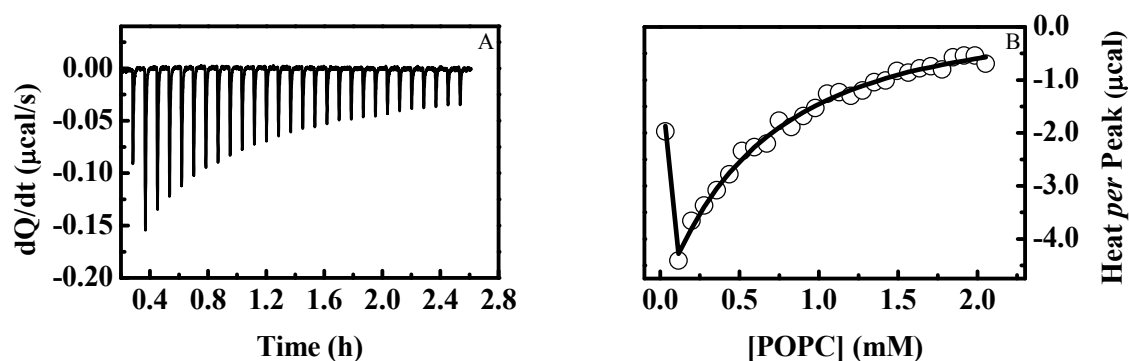


Figure V. 1 (A) Data from an uptake experiment at 37 °C, DCA 10 μ M (cell) and POPC 10 mM (syringe). The injection volumes were 1 x 4 μ L and the others 27 x 10 μ L. (B) Typical results obtained for the heat evolved (\circ) and theoretical fit with a $K_p^{obs}=2.2\times 10^3$, using a gamma of 0.5 (slow translocation). At 50% of titration the ratio of lipid to bound ligand was equal to 152.

Figure V. 1 shows that partition of DCA to the POPC membrane is exothermic. Results obtained show that 60 % of the ligand was titrated and the ratio of lipid to bound ligand in this experiment was always above 50. At 50 % of the titration there is 1 bounded molecule of BS per 152 lipid molecules. At this small local concentration of ligand no membrane perturbation is expected and therefore, the partition coefficient obtained is the intrinsic one. To determine the effect of hydrophobicity of BS in their partition to membranes, we carried the titration with CDCA and CA. We also addressed the effect of BS conjugation with glycine on partition. Figure V. 2 shows the different titration curves obtained for CDCA, CA and their glycine conjugates.

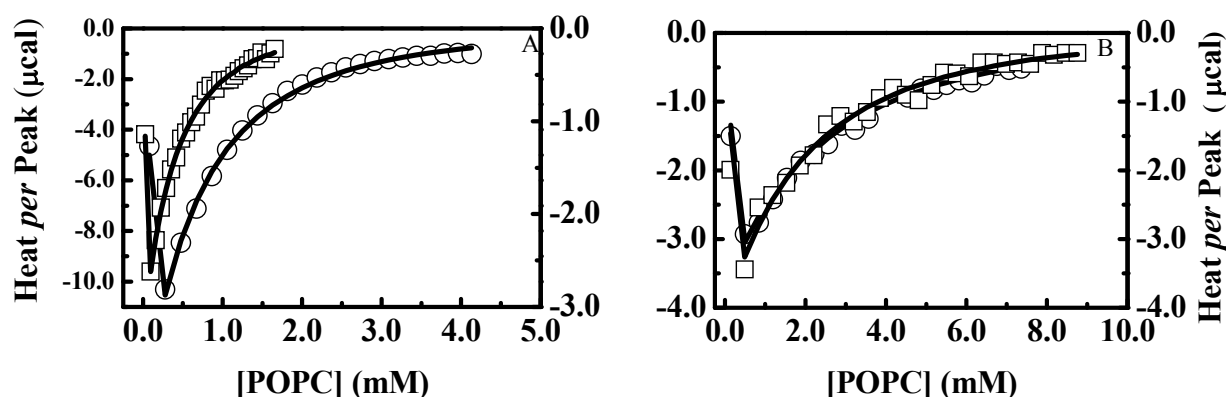


Figure V. 2 Comparison of titration curves and fit to the experimental results for the partition of conjugated and unconjugated BS to POPC LUV (syringe) at 37 °C: Panel A: GCDCA 20 uM (○) and CDCA 10 uM (□); Panel B: GCA 20 uM (○) and CA 30 uM (□). Average and standard deviation results for partition coefficient and enthalpy are given in Table V. 1.

From the above results we can observe that the partition of BS to POPC membranes decreases from CDCA to its conjugated form. The same trend was observed for DCA and its conjugated form as can be seen in Table V. 1. Relatively to the most hydrophilic BS, CA, its conjugation does not lead to any decrease on the partition into the POPC membranes. Herein, results assume an equilibration factor (γ) of 0.5 which considers slow translocation of the BS during the characteristic time of the titration. This assumption was used to define the most appropriate ligand and lipid concentrations. However, this value may not be correct to all BS used. In order to clarify this point, we employed a well known protocol [71] using a global fit for uptake and release experiments, allowing to know whether or not all the lipid was accessible during the time of the measurement.

Table V. 1 Partition constant and enthalpy contributions from the interaction of BS (unconjugated and Glycine conjugated) with lipid membranes composed of POPC and POPC/SpM/ Chol (1:1:1), using a translocation parameter of 0.5 or the value obtained by a global fit of the uptake and release experiments at 37 °C.

BS species	Uptake Protocol (assuming $\gamma=0.5$)				Uptake & Release Protocol (γ from the global fit)					
	K_p^{obs} ($\times 10^3$)		ΔH KJmol ⁻¹		K_p^{obs} ($\times 10^3$)		ΔH KJmol ⁻¹		γ	
	POPC	POPC/SpM/ Chol	POPC	POPC/SpM/ Chol	POPC	POPC/SpM/ Chol	POPC	POPC/SpM/ Chol	POPC	POPC/SpM/ Chol
DCA	2.2 ± 0.2	0.1 ± 0.1	-28 ± 4	110 ± 6	1.8 ± 0.3	0.1 ± 0.1	-23 ± 2	101 ± 36	0.8 ± 0.2	1.0 ± 0.1
CDCA	3.1 ± 0.1	0.2 ± 0.1	-12 ± 1	24 ± 10	2.10 ± 0.04	0.2 ± 0.1	-11.3 ± 0.1	31 ± 5	0.8 ± 0.1	1.0 ± 0.1
CA	0.3 ± 0.1		-5 ± 1		0.26 ± 0.01		-5.1 ± 0.1		1.0 ± 0.1	
GDCA	1.6 ± 0.1		-12 ± 1		1.9 ± 0.1		-11 ± 1		0.8 ± 0.1	
GCDCA	1.9 ± 0.2		-18 ± 3		2.0 ± 0.3		-13 ± 1		0.5 ± 0.1	
GCA	0.3 ± 0.2		-9 ± 2		0.20 ± 0.03		-12 ± 2		1.0 ± 0.1	

V. 4. 2 - Partition of BS into bilayers in liquid disordered phase (POPC)-release versus uptake protocol

In the release protocol it is important to ensure that at the beginning of the titration the lipid /BS ratio is the same as it is at 50% of a typical uptake partition experiment. Figure V. 3 illustrates the uptake and release experiments of CDCA (Panel A) and GCDCA (Panel B) to and from POPC membranes. From these experiments it is possible to determine the partition coefficient, the enthalpy associated to partition and the gamma factor. The gamma factor is a physical discriminator of how fast is the translocation process.

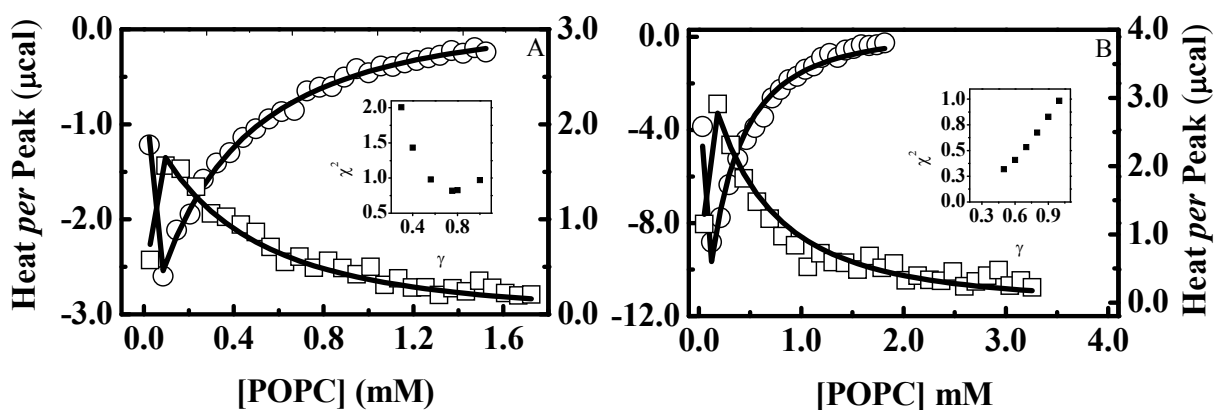


Figure V. 3 Titration curves obtained for uptake (○) and release (□) protocols with POPC membranes. Experiments at 37 °C, Plot A: CDCA partition profile obtained for both protocols with theoretical fit giving a K_p^{obs} of 2.1×10^3 , $\Delta H = -11 \text{ kJmol}^{-1}$ and $\gamma = 0.78$. Plot B: GCDCA partition profile obtained for both protocols with a fit to the experimental results giving a K_p^{obs} of 2.2×10^3 , $\Delta H = -13 \text{ kJmol}^{-1}$ and $\gamma = 0.5$. Insets show the dependence of the square deviation between the global best fit and the experimental results (χ^2) as a function of γ .

From the global fit to both experiments, γ is obtained from the minimum value of χ^2 , adjusting to several possible γ values (varying from 0.5 to 1). The graphs in the insets in both panels show the dependence of χ^2 on different values of γ . Results clearly show that depending of BS, γ and therefore the translocation rate can vary, being higher for the most hydrophilic BS used (CA and GCA).

Values obtained for partition of conjugated and non-conjugated BS indicate that, as expected, more hydrophobic BS partition more extensively to the POPC membranes

than those less hydrophobic. The trihydroxy BS showed a lower partition to the POPC membranes than the dihydroxy BS in both cases of conjugated and non-conjugated BS. The partition of BS decreases with the increase of CMC, indicating that the most soluble BS in water are partitioning less extensively to the membrane. The results show that for the glycine conjugated BS from which both partition and CMC were determined in this work showed that the logarithm of CMC correlate with the logarithm of partition coefficient, showing that partition coefficient can be predicted knowing the CMC of the BS.

Although several works are available in literature measuring partition of BS to lipid phase membranes, several inconsistencies were observed in this determinations [47; 48; 49; 50]. In most of these studies the lipid to bound ligand ratio was lower than 20 at 50 % of titration, which critically affects membrane properties by the presence of a too high BS concentration, compromising the partition value obtained from the experiment [75; 139].

Partition of DCA to EPC membranes was addressed by ITC and showed to be dependent on the lipid to bound ligand ratio used [49]. Although this was noticed this effect was not taken in consideration and the lipid to bound ligand ratio used in the mentioned experiments was between 7 and 10 at 50% of the titration, being the value obtained for the partition equal to 5.4×10^2 . This value is 10 times lower when compared with partition of DCA to POPC membranes obtained in this work. However we should highlight that the previous work was done at a lower temperature which have also a contribution on this decrease.

Another ITC work, where DCA and CA partition was addressed for POPC membranes, used lipid to bound ligand ratio at 50% of the titration equal to 2. However electrostatic correction was included in the partition model used to fit the experimental data, decreasing the error obtained for partition coefficient [50]. The values obtained are comparable to the ones determined in this work (see Table I. 8 and Table V. 1). Both works mentioned above assumed fast translocation meaning that the entire lipid was available for the BS partition. This affects the partition determined because an overestimation of translocation parameter (γ) necessarily overestimates the lipid phase volume considered leading to an underestimation of the observed partition coefficient. Our results show that a γ value of 1 is a valid assumption only in the case of trihydroxy conjugated and non-conjugated BS.

There were some attempts for measuring partition of conjugated and non-conjugated BS to lecithin and lecithin containing other lipids like SpM, PE, PS using ultracentrifugation, equilibrium dialysis and gel chromatography using labelled ^3H BS [36; 47; 48]. Again most of these studies are not determining the intrinsic partition coefficient due to the high local concentration used during the titration (see Chapter I, Table I. 8). However, the interaction of CA and UDCA with lecithin, and CA with lecithin/Chol (7:3) and lecithin/PE (7:3) were obtained with lipid to bound BS which was in the reasonable limits for a reliable determination. These results showed that for lecithin there is a decrease in partition for the most hydrophilic BS (CA when compared with UDCA). A comparable trend was obtained for the interaction of both conjugated and non-conjugated BS with POPC membranes in the presented work, showing a decrease of partition of BS to POPC membranes with the increase of hydrophilicity (Table V. 1). Although quantitatively the values obtained for CA are different, which can be a manifestation of different lipid composition of lecithin (several different PC) compared with POPC (used in the present work), the trend is similar to that obtained by our work.

The concentration of BS in all titrations used in our work was always lower than their CMC as the interaction of the monomer is different from the interaction of micelles which can solubilize membranes [7; 61]. The enthalpy variation obtained for the partition of BS to POPC membranes was negative for the different conjugated and non-conjugated BS used. The values available in literature for the transfer of DCA and CA to EPC membranes show that enthalpy variation obtained is positive [49]. Although in this work the heat flow from the calorimetric titration is exothermic. In another work the enthalpy variation obtained for the partition of CA and CDCA to POPC membranes is negative, comparable to the one obtained in this work [50]. These enthalpy results are in agreement with the results for partition of other amphiphiles to POPC membranes [143; 144; 145; 152].

In terms of translocation there is a clear distinction in the behaviour of the three different glycine conjugated BS. GCA is the most hydrophilic BS, it has the highest γ value indicating a faster translocation. On the other hand GCDCA has the lowest value of γ , stating that during the time scale of each measurement translocation does not occur. GDCA shows an intermediary behaviour. Fast translocation behaviour was also observed for the most hydrophilic non-conjugated BS CA. The reason for this behaviour can be related with the defect induced by the most hydrophilic BS (with more hydroxyl

Chapter V

groups) once in the membrane, leading to the translocation of the BS from one monolayer to the other. Order parameter measurements for cholic acid in lecithin large unilamellar vesicles indicated that this BS has a high destabilizing effect on the membranes [44]. From these results we can clearly conclude the BS partitioning the most to the membrane are the most hydrophobic though they are not the ones having the highest translocation rate.

V. 4. 3 - Partition of BS into membranes of POPC/SpM/Chol (1:1:1)-release versus uptake protocol

Partition of BS to lipid bilayers composed of POPC/SpM/Chol (1:1:1) was addressed for non-conjugated BS (DCA and CDCA). The approach was similar to the one used for POPC membranes. First the uptake experiments were done and then compared with the results from release experiments. Figure V. 4 shows results for DCA (Panel A) and CDCA (Panel B) using the uptake *versus* release protocol to and from the above mentioned lipid phase.

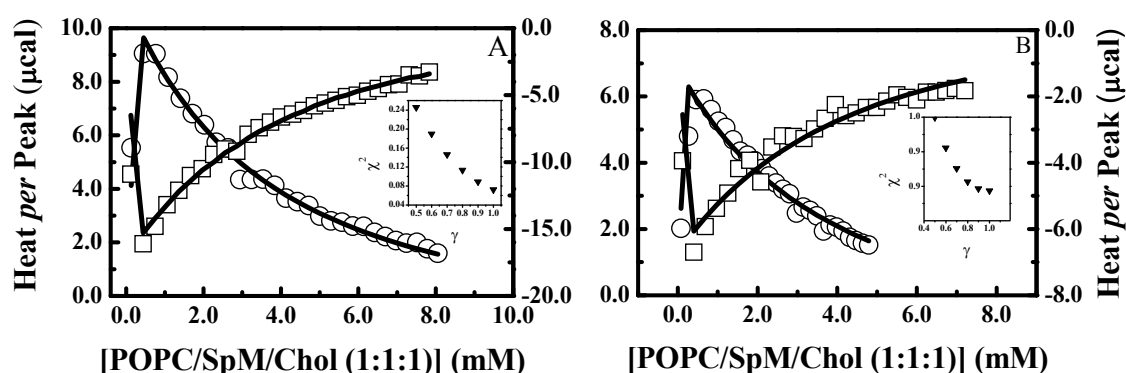


Figure V. 4 Titration curves obtained for uptake (○) and release (□) protocols with POPC/SpM/Chol (1:1:1) membranes. Experiments at 37 °C, Plot A: DCA partition profile obtained for both protocols giving a K_p^{obs} of 1.7×10^2 , $\Delta H = 75 \text{ KJmol}^{-1}$ and $\gamma = 1$. Plot B: CDCA partition profile obtained for both protocols giving a K_p^{obs} of 1.7×10^2 , $\Delta H = 28 \text{ KJ/mol}^{-1}$ and $\gamma = 1$. Insets show the dependence of the square deviation between the global best fit and the experimental results (χ^2) as a function of γ .

From these results obtained it is noticed that DCA and CDCA partition into the membrane composed of POPC/SpM/Chol (1:1:1) is less extensive than to POPC membranes. Considering previous studies of partition determination of CA to lecithin membranes in the presence and absence of cholesterol, it was shown a decrease of partition for the most ordered membranes containing cholesterol [48]. This result was expected due to the increase of order that cholesterol brings into the membrane and the same behaviour was shown for the partition of several amphiphiles for POPC/Chol and SpM/Chol membranes when compared with POPC membranes [143; 144; 145; 152].

Partition of both BS measured to the POPC/Chol/SpM (1:1:1) membranes was endothermic. Positive enthalpies variations were obtained for partitions of a large set of amphiphiles into lipid membranes in liquid order phase (phospholipids, lysolipids and dehydroergosterol) [143; 144; 145].

Literature results agree that POPC and SpM/Chol (60:40) are in the liquid disordered and ordered phase, respectively. However, for the membrane POPC/SpM/Chol (1:1:1) lipid composition there is no general consensus. One study refers that this lipid composition is thought to be in a regime of liquid order/ liquid disorder phase coexistence [1]. This has been questioned suggesting that this composition is already in the liquid ordered phase [146; 153].

From the results above discussed the enthalpy variation associated with partition into more disordered membranes is clearly negative but the enthalpies for more ordered membranes become less negative and the partition may even become endothermic. The same trend occurs with the partitions of the BS to POPC membranes, showing a clear exothermic behaviour, expected for this disordered membranes. The large endothermic enthalpy obtained for the partition of BS to POPC/SpM/Chol (1:1:1) membranes suggests that the BS could be partitioning to a liquid ordered phase or liquid order domains.

The translocation factor for the BS partition obtained for the POPC/SpM/Chol (1:1:1) was always equal to one and was higher than those observed for the POPC membranes. This is an unexpected result as the measured translocation rate of several amphiphiles in different type of membranes has shown that the fastest translocation occurs for POPC (liquid disordered state), decreases for POPC/Chol (50:50) and SPM/Chol (60:40), being these last two membranes thought to be in liquid ordered state [1]. Considering that translocation obtained for the BS in the POPC/SpM/Chol (1:1:1) is always higher than the one obtained for POPC membranes (liquid disordered phase) and the high positive enthalpies obtained from partition (characteristic of more ordered systems), these results may be consistent with a membrane having liquid order/disordered phase coexistence, although we should highlight it as an indirect evidence.

V. 4. 4 - Enthalpy contribution from buffer ionization

The overall enthalpy measured in a chemical reaction includes the contribution of the enthalpy of proton uptake or release to or from the buffer. In order to determine its contribution we followed the interaction of BS with POPC membranes in different buffers, namely phosphate, Tris-HCl and Hepes. These buffers are well known to have different ionization enthalpies [148].

The dependence of the observed partition enthalpy on the ionization enthalpy of the different buffers can give information relative to the number of protons released to the BS, enabling the discrimination of the intrinsic enthalpy due to partition. The results are shown in Figure V. 5.

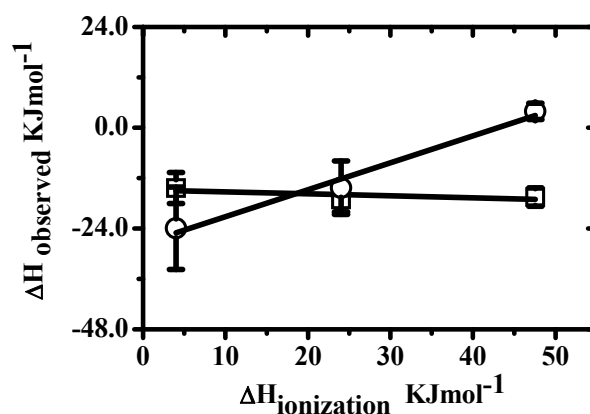


Figure V. 5 Dependence of the observed enthalpy variation associated with partition into POPC membranes for GDCA (□) and DCA (○), on the buffers ionization enthalpy. The enthalpy of ionization for the different buffers was obtained from [148]. The dependence obtained for the unconjugated BS, DCA, give an intrinsic enthalpy partition of -27 KJmol^{-1} and the number of protons released by the buffer to the BS is 0.6.

The enthalpy variation upon partition of non-conjugated BS DCA proved to be dependent on the enthalpy of buffer ionization, unlike the observation made with the glycine conjugated BS, GDCA.

The values obtained for the several unconjugated BS are shown in Table V. 2 as well as the corresponding change in pKa for the different BS upon partition.

Table V. 2 Variation in observed pKa due to the partition of BS from water to membranes of POPC. The pKa values of different BS in aqueous environment are also shown [23]. Information regarding the protons released or received by the buffer is shown and was obtained from the dependence of enthalpy of partition with enthalpy of ionization for the buffers considered.

BS	H ⁺ release from buffer	pKa Membrane	pKa Water	Δ pKa
DCA	0.63 ± 0.12	7.6	5.3	2.3
CDCA	0.78 ± 0.12	7.8	5.9	2.0
CA	0.83 ± 0.19	8.0	5.0	3.0
GDCA	-0.04 ± 0.06	4.7	4.7	0.0

Results show clearly that the partition process of non-conjugated BS to membranes involves change in their ionization state, contrary to observations made for conjugated BS (GDCA). Results also suggest that upon partition to the membrane the conjugated BS has its carboxylic group in a similar environment to the one it has when in bulk solution. For this reason no significant protonation was observed. A possible explanation is that unlike non-conjugated BS, glycine present in the conjugated BS can establish hydrogen bonds with membrane due to the extra amide group. This hydrogen bonding may allow BS stabilization in the membrane without any substantial gain by the protonation of the carboxylic group. In the case of the non-conjugated BS all of them seem to be stabilized by the protonation of the carboxylic group, being CA the BS changing the most its ionization state. CA is the most hydrophilic and therefore the one expected to partition the less and having a higher destabilizing effect on the membrane. This BS shows the highest protonation probably because they are less inserted in the membrane being more accessible to protonation than other more hydrophobic BS considerably deeper inserted in the membrane being for this reason less accessible to protonation.

The thermodynamic data for the non-conjugated BS interaction with POPC membranes after discarding the ionization enthalpy effects of the buffer are shown in Table V. 3.

Table V. 3 Thermodynamic data relative to the intrinsic partition of several non-conjugated BS to POPC lipid membranes at 37 °C.

BS	POPC		
	ΔH (KJmol ⁻¹)	ΔG (KJmol ⁻¹)	$T\Delta S$
DCA	-28 ± 4	-20 ± 2	-8
CDCA	-26 ± 4	-21 ± 2	-5
CA	-18 ± 6	-14 ± 2	-4

Thermodynamic data show that intrinsic enthalpy obtained for the non-conjugated BS is exothermic being more negative for the dihydroxy BS and less negative for the trihydroxy BS. The partition of non-conjugated BS to POPC membranes is enthalpic driven. The partition of apolar molecules to lipid membranes is normally considered to be a consequence of the hydrophobic effect which is characterized by an entropic contribution attributed to the water release from the solute hydration shell. Partition of BS to membranes reveals to be essentially due to large exothermic enthalpies and negative entropies which are in sharp contrast with the hydrophobic effect. In our measurements we used Hepes buffer which has a mean enthalpic contribution from the three buffers considered and enable to recover the partition of conjugated and non-conjugated BS to POPC membranes. The enthalpic contribution from phosphate buffer ionization was lower but it would interfere with the determinations of lipid concentrations based on quantification of phosphate in the membranes, being for this reason avoided.

The results clearly show that the choice of the buffer for certain amphiphiles is very important in the ITC measurements due to its enthalpic ionization contribution.

V. 5 - Conclusions

Duodenum content in the intestine is an intricate mixture of components, most of them very hydrophobic (e.g. cholesterol) which are solubilized with the help of BS. The surfactancy properties of BS are well known [6] as well as their perturbing effects on membranes, namely the solubilization limits [154; 155] and the effects of the order parameters of the palmitoyl chain of POPC [44]. The partition of BS to membranes is thought to occur through aqueous monomer interaction with the membrane [4]. To get a quantitative answer on the extent of the perturbation occurring in the membrane, the local concentration of BS in the membrane can be one of the parameters for consideration. For this reason the partition coefficient must be accurately measured. In this study we measured the partition of BS (CDCA, DCA, CA, GCDCA, GDCA, and GCA), non-conjugated and conjugated with glycine, into membranes composed of POPC and POPC/SpM/Chol (1:1:1) by ITC. Our results indicate that the partition to POPC membranes is higher for the most hydrophobic BS, CDCA and DCA, and lowest for the hydrophilic CA. The same trend is observed for the glycine conjugated BS, although there was no substantial difference between conjugated and non-conjugated BS. Most of the work available in literature in this area have been using too high lipid to bound ligand which clearly affects the observed partition. Moreover the partition model used also accounted for the translocation, using a global fit considering both uptake and release well establish protocols. This enabled the determination of the translocation which in some cases is in a different regime than the assumed fast translocation, which underestimates the values of observed partition obtained.

The partition to membranes in the liquid disordered state (POPC) was always higher than to POPC/SpM/ Chol (1:1:1) membranes. The enthalpies determined for the two types of membranes showed different behaviours, being exothermic for the POPC membranes and endothermic for POPC/SpM/Chol (1:1:1) membranes. Another complementary result is the translocation factor which differs among the different BS, being the translocation faster for the trihydroxy BS than for the dihydroxy. Although the γ parameter does not reveal a quantitative value for the translocation rate constant, it qualitatively expresses whether the translocation was fast or slow, discriminating if the lipid from both monolayers is or not available for the partition of the amphiphile considered. For the BS partition studied in membranes with different lipid composition, like CDCA and DCA, they showed a higher translocation on POPC/SpM/Chol (1:1:1)

membrane and an enthalpy of partition characteristic of a more ordered phase membrane. Altogether, these results suggest that POPC/SpM/Chol (1:1:1) membranes show liquid disorder/order phase coexistence.

The dependence of the partition enthalpy on the enthalpy of buffer ionization revealed that non-conjugated BS seems to be stabilized by the change in their ionization state when the partition to the membrane occurs, being this effect higher for the most hydrophilic BS. This is highlighted by the increase of pKa of BS from water to the membrane.

Partition of BS to POPC membranes is enthalpic driven, being more exothermic for the dihydroxy BS. Results also highlighted the fact that partition of BS to be lower in membranes composed of POPC/SpM/Chol (1:1:1), indicating these membranes to be less suitable to solubilization. Although they are more resistant, they exhibit a higher translocation factor which can be consistent with a passive diffusion view of the BS across gastrointestinal membrane and also at the canicular membrane when bile migrates from liver to the gallbladder. These results can have high relevance for drug delivery and pharmacokinetics field.

Chapter VI *General Conclusions*

VI. 1 - General conclusions

Cholesterol absorption through the intestinal epithelium is a very intricate process. There is some fundamental knowledge on the absorption process that is normally rationalized in two major mechanisms: the passive diffusion and the mediated transport. Evidences for both processes are found in literature but the weight from each of the processes is not known. Fundamental knowledge of passive diffusion mechanism could help the understanding of the overall process. It is clear that the absorption process goes through different steps. Before interaction with membrane cholesterol molecules need to be available for permeation. Due to their high hydrophobicity, they need to be solubilized in the so called intermixed dietary micelles and vesicles. These structures are composed essentially by BS, PL and cholesterol, although this is already a simplistic view of lumen content.

The first question addressed in this work regarded the effect of most prevalent BS, found in intestinal lumen, in respect to their cholesterol solubilization capacities. We develop a non-invasive method to determine cholesterol solubilized in the BS micelles [120]. From our studies it is clear that more hydrophilic BS solubilizes less cholesterol than hydrophobic BS, but we extended this knowledge for binary mixtures of BS and also to a physiologically relevant ternary mixture of BS. This understanding was important to rationalize strategies that could be helpful to decrease or increase cholesterol solubilization or others hydrophobic compounds. It is also important to notice that the micelle with more solubilized cholesterol does not mean that this system will deliver more cholesterol to the membranes. This will depend on the avidity of cholesterol for the membrane (partition coefficient) and also depends on the interaction of cholesterol with the micelle itself. The solubility in the micelle reflects the size of the reservoir of cholesterol that can be delivered to the membranes and it also affects the rate at which it occurs through changes in the concentration of cholesterol in the aqueous phase.

Another important observation is that micelles of hydrophilic BS are normally smaller than those formed by more hydrophobic BS. This can also be an argument for selectivity of certain type of micelles used on cholesterol delivery to membranes. These micelles will diffuse faster than bigger ones being more effective on the delivery of cholesterol at the gastrointestinal membranes. These arguments only reinforce the necessity to understand the solubilization process in a more detailed way than until now.

The solubilization of cholesterol in the several simple and composed micelles showed several important results. The dependence of cholesterol solubility with total cholesterol showed a linear dependence until a plateau was attained, confirming the cholesterol solubility limit. Moreover, the solubility of cholesterol obtained *per* micelle gave different average values for distinct BS being usually smaller than 1. Both results were interpreted as indicative that solubilization of sterol by the micelles is more related to a partition phenomena than to a binding event.

From our results the binary mixtures showed some distinct solubilization capacities when compared to their individual behaviour. The GDCA/GCA mixture was the one that showed higher solubilization if only mixed systems are considered. The GCA/GCDCA showed a higher solubility for cholesterol than both individual BS species. This is an unexpected result and shows that the mixtures of these BS increase their cholesterol solubilizing capacities. This was not observed in the other binary mixtures, where normally the value obtained for the solubilization of cholesterol is an average of the solubilities obtained for single BS. These results clearly show that some proportions of BS can affect solubility of cholesterol and this can be a specific target for decreasing cholesterol solubilization. Moreover, the solubilization of BS at intestinal lumen is not optimized for the highest or lowest solubilization, but is regulated for a trade off between cholesterol solubility at intestinal lumen and absorption through GIM. This is achieved having micelles with a low CMC, forming micelles at a lower value of solubilizer and having a moderate solubilizing capacity.

Another question addressed in this work has to do with the effect of phytosterols, fatty acids (saturated and unsaturated) and tocopherol in the solubilization of cholesterol by the BS micelles. The use of competitors in human diet has been used as a strategy for the reduction of cholesterol absorption. Two possible mechanisms have been described in literature explaining their inhibitory effects (co-solubilization and co-precipitation). Also in the literature there are some inconsistencies related with the weight effects of sterols and stanols in the solubilization of cholesterol. Our results showed that stigmasterol has a higher inhibitory skill on cholesterol solubility than stigmastanol. Phytosterols seem to reduce the amount of cholesterol solubilized via both co-solubilization and co-precipitation, based into two fundamental observations: a) the dependence of cholesterol and stigmasterol solubilization in micelles with the increase stigmasterol/cholesterol ratio showed a solubility limit for stigmasterol increasing and a decrease on cholesterol solubilization in the micelle; b) the overall

sterol at the micelle decrease when compared with the capacity for cholesterol in absence of phytosterols.

The vitamin (α -tocopherol) and the unsaturated FA (OA) showed smaller decreasing effects on cholesterol solubility than phytosterols, nevertheless being higher for the vitamin. However they showed similar mechanisms of action, namely both inhibitors were completely soluble in the micellar solutions and their presence in micelles decreased the solubility of cholesterol. This indicates that although their effect is smaller than that of phytosterols, both vitamins and unsaturated FA decrease cholesterol solubility and can be useful for decreasing cholesterol intake in the intestine. Saturated FA (PA) increased the solubility of cholesterol in the micelles.

The interaction of conjugated and non conjugated BS with model lipid membranes, that could mimic the apical and basolateral membranes of intestinal epithelium, was another subject studied in this work by isothermal titration calorimetry. The partition for two membranes was characterized, namely, POPC and POPC/SpM/Chol (1:1:1) membranes. The results showed that the most hydrophobic BS partition more extensively for the membranes than the hydrophilic ones. The difference of the observed partition between non-conjugated and conjugated was very similar for POPC membranes. The partition for membranes of POPC/SpM/Chol (1:1:1) decreased when compared with partition obtained for POPC.

The translocation parameter, that is the fraction of lipid accessible to BS during the titration, assuming the value 1 when all lipid is available (fast translocation), and 0.5, when only half of the lipid is available for translocation (slow translocation), was also measured. Translocation showed to be fastest for hydrophilic BS (CA and GCA) and slowest for the hydrophobic BS. In this latest GCDCA showed to be particularly slow. The translocation factor increase when passing from POPC membranes in the liquid disorder state to the membranes of POPC/SpM/Chol (1:1:1). The positive enthalpy variation obtained for the partition of the BS with the POPC/SpM/Chol (1:1:1) membrane allied with the highest translocation obtained for this membranes when compared with the POPC membranes were interpreted as arguments for considering POPC/SpM/Chol (1:1:1) membrane as being in a liquid order/liquid disorder phase coexistence state.

The dependence of enthalpy of partition was studied as function of buffer ionization enthalpy for unconjugated and conjugated BS to evaluate changes in the ionization of BS upon interaction with the membranes. The non-conjugated BS showed

to be strongly dependent on the enthalpy associated with the ionization of the buffer, contrary to that observed for conjugated BS. This allowed obtaining the number of protons transferred as well as the intrinsic enthalpy variation upon partition to the membranes. The understanding of the interaction of BS with membranes is a very important process, namely for determining the local concentration of BS at the membranes, that can be important to interpret enterohepatic re-circulation of BS mechanisms, the effects of BS on membrane permeability and also their surfactancy effects on the biological membranes (cytotoxicity of BS).

The study presented here gives some important contribution for the field of passive absorption in the intestine. Previous to absorption, the hydrophobic molecules or drugs need to be solubilized in BS micelles. They seem to have a crucial role for cholesterol absorption but they are also very important for drug delivery. Results obtained indicate that the solubilization of cholesterol by BS micelles in the intestinal lumen is a very important process, which conditions the availability of the cholesterol (and other hydrophobic molecules). The co-solubilizers can be either BS themselves or other molecules like phytosterols, FA, vitamins and drugs, which depending on their nature, structure and concentration, can have completely different actions.

The BS can also interact with membranes changing their properties, which can alter the passive diffusion of several molecules through the membrane. The determination of the solubilization and partition parameters of BS can improve the knowledge on pharmacokinetics field and develop better strategies for inducing or reducing the absorption through intestinal epithelium. Further studies on this area can help in the development of better strategies to reduce cholesterol intake in human and into the development of more efficient carriers of drugs using BS.

VI. 2 - Pitfalls and future perspectives

The argument that this work is a vision too simplistic of reality can be valid but this has been a deliberate option. To understand a complex system the approach can be done by decrease of the system complexity to the simplest possible, and then increase complexity step by step. Taking this in consideration an evaluation of the cholesterol solubilization limit in a single mixture of BS (most representatives in the biological context) at a relevant concentration was determined. Knowing this, the cholesterol solubilization index was addressed in binary and ternary BS mixtures. In a biological context the presence of several other contributors for the cholesterol solubilization should not be ignored, namely phospholipids, fatty acids, vitamins and others.

The methodology developed in this study to follow the solubility of sterol in the micelle used NMR spectroscopy with an enriched ^{13}C cholesterol molecule. One question that can arise is why it was used cholesterol labelled in ^{13}C if we could see the alkene proton of cholesterol by ^1H NMR. The answer is simple: the signal in ^1H NMR spectrum is seen at 5.4 ppm (near the proton signal of water), being difficult to measure without distortion of the signal. ^{13}C NMR allows us to follow cholesterol inside the micelles. Then, when adding oleic acid or stigmasterol to the system, we can follow both competitor and cholesterol, gathering ^1H and ^{13}C NMR information. Another reason for doing so is the presence in an *in vivo* context of several compounds with double bonds able to interfere with the quantification of cholesterol. This approach was addressed considering the possibility of being used for a more complex physiological mixture. This method in future can be used to follow the transfer of cholesterol from BS micelles to membranes or to cellular lines, in the presence and absence of co-solubilizers. Another important study in the future is to evaluate the effect of other sterols and stanols with different side chains on cholesterol solubilization. The effect of polyunsaturated FA (e.g. Omega 3, Omega 6) should be evaluated to observe if they are more effective on the decrease of cholesterol solubility by BS micelles than the unsaturated oleic acid. Another important evaluation is concerned with possible synergies between all of different inhibitors of cholesterol solubilization. Does the mixture of vitamins and phytosterols will decrease more cholesterol solubility in BS micelles than each component separately? Are the effects additive?

Chapter VI

The transfer of cholesterol between different BS micelles to model membranes would give the relation between solubilization and partition that can best characterize absorption mechanism in intestinal epithelium.

This work should be extended to cell lines mimetizing gastrointestinal membrane (e.g. Caco cells), the strategy can be using labelled cholesterol in ^{14}C and determining the cholesterol inside of different compartments, that should mimetize intestinal lumen (donor compartment) and blood (acceptor compartment). This will have profound implications for the understanding of passive absorption process but also to understand the weight of passive diffusion on the overall process of absorption.

VII. 1 - Bibliography

- [1] R.F.M. De Almeida, A. Fedorov, And M. Prieto, *Sphingomyelin/Phosphatidylcholine/Cholesterol Phase Diagram: Boundaries And Composition Of Lipid Rafts. Biophysical Journal* 85 (2003) 2406-2416.
- [2] D.Y. Hui, And P.N. Howles, *Molecular Mechanisms Of Cholesterol Absorption And Transport In The Intestine. Seminars In Cell & Developmental Biology* 16 (2005) 183-192.
- [3] K. Simons, And W.L.C. Vaz, *Model Systems, Lipid Rafts, And Cell Membranes. Annual Review Of Biophysics And Biomolecular Structure* 33 (2004) 269-295.
- [4] G. Thompson, *Fat Absorption And Metabolism. Gastroenterologia Japonica* 19 (1984) 251-259.
- [5] M.C. Carey, D.M. Small, And C.M. Bliss, *Lipid Digestion And Absorption. Annual Review Of Physiology* 45 (1983) 651-677.
- [6] J.S. Patton, And M.C. Carey, *Watching Fat Digestion. Science* 204 (1979) 145-148.
- [7] W.J. Simmonds, *Role Of Micellar Solubilization In Lipid Absorption. Australian Journal Of Experimental Biology And Medical Science* 50 (1972) 403-&.
- [8] K. Matsuoka, M. Suzuki, C. Honda, K. Endo, And Y. Moroi, *Micellization Of Conjugated Chenodeoxy- And Ursodeoxycholates And Solubilization Of Cholesterol Into Their Micelles: Comparison With Other Four Conjugated Bile Salts Species. Chemistry And Physics Of Lipids* 139 (2006) 1-10.
- [9] A.F. Hofmann, And D.M. Small, *Detergent Properties Of Bile Salts - Correlation With Physiological Function. Annual Review Of Medicine* 18 (1967) 333-&.
- [10] E.A. Trautwein, G. Duchateau, Y.G. Lin, S.M. Mel'nikov, H.O.F. Molhuizen, And F.Y. Ntanios, *Proposed Mechanisms Of Cholesterol-Lowering Action Of Plant Sterols. European Journal Of Lipid Science And Technology* 105 (2003) 171-185.

- [11] E. Levy, S. Spahis, D. Sinnett, N. Peretti, F. Maupas-Schwalm, E. Delvin, M. Lambert, And M.A. Lavoie, *Intestinal Cholesterol Transport Proteins: An Update And Beyond. Current Opinion In Lipidology* 18 (2007) 310-318.
- [12] K. Klappe, I. Hummel, D. Hoekstra, And J.W. Kok, *Lipid Dependence Of ABC Transporter Localization And Function. Chemistry And Physics Of Lipids* 161 (2009) 57-64.
- [13] T.T. Kararli, *Comparisson Of The Gastrointestinal Anatomy, Physiology And Biochemistry Of Humans And Commonly Used Laboratory-Animals. Biopharmaceutics & Drug Disposition* 16 (1995).
- [14] J.L. Madara, *Handbook Of Physiology, The Gastrointestinal System, Intestinal Absorption And Secretion: .Functional Morphology Of Epithelium Of The Small Intestine. Compr Physiol* 2011, Supplement 19.
- [15] I. Fox, *Human Physiology, Wm. C. Brown Publishers, 1996.*
- [16] J.E. Staggers, O. Hernell, R.J. Stafford, And M.C. Carey, *Physical-Chemical Behavior Of Dietary And Biliary Lipids During Intestinal Digestion And Absorption .1. Phase-Behavior And Aggregation States Of Model Lipid Systems Patterned After Aqueous Duodenal Contents Of Healthy Adult Human-Beings. Biochemistry* 29 (1990) 2028-2040.
- [17] A.F. Hofmann, And B. Borgstrom, *Intraluminal Phase Of Fat Digestion In Man - Lipid Content Of Micellar + Oil Phases Of Intestinal Content Obtained During Fat Digestion + Absorption. Journal Of Clinical Investigation* 43 (1964) 247-&.
- [18] O. Hernell, J.E. Staggers, And M.C. Carey, *Physical-Chemical Behavior Of Dietary And Biliary Lipids During Intestinal Digestion And Absorption. 2. Phase Analysis And Aggregation States Of Luminal Lipids During Duodenal Fat Digestion In Healthy Adult Human Beings. Biochemistry* 29 (1990) 2041-2056.
- [19] A. Adef, *Absorption And Drug Development: Solubility, Permeability, And Charge State, 2003.*

- [20] J.N. Israelachvili, D.J. Mitchell, And B.W. Ninham, *Theory Of Self-Assembly Of Lipid Bilayers And Vesicles. Biochimica Et Biophysica Acta* 470 (1977) 185-201.
- [21] J. Israelachvili, *Intermolecular And Surface Forces*, Elsevier, Academic Press Publications, Amsterdam, 2011.
- [22] M.C. Carey, And D.M. Small, *Micellar Properties Of Dihydroxy And Trihydroxy Bile Salts - Effects Of Counterion And Temperature. Journal Of Colloid And Interface Science* 31 (1969) 382-&.
- [23] M.C. Carey, And D.M. Small, *Micelle Formation By Bile-Salts - Physical-Chemical And Thermodynamic Considerations. Archives Of Internal Medicine* 130 (1972) 506-&.
- [24] D.J. Cabral, J.A. Hamilton, And D.M. Small, *The Ionization Behavior Of Bile-Acids In Different Aqueous Environments. Journal Of Lipid Research* 27 (1986) 334-343.
- [25] A. Roda, A.F. Hofmann, And K.J. Mysels, *The Influence Of Bile-Salt Structure On Self-Association In Aqueous-Solutions. Journal Of Biological Chemistry* 258 (1983) 6362-6370.
- [26] D.K. P. Nair, *The Bile Acids. Chemistry, Physiology, And Metabolism*, Plenum Press, 1971.
- [27] R. Ninomiya, K. Matsuoka, And Y. Moroi, *Micelle Formation Of Sodium Chenodeoxycholate And Solubilization Into The Micelles: Comparison With Other Unconjugated Bile Salts. Biochimica Et Biophysica Acta-Molecular And Cell Biology Of Lipids* 1634 (2003) 116-125.
- [28] M.C. Carey, J.C. Montet, M.C. Phillips, M.J. Armstrong, And N.A. Mazer, *Thermodynamic And Molecular-Basis For Dissimilar Cholesterol-Solubilizing Capacities By Micellar Solutions Of Bile-Salts - Cases Of Sodium Chenodeoxycholate And Sodium Ursodeoxycholate And Their Glycine And Taurine Conjugates. Biochemistry* 20 (1981) 3637-3648.

- [29] S.M. Mel'nikov, J. Ten Hoorn, And A. Eijkelenboom, *Effect Of Phytosterols And Phytostanols On The Solubilization Of Cholesterol By Dietary Mixed Micelles: An In Vitro Study. Chemistry And Physics Of Lipids* 127 (2004) 121-141.
- [30] K. Matsuoka, M. Maeda, And Y. Moroi, *Micelle Formation Of Sodium Glyco- And Taurocholates And Sodium Glyco- And Taurodeoxycholates And Solubilization Of Cholesterol Into Their Micelles. Colloids And Surfaces B-Biointerfaces* 32 (2003) 87-95.
- [31] R.D. Stevens, A.A. Ribeiro, L. Lack, And P.G. Killenberg, *Proton Magnetic-Resonance Studies Of The Aggregation Of Taurine-Conjugated Bile-Salts. Journal Of Lipid Research* 33 (1992) 21-29.
- [32] H. Igimi, And M.C. Carey, *Cholesterol Gallstone Dissolution In Bile - Dissolution Kinetics Of Crystalline (Anhydrate And Monohydrate) Cholesterol With Chenodeoxycholate, Ursodeoxycholate, And Their Glycine And Taurine Conjugates. Journal Of Lipid Research* 22 (1981) 254-270.
- [33] P. Garidel, A. Hildebrand, R. Neubert, And A. Blume, *Thermodynamic Characterization Of Bile Salt Aggregation As A Function Of Temperature And Ionic Strength Using Isothermal Titration Calorimetry. Langmuir* 16 (2000) 5267-5275.
- [34] Neiderhi.Dh, And H.P. Roth, *Cholesterol Solubilization By Solutions Of Bile Salts And Bile Salts Plus Lecithin. Proceedings Of The Society For Experimental Biology And Medicine* 128 (1968).
- [35] G. Salvioli, H. Igimi, And M.C. Carey, *Cholesterol Gallstone Dissolution In Bile - Dissolution Kinetics Of Crystalline Cholesterol Monohydrate By Conjugated Chenodeoxycholate-Lecithin And Conjugated Ursodeoxycholate-Lecithin Mixtures - Dissimilar Phase-Equilibria And Dissolution Mechanisms. Journal Of Lipid Research* 24 (1983) 701-720.
- [36] P. Schurtenberger, N. Mazer, And W. Kanzig, *Micelle To Vesicle Transition In Aqueous-Solutions Of Bile-Salt And Lecithin. Journal Of Physical Chemistry* 89 (1985) 1042-1049.

- [37] N.A. Mazer, G.B. Benedek, And M.C. Carey, *Quasi-Elastic Light-Scattering-Studies Of Aqueous Biliary Lipid Systems - Mixed Micelle Formation In Bile-Salt Lecithin Solutions. Biochemistry* 19 (1980) 601-615.
- [38] M.C. Carey, *Critical Tables For Calculating Cholesterol Saturation Of Native Bile. Journal Of Lipid Research* 19 (1978) 945-955.
- [39] G.R. Thompson, And S.M. Grundy, *History And Development Of Plant Sterol And Stanol Esters For Cholesterol-Lowering Purposes. American Journal Of Cardiology* 96 (2005) 3D-9D.
- [40] K. Matsuoka, E. Rie, S. Yui, C. Honda, And K. Endo, *Competitive Solubilization Of Cholesterol And Beta-Sitosterol With Changing Biliary Lipid Compositions In Model Intestinal Solution. Chemistry And Physics Of Lipids* 165 (2012) 7-14.
- [41] M.J. Armstrong, And M.C. Carey, *Thermodynamic And Molecular Determinants Of Sterol Solubilities In Bile-Salt Micelles. Journal Of Lipid Research* 28 (1987) 1144-1155.
- [42] A.W. Brown, J. Hang, P.H. Dussault, And T.P. Carr, *Phytosterol Ester Constituents Affect Micellar Cholesterol Solubility In Model Bile. Lipids* 45 (2010) 855-862.
- [43] P. Garidel, A. Hildebrand, K. Knauf, And A. Blume, *Membranolytic Activity Of Bile Salts: Influence Of Biological Membrane Properties And Composition. Molecules* 12 (2007).
- [44] J. Ulmius, G. Lindblom, H. Wennerstrom, L.B.A. Johansson, K. Fontell, O. Soderman, And G. Arvidson, *Molecular-Organization In The Liquid-Crystalline Phases Of Lecithin Sodium Cholate Water-Systems Studied By Nuclear Magnetic-Resonance. Biochemistry* 21 (1982) 1553-1560.
- [45] J.L. Thewalt, And M. Bloom, *Phosphatidylcholine - Cholesterol Phase-Diagrams. Biophysical Journal* 63 (1992) 1176-1181.
- [46] T.M. Ferreira, F. Coreta-Gomes, O.H. Ollila, M.J. Moreno, W.L. Vaz, And D. Topgaard, *Cholesterol And POPC Segmental Order Parameters In Lipid Membranes:*

Solid State (1)H-(13)C NMR And MD Simulation Studies. Phys Chem Chem Phys 21 (2012) 21.

[47] R. Schubert, K. Beyer, H. Wolburg, And K.H. Schmidt, *Structural-Changes In Membranes Of Large Unilamellar Vesicles After Binding Of Sodium Cholate. Biochemistry* 25 (1986) 5263-5269.

[48] R. Schubert, And K.H. Schmidt, *Structural-Changes In Vesicle Membranes And Mixed Micelles Of Various Lipid Compositions After Binding Of Different Bile-Salts. Biochemistry* 27 (1988) 8787-8794.

[49] F. Ollila, And J.P. Slotte, *A Thermodynamic Study Of Bile Salt Interactions With Phosphatidylcholine And Sphingomyelin Unilamellar Vesicles. Langmuir* 17 (2001) 2835-2840.

[50] A. Hildebrand, K. Beyer, R. Neubert, P. Garidel, And A. Blume, *Temperature Dependence Of The Interaction Of Cholate And Deoxycholate With Fluid Model Membranes And Their Solubilization Into Mixed Micelles. Colloids And Surfaces B-Biointerfaces* 32 (2003).

[51] A.F. Hofmann, And L.R. Hagey, *Bile Acids: Chemistry, Pathochemistry, Biology, Pathobiology, And Therapeutics. Cellular And Molecular Life Sciences* 65 (2008) 2461-2483.

[52] M.C. Carey, *Aqueous Bile Salt-Lecithin-Cholesterol Systems - Equilibrium Aspects. Hepatology* 4 (1984) S151-S154.

[53] J.M. Donovan, And A.A. Jackson, *Transbilayer Movement Of Fully Ionized Taurine-Conjugated Bile Salts Depends Upon Bile Salt Concentration, Hydrophobicity, And Membrane Cholesterol Content. Biochemistry* 36 (1997) 11444-11451.

[54] K. John, J. Kubelt, P. Muller, D. Wustner, And A. Herrmann, *Rapid Transbilayer Movement Of The Fluorescent Sterol Dehydroergosterol In Lipid Membranes. Biophysical Journal* 83 (2002) 1525-1534.

- [55] *Haberlan.Me, And J.A. Reynolds, Self-Association Of Cholesterol In Aqueous-Solution. Proceedings Of The National Academy Of Sciences Of The United States Of America* 70 (1973) 2313-2316.
- [56] *A. Missner, And P. Pohl, 110 Years Of The Meyer-Overton Rule: Predicting Membrane Permeability Of Gases And Other Small Compounds. Chemphyschem* 10 (2009) 1405-1414.
- [57] *A.B.R. Thomson, C. Schoeller, M. Keelan, L. Smith, And M.T. Clandinin, Lipid Absorption - Passing Through The Unstirred Layers, Brush-Border Membrane, And Beyond. Canadian Journal Of Physiology And Pharmacology* 71 (1993).
- [58] *H. Westergaard, And J.M. Dietschy, Mechanism Whereby Bile-Acid Micelles Increase Rate Of Fatty-Acid And Cholesterol Uptake Into Intestinal Mucosal Cell. Journal Of Clinical Investigation* 58 (1976) 97-108.
- [59] *H. Danielsson, And J. Sjoval, Sterols And Bile Acids, Elsevier, 1985.*
- [60] *W.J. Simmonds, A.F. Hofmann, And E. Theodor, Absorption Of Cholesterol From A Micellar Solution - Intestinal Perfusion Studies In Man. Journal Of Clinical Investigation* 46 (1967) 874-&.
- [61] *S.M. Watt, And W.J. Simmonds, Specificity Of Bile-Salts In Intestinal-Absorption Of Micellar Cholesterol In Rat. Clinical And Experimental Pharmacology And Physiology* 3 (1976).
- [62] *E.B. Feldman, And C.Y. Cheng, Mucosal Uptake Invitro Of Cholesterol From Bile-Salt And Surfactant Solutions. American Journal Of Clinical Nutrition* 28 (1975) 692-698.
- [63] *A.F. Hofmann, And K.J. Mysels, Bile Salts As Biological Surfactants. Colloids And Surfaces* 30 (1988) 145-173.
- [64] *L. Jia, J.L. Betters, And L. Yu, Niemann-Pick C1-Like 1 (NPC1L1) Protein In Intestinal And Hepatic Cholesterol Transport. Annual Review Of Physiology, Vol 73* 73 (2011).

- [65] D. Voet, J. Voet, And C. Pratt, *Fundamentals Of Biochemistry*, John Wiley & Sons, Inc, 1998.
- [66] R.J. Abraham, J. Fisher, And P. Loftus, *Introduction To NMR Spectroscopy*, John Wiley & Sons, Essex, 1988.
- [67] V. Gil, And C. Geraldés, *Ressonância Magnética Nuclear: Fundamentos, Métodos E Aplicações*, Fundação Calouste Gulbenkian, 2002.
- [68] T. Claridge, *High-Resolution NMR Technique In Organic Chemistry*, Pergamon, 1999.
- [69] A. Velázquez-Campoy, And E. Freire, *ITC In The Post-Genomic Era... ? Priceless. Biophysical Chemistry* 115 (2005) 115-124.
- [70] H. Heerklotz, *The Microcalorimetry Of Lipid Membranes. Journal Of Physics-Condensed Matter* 16 (2004) R441-R467.
- [71] H.H. Heerklotz, H. Binder, And R.M. Epand, *A "Release" Protocol For Isothermal Titration Calorimetry. Biophysical Journal* 76 (1999) 2606-2613.
- [72] E. Freire, A. Schoen, And A. Velázquez-Campoy, *Isothermal Titration Calorimetry: General Formalism Using Binding Polynomials. Methods In Enzymology: Biothermodynamics, Vol 455, Part A 455 (2009) 127-155.*
- [73] M.C. Wiener, And S.H. White, *Structure Of A Fluid Dioleoylphosphatidylcholine Bilayer Determined By Joint Refinement Of X-Ray And Neutron-Diffraction Data .2. Distribution And Packing Of Terminal Methyl-Groups. Biophysical Journal* 61 (1992) 428-433.
- [74] A.I. Greenwood, S. Tristram-Nagle, And J.F. Nagle, *Partial Molecular Volumes Of Lipids And Cholesterol. Chemistry And Physics Of Lipids* 143 (2006) 1-10.
- [75] M.J. Moreno, M. Bastos, And A. Velázquez-Campoy, *Partition Of Amphiphilic Molecules To Lipid Bilayers By Isothermal Titration Calorimetry. Analytical Biochemistry* 399 (2010).

- [76] M.H. Oosterveer, A. Grefhorst, A.K. Groen, And F. Kuipers, *The Liver X Receptor: Control Of Cellular Lipid Homeostasis And Beyond Implications For Drug Design*. *Progress In Lipid Research* 49 (2010) 343-352.
- [77] D. Meder, M.J. Moreno, P. Verkade, W.L.C. Vaz, And K. Simons, *Phase Coexistence And Connectivity In The Apical Membrane Of Polarized Epithelial Cells*. *Proceedings Of The National Academy Of Sciences Of The United States Of America* 103 (2006) 329-334.
- [78] D. Lingwood, And K. Simons, *Lipid Rafts As A Membrane-Organizing Principle*. *Science* 327 (2010) 46-50.
- [79] N. Taieb, N. Yahi, And J. Fantini, *Rafts And Related Glycosphingolipid-Enriched Microdomains In The Intestinal Epithelium: Bacterial Targets Linked To Nutrient Absorption*. *Advanced Drug Delivery Reviews* 56 (2004) 779-794.
- [80] F. Schroeder, A.M. Gallegos, B.P. Atshaves, S.M. Storey, A.L. McIntosh, A.D. Petrescu, H. Huang, O. Starodub, H. Chao, H.Q. Yang, A. Frolov, And A.B. Kier, *Recent Advances In Membrane Microdomains: Rafts, Caveolae, And Intracellular Cholesterol Trafficking*. *Experimental Biology And Medicine* 226 (2001) 873-890.
- [81] J.C.M. Holthuis, G. Van Meer, And K. Huitema, *Lipid Microdomains, Lipid Translocation And The Organization Of Intracellular Membrane Transport (Review)*. *Molecular Membrane Biology* 20 (2003) 231-241.
- [82] T. Rezen, D. Rozman, J.M. Pascussi, And K. Monostory, *Interplay Between Cholesterol And Drug Metabolism*. *Biochimica Et Biophysica Acta-Proteins And Proteomics* 1814 (2011) 146-160.
- [83] S. Santosa, K.A. Varady, S. Abumweis, And P.J.H. Jones, *Physiological And Therapeutic Factors Affecting Cholesterol Metabolism: Does A Reciprocal Relationship Between Cholesterol Absorption And Synthesis Really Exist?* *Life Sciences* 80 (2007) 505-514.
- [84] L.A. Woollett, Y. Wang, D.D. Buckley, L. Yao, S. Chin, N. Granholm, P.J.H. Jones, K.D.R. Setchell, P. Tso, And J.E. Heubi, *Micellar Solubilisation Of Cholesterol Is Essential For Absorption In Humans*. *Gut* 55 (2006) 197-204.

- [85] M.D. Siperstein, I.L. Chaikoff, And W.O. Reinhardt, C-14-Cholesterol .5. Obligatory Function Of Bile In Intestinal Absorption Of Cholesterol. *Journal Of Biological Chemistry* 198 (1952) 111-114.
- [86] A.F. Hofmann, Function Of Bile Salts In Fat Absorption - Solvent Properties Of Dilute Micellar Solutions Of Conjugated Bile Salts. *Biochemical Journal* 89 (1963) 57-68.
- [87] M.D. Wilson, And L.L. Rudel, Review Of Cholesterol Absorption With Emphasis On Dietary And Biliary Cholesterol. *Journal Of Lipid Research* 35 (1994) 943-955.
- [88] S.D. Turley, And J.M. Dietschy, Sterol Absorption By The Small Intestine. *Current Opinion In Lipidology* 14 (2003) 233-240.
- [89] D.Q.H. Wang, S. Tazuma, D.E. Cohen, And M.C. Carey, Feeding Natural Hydrophilic Bile Acids Inhibits Intestinal Cholesterol Absorption: Studies In The Gallstone-Susceptible Mouse. *American Journal Of Physiology-Gastrointestinal And Liver Physiology* 285 (2003) G494-G502.
- [90] L.M.B.B. Estronca, M.J. Moreno, And W.L.C. Vaz, Kinetics And Thermodynamics Of The Association Of Dehydroergosterol With Lipid Bilayer Membranes. *Biophys. J.* 93 (2007) 4244-4253.
- [91] M.C. Phillips, W.J. Johnson, And G.H. Rothblat, Mechanisms And Consequences Of Cellular Cholesterol Exchange And Transfer. *Biochimica Et Biophysica Acta* 906 (1987) 223-276.
- [92] S. Meaney, K. Bodin, U. Diczfalusy, And I. Bjorkhem, On The Rate Of Translocation In Vitro And Kinetics In Vivo Of The Major Oxysterols In Human Circulation: Critical Importance Of The Position Of The Oxygen Function. *Journal Of Lipid Research* 43 (2002) 2130-2135.
- [93] M.C. Carey, And D.M. Small, Physical-Chemistry Of Cholesterol Solubility In Bile - Relationship To Gallstone Formation And Dissolution In Man. *Journal Of Clinical Investigation* 61 (1978) 998-1026.

- [94] D.Q.H. Wang, D.E. Cohen, And M.C. Carey, *Biliary Lipids And Cholesterol Gallstone Disease. Journal Of Lipid Research* 50 (2009) S406-S411.
- [95] R.N. Redinger, And D.M. Small, *Bile Composition, Bile-Salt Metabolism And Gallstones. Archives Of Internal Medicine* 130 (1972) 618-630.
- [96] L.J. Schoenfield, J.M. Lachin, R.A. Baum, R.L. Habig, R.F. Hanson, T. Hersh, N.C. Hightower, A.F. Hofmann, E.C. Lasser, J.W. Marks, H. Mekhjian, R. Okun, R.A. Schaefer, L. Shaw, R.D. Soloway, J.L. Thistle, F.B. Thomas, And M.P. Tyor, *Chenodiol (Chenodeoxycholic Acid) For Dissolution Of Gallstones - The National Cooperative Gallstone Study - A Controlled Trial Of Efficacy And Safety. Annals Of Internal Medicine* 95 (1981) 257-282.
- [97] Danzinge.Rg, J.L. Thistle, Schoenfi.Lj, And A.F. Hofmann, *Dissolution Of Cholesterol Gallstones By Chenodeoxycholic Acid. New England Journal Of Medicine* 286 (1972) 1-8.
- [98] J.T. Bashour, And L. Bauman, *The Solubility Of Cholesterol In Bile Salt Solutions. Journal Of Biological Chemistry* 121 (1937) 1-3.
- [99] G.A.N. Gowda, O.B. Ijare, B.S. Somashekar, A. Sharma, V.K. Kapoor, And C.L. Khetrapal, *Single-Step Analysis Of Individual Conjugated Bile Acids In Human Bile Using H-1 NMR Spectroscopy. Lipids* 41 (2006) 591-603.
- [100] G.A.N. Gowda, B.S. Somashekar, O.B. Ijare, A. Sharma, V.K. Kapoor, And C.L. Khetrapal, *One-Step Analysis Of Major Bile Components In Human Bile Using H-1 NMR Spectroscopy. Lipids* 41 (2006) 577-589.
- [101] A.A. Ribeiro, And E.A. Dennis, *Proton Magnetic-Resonance Relaxation Studies On Structure Of Mixed Micelles Of Triton-X-100 And Dimyristoylphosphatidylcholine. Biochemistry* 14 (1975) 3746-3755.
- [102] J.P.M. Ellul, G.M. Murphy, H.G. Parkes, R.Z. Slapa, And R.H. Dowling, *Nuclear-Magnetic-Resonance Spectroscopy To Determine The Micellar Cholesterol In Human Bile. Febs Letters* 300 (1992) 30-32.

- [103] J.M. Donovan, A.A. Jackson, And M.C. Carey, *Molecular-Species Composition Of Inter-Mixed Micellar/Vesicular Bile-Salt Concentrations In Model Bile - Dependence Upon Hydrophilic-Hydrophobic Balance. Journal Of Lipid Research 34 (1993) 1131-1140.*
- [104] D.Q.H. Wang, And M.C. Carey, *Characterization Of Crystallization Pathways During Cholesterol Precipitation From Human Gallbladder Biles: Identical Pathways To Corresponding Model Biles With Three Predominating Sequences. Journal Of Lipid Research 37 (1996) 2539-2549.*
- [105] M.J. Armstrong, And M.C. Carey, *The Hydrophobic-Hydrophilic Balance Of Bile-Salts - Inverse Correlation Between Reverse-Phase High-Performance Liquid-Chromatographic Mobilities And Micellar Cholesterol-Solubilizing Capacities. Journal Of Lipid Research 23 (1982) 70-80.*
- [106] R.M.M. Brito, And W.L.C. Vaz, *Determination Of The Critical Micelle Concentration Of Surfactants Using The Fluorescent-Probe N-Phenyl-1-Naphthylamine. Analytical Biochemistry 152 (1986) 250-255.*
- [107] D.M. Small, S.A. Penkett, And D. Chapman, *Studies On Simple And Mixed Bile Salt Micelles By Nuclear Magnetic Resonance Spectroscopy. Biochimica Et Biophysica Acta 176 (1969) 178-189.*
- [108] C.F. Schmidt, J.K. Chun, A.V. Broccoli, And R.P. Taylor, *Physical Studies Of Interaction Between Detergent-Solubilized Cholesterol And PC Vesicles. Chemistry And Physics Of Lipids 22 (1978) 125-133.*
- [109] O. Ijare, B. Somashekar, Y. Jadegoud, And G. Nagana Gowda, *¹H And ¹³C NMR Characterization And Stereochemical Assignments Of Bile Acids In Aqueous Media. Lipids 40 (2005) 1031-1041.*
- [110] M. Janich, J. Lange, H. Graener, And R. Neubert, *Extended Light Scattering Investigations On Dihydroxy Bile Salt Micelles In Low-Salt Aqueous Solutions. Journal Of Physical Chemistry B 102 (1998) 5957-5962.*

- [111] N.A. Mazer, M.C. Carey, R.F. Kwasnick, And G.B. Benedek, *Quasi-Elastic Light-Scattering Studies Of Aqueous Biliary Lipid Systems - Size, Shape, And Thermodynamics Of Bile-Salt Micelles*. *Biochemistry* 18 (1979) 3064-3075.
- [112] J.P. Kratochvil, W.P. Hsu, And D.I. Kwok, *How Large Are The Micelles Of Di-Alpha-Hydroxy Bile-Salts At The Critical Micellization Concentrations In Aqueous-Electrolyte Solutions - Results For Sodium Taurodeoxycholate And Sodium Deoxycholate*. *Langmuir* 2 (1986) 256-258.
- [113] P. Schurtenberger, N. Mazer, And W. Kanzig, *Static And Dynamic Light-Scattering Studies Of Micellar Growth And Interactions In Bile-Salt Solutions*. *Journal Of Physical Chemistry* 87 (1983) 308-315.
- [114] S.Y. Oh, M.E. McDonnell, R.T. Holzbach, And A.M. Jamieson, *Diffusion-Coefficients Of Single Bile-Salt And Bile Salt-Mixed Lipid Micelles In Aqueous-Solution Measured By Quasi-Elastic Laser-Light Scattering*. *Biochimica Et Biophysica Acta* 488 (1977) 25-35.
- [115] A. Coello, F. Meijide, E.R. Nunez, And J.V. Tato, *Aggregation Behavior Of Bile Salts In Aqueous Solution*. *Journal Of Pharmaceutical Sciences* 85 (1996) 9-15.
- [116] J.R. Lakowicz, *Principles Of Fluorescence Spectroscopy*, Kluwer Academic/Plenum Publishers, New York, 1999.
- [117] L. Korson, Drosthan.W, And F.J. Millero, *Viscosity Of Water At Various Temperatures*. *Journal Of Physical Chemistry* 73 (1969) 34-39.
- [118] K. Matsuoka, T. Hirosawa, C. Honda, K. Endo, Y. Moroi, And O. Shibata, *Thermodynamic Study On Competitive Solubilization Of Cholesterol And P-Sitosterol In Bile Salt Micelles*. *Chemistry And Physics Of Lipids* 148 (2007) 51-60.
- [119] E. Melo, A.A. Freitas, Y.W. Chang, And F.H. Quina, *On The Significance Of The Solubilization Power Of Detergents*. *Langmuir* 17 (2001) 7980-7981.
- [120] F.M. Coreta-Gomes, W.L. Vaz, E. Wasielewski, C.F. Geraldés, And M.J. Moreno, *Quantification Of Cholesterol Solubilized In Bile Salt Micellar Aqueous Solutions Using (13)C Nuclear Magnetic Resonance*. *Anal Biochem* 427 (2012) 41-8.

- [121] C.K. Glass, And J.L. Witztum, *Atherosclerosis: The Road Ahead*. *Cell* 104 (2001).
- [122] E. Goddard, *Molecular Association in Biological And Related Systems*, American Chemical Society Publications, USA, 1968.
- [123] K. Matsuoka, E. Kajimoto, M. Horiuchi, C. Honda, And K. Endo, *Competitive Solubilization Of Cholesterol And Six Species Of Sterol/Stanol In Bile Salt Micelles*. *Chemistry And Physics Of Lipids* 163 (2010) 397-402.
- [124] K. Matsuoka, T. Nakazawa, A. Nakamura, C. Honda, K. Endo, And M. Tsukada, *Study Of Thermodynamic Parameters For Solubilization Of Plant Sterol And Stanol In Bile Salt Micelles*. *Chemistry And Physics Of Lipids* 154 (2008) 87-93.
- [125] E. Ros, *Intestinal Absorption Of Triglyceride And Cholesterol. Dietary And Pharmacological Inhibition To Reduce Cardiovascular Risk*. *Atherosclerosis* 151 (2000) 357-379.
- [126] A.B.R. Thomson, M. Keelan, M.L. Garg, And M.T. Clandinin, *Intestinal Aspects Of Lipid Absorption - In Review*. *Canadian Journal Of Physiology And Pharmacology* 67 (1989).
- [127] J. Plat, And R.P. Mensink, *Plant Stanol And Sterol Esters In The Control Of Blood Cholesterol Levels: Mechanism And Safety Aspects*. *American Journal Of Cardiology* 96 (2005) 15D-22D.
- [128] P.B. Nielsen, A. Mullertz, T. Norling, And H.G. Kristensen, *The Effect Of Alpha-Tocopherol On The In Vitro Solubilisation Of Lipophilic Drugs*. *International Journal Of Pharmaceutics* 222 (2001) 217-224.
- [129] S. Rozner, A. Aserin, And N. Garti, *Competitive Solubilization Of Cholesterol And Phytosterols In Nonionic Microemulsions Studied By Pulse Gradient Spin-Echo NMR*. *Journal Of Colloid And Interface Science* 321 (2008) 418-425.
- [130] S. Nagadome, Y. Okazaki, S. Lee, Y. Sasaki, And G. Sugihara, *Selective Solubilization Of Sterols By Bile Salt Micelles In Water: A Thermodynamic Study*. *Langmuir* 17 (2001) 4405-4412.

- [131] K. Matsuoka, Y. Kuranaga, And Y. Moroi, *Solubilization Of Cholesterol And Polycyclic Aromatic Compounds Into Sodium Bile Salt Micelles (Part 2)*. *Biochimica Et Biophysica Acta-Molecular And Cell Biology Of Lipids* 1580 (2002) 200-214.
- [132] E.D. Jesch, And T.P. Carr, *Sitosterol Reduces Micellar Cholesterol Solubility In Model Bile*. *Nutrition Research* 26 (2006) 579-584.
- [133] S.M. Mel'nikov, J. Ten Hoorn, And B. Bertrand, *Can Cholesterol Absorption Be Reduced By Phytosterols And Phytostanols Via A Cocrystallization Mechanism?* *Chemistry And Physics Of Lipids* 127 (2004) 15-33.
- [134] A. Von Bonsdorff-Nikander, L. Christiansen, L. Huikko, A.M. Lampi, V. Piironen, J. Yliruusi, And A.M. Kaukonen, *A Comparison Of The Effect Of Medium- Vs. Long-Chain Triglycerides On The In Vitro Solubilization Of Cholesterol And/Or Phytosterol Into Mixed Micelles*. *Lipids* 40 (2005) 181-190.
- [135] Y.F. Shiau, P. Fernandez, M.J. Jackson, And S. Mcmonagle, *Mechanisms Maintaining A Low-PH Microclimate In The Intestine* *American Journal Of Physiology* 248 (1985) G608-G617.
- [136] O. Abian, P. Alfonso, A. Velazquez-Campoy, P. Giraldo, M. Pocovi, And J. Sancho, *Therapeutic Strategies For Gaucher Disease: Miglustat (NB-DNJ) As A Pharmacological Chaperone For Glucocerebrosidase And The Different Thermostability Of Velaglucerase Alfa And Imiglucerase*. *Molecular Pharmaceutics* 8 (2011) 2390-2397.
- [137] T.E. Thompson, And T.W. Tillack, *Organization Of Glycosphingolipids In Bilayers And Plasma-Membranes Of Mammalian-Cells*. *Annual Review Of Biophysics And Biophysical Chemistry* 14 (1985) 361-386.
- [138] P. Schurtenberger, N.A. Mazer, And W. Kanzig, *Dynamic Laser-Light Scattering Studies Of The Micelle To Vesicle Transition In Model And Native Bile*. *Hepatology* 4 (1984) S143-S147.
- [139] P.T. Martins, A. Velazquez-Campoy, W.L.C. Vaz, R.M.S. Cardoso, J. Valerio, And M.J. Moreno, *Kinetics And Thermodynamics Of Chlorpromazine Interaction With*

Lipid Bilayers: Effect Of Charge And Cholesterol. Journal Of The American Chemical Society 134 (2012).

[140] H. Heerklotz, *Interactions Of Surfactants With Lipid Membranes. Quarterly Reviews Of Biophysics* 41 (2008) 205-264.

[141] H. Heerklotz, A.D. Tsamaloukas, And S. Keller, *Monitoring Detergent-Mediated Solubilization And Reconstitution Of Lipid Membranes By Isothermal Titration Calorimetry. Nature Protocols* 4 (2009) 686-697.

[142] M.S.C. Abreu, L. Estroñca, M.J. Moreno, And W.L.C. Vaz, *Binding Of A Fluorescent Lipid Amphiphile To Albumin And Its Transfer To Lipid Bilayer Membranes. Biophysical Journal* 84 (2003).

[143] M.S.C. Abreu, M.J. Moreno, And W.L.C. Vaz, *Kinetics And Thermodynamics Of Association Of A Phospholipid Derivative With Lipid Bilayers In Liquid-Disordered And Liquid-Ordered Phases. Biophysical Journal* 87 (2004).

[144] L.M.B.B. Estroñca, M.J. Moreno, And W.L.C. Vaz, *Kinetics And Thermodynamics Of The Association Of Dehydroergosterol With Lipid Bilayer Membranes. Biophysical Journal* 93 (2007) 4244-4253.

[145] J.L. Sampaio, M.J. Moreno, And W.L.C. Vaz, *Kinetics And Thermodynamics Of Association Of A Fluorescent Lysophospholipid Derivative With Lipid Bilayers In Liquid-Ordered And Liquid-Disordered Phases. Biophysical Journal* 88 (2005) 4064-4071.

[146] I.V. Ionova, V.A. Livshits, And D. Marsh, *Phase Diagram Of Ternary Cholesterol/Palmitoylsphingomyelin/Palmitoyl-oleoyl-Phosphatidylcholine Mixtures: Spin-Label EPR Study Of Lipid-Raft Formation. Biophysical Journal* 102 (2012) 1856-1865.

[147] S.L. Veatch, And S.L. Keller, *Separation Of Liquid Phases In Giant Vesicles Of Ternary Mixtures Of Phospholipids And Cholesterol. Biophysical Journal* 85 (2003) 3074-3083.

- [148] H. Fukada, And K. Takahashi, *Enthalpy And Heat Capacity Changes For The Proton Dissociation Of Various Buffer Components In 0.1 M Potassium Chloride. Proteins-Structure Function And Genetics* 33 (1998) 159-166.
- [149] A. Velazquez-Campoy, And E. Freire, *Isothermal Titration Calorimetry To Determine Association Constants For High-Affinity Ligands. Nature Protocols* 1 (2006) 186-191.
- [150] G.R. Bartlett, *Phosphorus Assay In Column Chromatography. Journal Of Biological Chemistry* 234 (1959) 466-468.
- [151] R.P. Taylor, A.V. Broccoli, And C.M. Grisham, *Enzymatic And Colorimetric Determination Of Total Serum-Cholesterol - Undergraduate Biochemistry Laboratory Experiment. Journal Of Chemical Education* 55 (1978) 63-64.
- [152] R.M.S. Cardoso, P.A.T. Martins, F. Gomes, S. Doktorovova, W.L.C. Vaz, And M.J. Moreno, *Chain-Length Dependence Of Insertion, Desorption, And Translocation Of A Homologous Series Of 7-Nitrobenz-2-Oxa-1,3-Diazol-4-Yl-Labeled Aliphatic Amines In Membranes. Journal Of Physical Chemistry B* 115 (2011).
- [153] S.L. Veatch, And S.L. Keller, *Miscibility Phase Diagrams Of Giant Vesicles Containing Sphingomyelin. Physical Review Letters* 94 (2005).
- [154] N.A. Mazer, And M.C. Carey, *Quasi-Elastic Light-Scattering-Studies Of Aqueous Biliary Lipid Systems - Cholesterol Solubilization And Precipitation In Model Bile Solutions. Biochemistry* 22 (1983) 426-442.
- [155] J.M. Donovan, N. Timofeyeva, And M.C. Carey, *Influence Of Total Lipid-Concentration, Bile-Salt Lecithin Ratio, And Cholesterol Content On Inter-Mixed Micellar/Vesicular (Non-Lecithin-Associated) Bile-Salt Concentrations In Model Bile. Journal Of Lipid Research* 32 (1991) 1501-1512.